

SCALE FORMATION IN SALINE WATER DISTILLATION

A Thesis submitted for the degree of
DOCTOR OF PHILOSOPHY
in the University of London

by

Douglas Ian Turner , B.Eng.

Department of Chemical Engineering,
Imperial College of Science and Technology,
London, S.W.7.

November, 1965.

ABSTRACT

One of the principal steps in the formation of a calcium sulphate deposit on a surface under isothermal conditions is shown to be the nucleation of crystals in the bulk of the solution followed by their attachment to the surface. The ease of attachment of the crystals depends on the supersaturation and agitation of the solution as well as on the smoothness of the surface, but it appears to be independent of the surface material. It is shown that by controlling the number of crystals in the bulk of the solution or the access of these crystals to the surface, the number of crystals attached can be controlled.

The rate of nucleation of hemihydrate and dihydrate has been measured under isothermal conditions. The induction time for the hemihydrate is shorter than that for the dihydrate in simple calcium sulphate solutions; the induction time for the hemihydrate is reduced even further in mixed calcium chloride and sodium sulphate solutions.

The growth rates at controlled levels of supersaturation and stirring velocity both of single hemihydrate and dihydrate crystals in the bulk of the solution and of massive deposits of these crystals on a metal surface have been measured, and a direct relationship is indicated. From the effect of stirring on the growth rate of single crystals, the relative contributions

of mass transfer and surface reaction to the overall growth rate of the dihydrate are found, and it is shown that the growth rate is controlled to some extent by the rate of mass transfer except at low supersaturations and high stirring rates. When mass transfer effects are eliminated, the surface reaction rate is found to be approximately proportional to the second power of the supersaturation. Also, it is shown that the growth of the hemihydrate can be inhibited by a coating of glass dust on the crystal surface.

ACKNOWLEDGEMENTS

The author would like to express his especial appreciation to Dr. R. F. Strickland-Constable for his helpful guidance and valuable advice throughout this course of study. He is also indebted to Professor K. G. Denbigh in whose department this work was carried out.

Grateful acknowledgement is made to The Admiralty (Ministry of Defence (Navy)) for providing financial assistance. The author would also like to thank Dr. R. G. H. Watson and Mr. D. W. Butcher of The Admiralty Materials Laboratory for several stimulating and useful discussions.

CONTENTS

TITLE		1
ABSTRACT		2
ACKNOWLEDGEMENTS		4
CONTENTS		5
CHAPTER 1.	INTRODUCTION	
1.1	The Scale Problem	9
1.2	Previous Studies on Calcium Sulphate Scale Formation	12
1.3	The Scope of the Present Work	15
CHAPTER 2.	THE FORMATION OF CALCIUM SULPHATE NUCLEI IN THE BULK OF THE SOLUTION	
2.1	Introduction	19
2.2	The Forms of Calcium Sulphate	22
2.3	Apparatus	29
2.4	The Effect of Temperature and Super- saturation on the Relative Amounts of Dihydrate and Hemihydrate Formed in Solution	29
2.5	The Rate of Nucleation in Unstirred Calcium Sulphate Solutions	37
2.5.1	Induction Times in Heated Solutions	39
2.5.2	Induction Times in Mixed Solutions	51
2.6	The Rate of Nucleation in Stirred Calcium Sulphate Solutions	55
2.7	Summary	60

CHAPTER 3.	THE GROWTH RATE OF DIHYDRATE CRYSTALS	
3.1	Introduction	62
3.2	Growth Rates of Unstirred Crystals	70
3.3	Growth Rates of Stirred Crystals	79
3.4	The Effect of Crystal Size on Growth Rate	93
3.5	Summary	94
CHAPTER 4.	THE GROWTH RATE OF HEMIHYDRATE CRYSTALS	
4.1	Introduction	96
4.2	Growth Rates of Unstirred Crystals	96
4.3	Growth Rates of Stirred Crystals	99
4.3.1	Preliminary Measurements of the Stirred Growth Rate	99
4.3.2	Effect of Impurities on the Growth of Hemihydrate	102
4.4	The Growth Rates of Hemihydrate and Dihydrate in 1.0 Molar Sodium Chloride Solutions	110
4.5	Summary	111
CHAPTER 5.	THE FORMATION OF MASSIVE DEPOSITS OF DIHYDRATE AND HEMIHYDRATE	
5.1	Introduction	113
5.2	Exploratory Investigations of Deposition on Unheated Metal Surfaces	114

5.3	Exploratory Investigations of Deposition on a Heated Metal Surface	120
5.4	The Rate of Deposition on a Metal Surface : Isothermal Conditions	125
5.5	Summary	137
CHAPTER 6.	THE FORMATION OF CALCIUM SULPHATE DEPOSITS ON CRYSTAL SURFACES	
6.1	Introduction	139
6.2	Examination of the Dihydrate Deposits Formed on Stirred Unheated Metal Surfaces	141
6.3	Nucleation of Dihydrate Crystals in the Presence of an Unstirred Dihydrate Seed Crystal	143
6.4	The Effect of the Number of Crystals in the Solution on the Deposit Density on Crystal Surfaces	146
6.4.1	The Effect of the Addition of Barium Ion on Nucleation in the Solution	146
6.4.2	The Effect of the Volume of Solution in Contact with the Seed Crystal	148
6.4.3	The Effect of the Addition of Dihydrate Crystals on the Number of Crystals on the Seed Crystal	154
6.5	The Effect of Stirring on the Number of Dihydrate Crystals on a Seed Crystal Surface	156
6.6	Summary	162

CHAPTER 7.	SUMMARY AND DISCUSSION OF RESULTS	
7.1	The Mechanism of Calcium Sulphate Deposition on an Unheated Surface	165
7.2	Nucleation of Calcium Sulphate Dihydrate and Hemihydrate	172
7.3	Growth of Calcium Sulphate Dihydrate and Hemihydrate	174
APPENDIX 1	EXPERIMENTAL RESULTS	185
APPENDIX 2	PHYSICAL DATA	238
APPENDIX 3	NOMENCLATURE	239
APPENDIX 4	REFERENCES	242

CHAPTER 1

Introduction

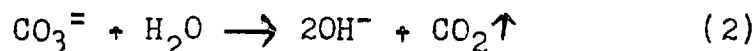
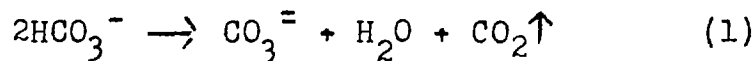
1.1 The Scale Problem

Sea water is a rather complex aqueous solution containing many inorganic salts as well as lesser amounts of organic materials. When it is distilled to produce fresh water, the concentration of the dissolved salts increases as water is removed. Since normal sea water is greatly undersaturated in most of these salts, a considerable amount of water could be removed were it not for a few salts having low solubilities which decrease with increasing temperature. If the concentration of these salts exceeds the solubility, a scale forms on the most convenient surface. Because of their negative solubilities, this generally occurs on the hottest surface in contact with the solution and causes a reduction in efficiency of distillation.

As many as fifty elements have been detected in sea water¹, but nine of these comprise over 99% by weight of the total dissolved solid constituents. A typical formula for preparing synthetic sea water² incorporating the major elements present in natural sea water is shown below.

CONSTITUENT	CONCENTRATION (parts per million)
Sodium chloride	27,200
Magnesium chloride	3,800
Magnesium sulphate	1,600
Calcium sulphate	1,300
Potassium sulphate	900
Calcium carbonate	100
Magnesium bromide	100
	<hr style="width: 10%; margin: 0 auto;"/>
	35,000

There are three salts which form the major proportion of the scales produced in sea water distillation. These are calcium carbonate, magnesium hydroxide and calcium sulphate. The first two salts are formed because of the production of carbonate and hydroxyl ions when sea water is heated:



When the sea water becomes supersaturated in the two salts, deposition occurs. The simplest and most effective method of control is to entirely prevent deposition by reducing the pH of the sea water to a slightly acidic value. Since the above reactions proceed only when the sea water is alkaline, they can be repressed by the addition of an acid or an acidic salt. In this way, the concentration of the

two salts never reaches solubility during distillation.

Calcium sulphate, on the other hand, is formed in sea water distillation by concentration of the calcium and sulphate ions present initially in sea water. When the concentration exceeds the solubility, calcium sulphate deposits as a scale. Its formation can be prevented by keeping the sea water unsaturated in calcium sulphate during operation, but this allows only about two thirds of the total water to be removed. Although there are various ways of improving this yield (by suspending calcium sulphate crystals in the sea water for example), calcium sulphate scale is less readily prevented than the carbonate or hydroxide scales. For this reason, the present work has been confined to a study of the kinetics of calcium sulphate deposition.

Considerable research on scaling has been undertaken but surprisingly little of this has been concerned with the fundamental mechanisms involved. It appeared, however, that before any meaningful study on scaling in sea water can be undertaken, it would be advisable to make a study on scaling in pure solutions. This is because of the extremely complex nature of sea water. It is known, for example, that the solubilities of the scale-forming salts are affected by some of the major constituents of sea water and it is not unreasonable to expect that both

the inorganic and organic constituents will influence the nucleation and growth rates and habits of the scale-forming salts. In fact, Ridge et al.^{3,4}, McCartney and Alexander⁵ and Cunningham et al.⁶ have found that the addition of small amounts of various inorganic and organic materials to calcium sulphate slurries has a pronounced effect on the setting time of the plaster and on the size and shape of the calcium sulphate crystals. The present work has therefore been confined to a study of the kinetics of calcium sulphate scale formation in pure solutions as an approach to understanding the formation of scale in more complex solutions.

1.2 Previous Studies on Calcium Sulphate Scale Formation

Several views have been advanced on the mechanism of scale deposition. Partridge⁷ published a good review of the important contributions prior to 1930, and a more recent review has been carried out by Badger⁸.

The observation that calcium sulphate scale grew most rapidly in the hottest parts of a boiler was first made over 100 years ago by Couste⁹. More recently, Hall^{10,11} found that salts with a negative solubility curve

tended to deposit as adherent scales directly onto hotter surfaces whereas salts having the normal positive solubility curve deposited chiefly as non-adherent crystals in the cooler parts of the solution.

Partridge⁷ investigated the formation of calcium sulphate scales from pure solutions boiling on a heated surface. He showed that the mechanism of deposition was nucleation and growth of crystals at the triple interface formed by the bubble, the solution and the heated surface. This was indicated by the ring of crystals remaining on the heated surface after the bubble had detached itself. He postulated that because of increased resistance to heat transfer in the bubble of vapour, local overheating of the heat transfer surface occurred causing increased evaporation of water into the bubble from the thin edge of solution at the triple interface. This would result in a higher degree of supersaturation at the triple interface causing rapid deposition there.

Freeborn¹² extended this work to pure boiling solutions of other salts found in natural waters. He found that salts with negative solubility curves generally gave permanent rings on the heated surface whereas those with positive solubility curves exhibited transient rings that redissolved after the bubble detached from the surface. Golightly and McCartney¹³ obtained similar results

in a study of the effect of air bubbles on the deposition of calcium sulphate on a heated surface.

Gordon and Smith¹⁴ made the first systematic quantitative study on the kinetics of calcium sulphate scale formation in pure solutions. The induction time, or the time elapsed when the first calcium sulphate deposit was observed on the heated surfaces, was taken as a measure of the rate of initiation of scale. The rate was found to be dependent on both solution temperature and supersaturation, but neither boiling nor solution velocity was observed to have an effect. The addition of calcium sulphate crystals to the solutions decreased the induction time for scale formation in some cases, suggesting that the seeding of solutions as a scale prevention technique may not be as effective as has been assumed. The rate of growth of the scale on the heated surface was measured indirectly from the decrease in heat transfer coefficient as the scale was deposited. A finite supersaturation appeared to be necessary in order for the scale to deposit.

All of these studies on calcium sulphate scale formation have been concerned with deposition on heated surfaces, this being a process to which calcium sulphate is susceptible because of its negative solubility. Many investigations have been made of calcium sulphate deposition under isothermal conditions, but these have been

confined to the precipitation of crystals in the bulk of the solution at rather lower temperatures. For example, Lurie et al.¹⁵ measured the decrease in concentration of a supersaturated calcium sulphate solution as gypsum crystals nucleated and grew at room temperature. Visual detection of the onset of nucleation was made before any measurable change in the conductivity of the solution was noted. Stirring the solution was observed to have no effect whereas the addition of certain compounds had a very significant effect on the nucleation rate.

Schierholtz¹⁶ carried out similar experiments at 25°C and concluded that the reaction rate was first order with respect to concentration. Other studies^{17,18} made at temperatures up to 60°C, however, indicated that the reaction rate was second order with respect to supersaturation. Also, in these, stirring of the solution was found to increase the nucleation rate.

1.3 The Scope of the Present Work

It is apparent that there is a need for more fundamental information on the mechanisms involved in scale formation in the absence of boiling. In this connection, some of the questions that can be posed are: Where do the nuclei of the scaling salts form? How are they attached to the surface? How does the scale grow? Is it composed

of single crystals? A number of mechanisms are possible, but the most probable would seem to be one or more of the following:

- (A) The formation of many nuclei directly on the metal surface followed by growth of these nuclei to give a fine polycrystalline mass.
- (B) The formation of nuclei directly on the metal surface as in (A), followed by growth of these nuclei and the formation of further nuclei on the growing crystals.
- (C) The formation of nuclei in the bulk of the solution (presumably on heterogenous particles) followed by attachment of these nuclei to the metal surface, growth of the attached nuclei, and the attachment of further nuclei.

In particular, there is a lack of data on the nucleation and growth of calcium sulphate at the temperatures of interest in saline water distillation. There has, for instance, been little work done at these temperatures on the rates of nucleation and growth of specific forms of calcium sulphate although as many as six of these have been postulated.¹⁹

The present work has involved a study of the kinetics of formation and growth of calcium sulphate dihydrate and hemihydrate, forms of calcium sulphate frequently encountered in scales produced in sea water

distillation. This work has two essential features. Firstly, as mentioned earlier, pure solutions were used in order to observe the kinetics of crystal formation unhindered by the effects of the many other constituents present in sea water. And secondly, because of the near impossibility of accurately defining the supersaturation in a solution having temperature as well as concentration gradients, this work was carried out as far as possible under isothermal conditions.

In the following chapters, experimental evidence is advanced in support of a proposed mechanism for the formation and build-up of scale on an unheated surface, rather like the mechanism described in (C) above. In this, crystal nuclei initially form on a metal surface either by direct nucleation on the surface or by attachment of nuclei which have formed in the bulk of the solution, and these nuclei then grow while further nuclei formed in the bulk of the solution attach to the deposit. Each of the steps in this mechanism was investigated in turn. In the first instance, the rate of and factors affecting the formation of nuclei of the two hydrates in the bulk of the solution were investigated. Following this, the rates of growth were measured both for single crystals in the bulk of the solution and for massive deposits on a metal surface, and a direct relationship of the

two growth rates has been indicated. Both of these growth rates were obtained at controlled stirring rates so that the effect of the relative velocity between the crystal and the solution could be determined. Finally, the attachment to the surface of a seed crystal, of crystals nucleated in the bulk of the solution, was investigated. In the present work, crystals were not observed to nucleate directly on another crystal surface.

CHAPTER 2
THE FORMATION OF CALCIUM SULPHATE NUCLEI
IN THE BULK OF THE SOLUTION

2.1 Introduction

The process of scale formation must involve two stages namely, the nucleation of crystals and their subsequent growth. In this chapter, we shall consider the first stage, that of the formation of new crystals.

Although nucleation can either occur spontaneously in the bulk of a supersaturated solution (homogenous) or be induced by the presence of other materials (heterogeneous), it is considered in most cases to be of the latter type due to the difficulty of ensuring the complete removal of foreign materials from the solution. Depending on the crystal, these materials can be of many types ranging from other dissolved salts to common dust. The walls of the solution container may also induce nucleation. The nucleated crystals may first be detected in the bulk of the solution or on the container walls but this may not in either case be the original site of nucleation.

Expressions for the rate of homogeneous nucleation have been derived from thermodynamic and kinetic theory by Volmer²⁰, Becker and Döring²¹ and others. Since the equation derived from this theory has received considerable experimental confirmation, it has been adopted

here to enable the results of the present work to be discussed and correlated. Very briefly, the theory can be described as follows.

When a new crystal is created in a supersaturated solution, there will be a change in the total free energy, ΔG . For a spherical particle of radius r , and specific surface free energy σ , this change in total free energy is:

$$\Delta G = \frac{4}{3} \pi r^2 \sigma \quad (3)$$

If this particle has a radius less than the critical radius r_c , it will dissolve; if the radius is greater, the particle will continue to grow. This dependence of solubility on crystal size is expressed by the Ostwald-Freundlich equation:

$$\ln \frac{c_r}{c^*} = \frac{2M\sigma}{RT\rho r} \quad (4)$$

where c_r is the solubility of a particle of radius r ; c^* is the solubility of a large particle ($r \rightarrow \infty$); M is the molecular weight of the crystal; ρ is the density of the particle; R is the gas constant and T is the absolute temperature. This equation has been found²² to adequately describe the solubility of calcium sulphate dihydrate crystals with sizes from 0.5 to 50 microns.

Combining these two equations and setting c_r/c^* equal to S , the supersaturation, gives:

$$\Delta G = \frac{16\pi\sigma^3 M^2}{3(RT\rho \ln S)^2} \quad (5)$$

The rate of nucleation, N , can then be expressed in an equation similar in form to the Arrhenius equation:

$$N = A' \exp \left[-\frac{\Delta G}{kT} \right] \quad (6)$$

$$= A' \exp \left[-\frac{16\pi\sigma^3 M^2}{3kR^2 T^3 \rho^2 (\ln S)^2} \right] \quad (7)$$

where k is the Boltzmann constant. The pre-exponential term, A' , is relatively insensitive to changes in temperature or supersaturation, and the predominant effect on the rate of nucleation is contributed by the $(\ln S)^2$ term.

In the case of heterogeneous nucleation, the change in the total free energy, $\Delta G'$, is less than that associated with homogeneous nucleation, ΔG . This would result in an increase in the value of N in equation 6.

In this chapter, measurements on the rate of nucleation of calcium sulphate dihydrate and hemihydrate in solutions of known supersaturation in the temperature range, $70^\circ - 110^\circ\text{C}$, are reported. Since both hydrates nucleate in this temperature range, the effect of temperature and supersaturation on the relative amounts of the two hydrates nucleated was also investigated. Before reporting this work however, a brief description of the various forms of calcium sulphate and their properties will be given.

2.2 The Forms of Calcium Sulphate

There are three basic forms of calcium sulphate: the dihydrate ($\text{CaSO}_4 \cdot 2\text{H}_2\text{O}$), the hemihydrate ($\text{CaSO}_4 \cdot \frac{1}{2}\text{H}_2\text{O}$), and the anhydrite (CaSO_4). Various modifications of the hemihydrate have been postulated however, and there has been considerable controversy as to the total number of unique forms.

The first comprehensive investigation of the various forms of calcium sulphate was carried out over 60 years ago by van't Hoff et al.²³ who concluded that as well as the above forms, there existed a fourth called "soluble anhydrite". This could be prepared by dehydration of the hemihydrate and was so-called because its solubility was much higher than that of the anhydrite, which was renamed "insoluble anhydrite".

Later investigators suggested, however, that the hemihydrate was a zeolitic material and that "soluble anhydrite" was merely a dehydrated form and not a distinct compound. A crystal structure for the hemihydrate was proposed^{24,25} in which a very stable lattice of calcium and sulphate ions formed channels in which the water molecules were weakly held and hence dehydration could be effected without disruption of the lattice.

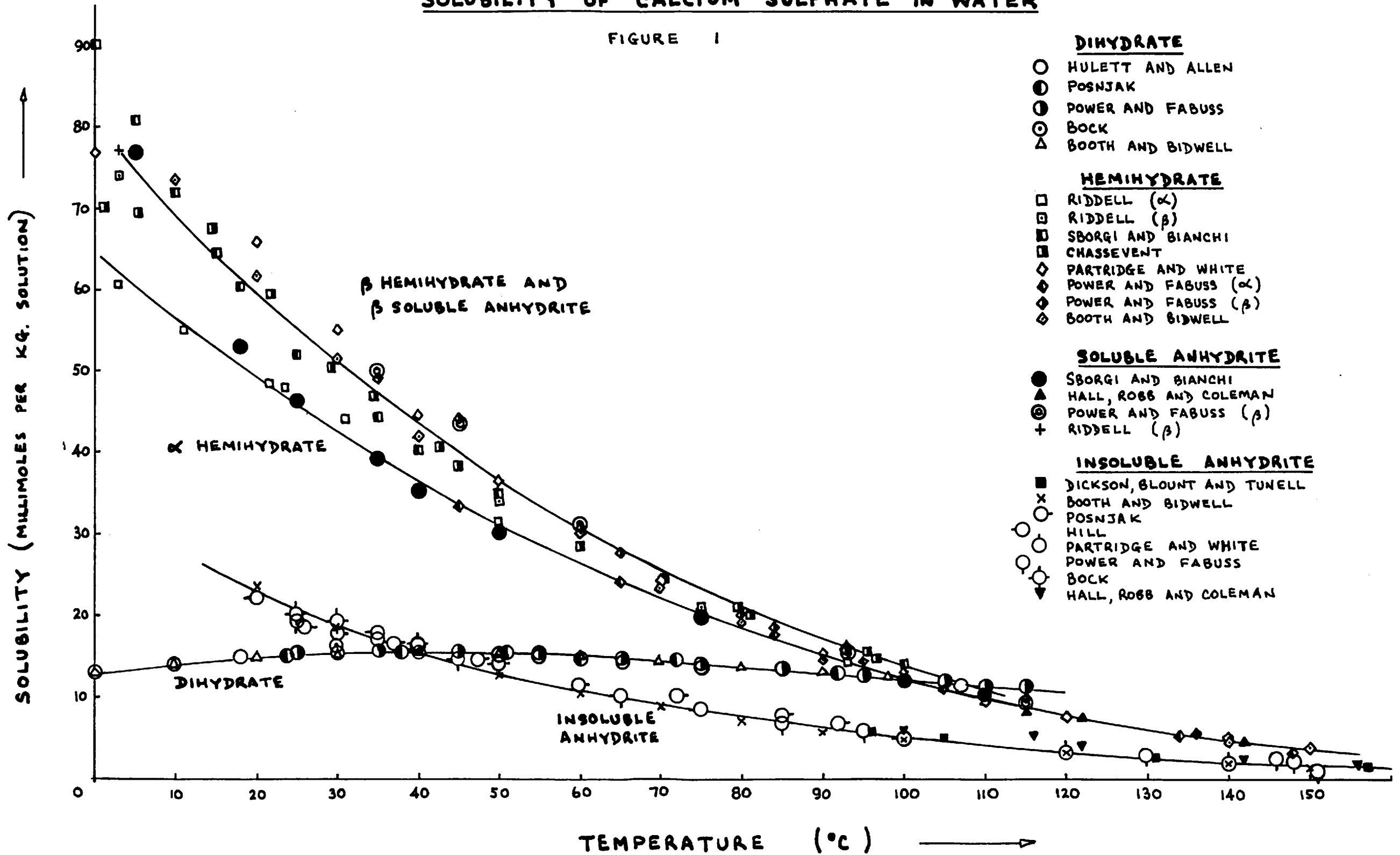
The question of the existence of "soluble anhydrite" as a separate form was not entirely resolved by Xray

diffraction data. Partridge et al.²⁶ concluded on the basis of their diffraction data that the crystal structures of hemihydrate and "soluble anhydrite" were identical and that the "soluble anhydrite" did not represent a separate form. On the other hand, Weiser et al.²⁷ and Posnjak²⁸ detected slight differences in the diffraction data for these two forms and reported that hemihydrate behaved in all essential respects like a true chemical hydrate. Bunn²⁹ however reported that there were slight differences in the diffraction patterns for four forms of $\text{CaSO}_4 \cdot x\text{H}_2\text{O}$ where x was 0.65, 0.48, 0.19 and 0.02. He showed that these forms had the same essential structure with only slight differences in the unit cell dimensions. He attributed this distortion of the crystal lattice to the disturbance of the balance of forces caused by the removal or addition of water molecules. Thus he concluded that hemihydrate was a zeolitic material.

In 1941 Kelley et al.¹⁹, after making an extensive study of their own measurements and those of others on the thermodynamic properties of calcium sulphate, concluded that there are not four, but six unique forms: dihydrate, α hemihydrate, β hemihydrate, α soluble anhydrite, β soluble anhydrite and insoluble anhydrite. The existence of these as separate forms was proposed on the basis of the markedly different energy contents associated

SOLUBILITY OF CALCIUM SULPHATE IN WATER

FIGURE 1



with each form. The two types of hemihydrate were prepared by different methods and each gave a corresponding soluble anhydrite on dehydration. The more stable α hemihydrate was prepared in solution or by dehydration of the dihydrate in an atmosphere saturated with steam whereas the β hemihydrate was prepared by dehydration of dihydrate in an atmosphere greatly undersaturated with steam. The latter was found to have a higher energy content and a somewhat higher solubility than the former.

More recently, Power and Fabuss³⁰ have reported measurements on the solubilities and stabilities in water for all of these forms except α soluble anhydrite. These solubilities are illustrated along with most of the previously published solubility data^{26,28,31-39} in figure 1. It is evident that the solubility data for both the dihydrate and the insoluble anhydrite are in good agreement whereas those for the hemihydrate and the soluble anhydrite show considerable scatter, particularly at the lower temperatures. However, these latter solubilities fall roughly onto two curves corresponding to the α and β forms.

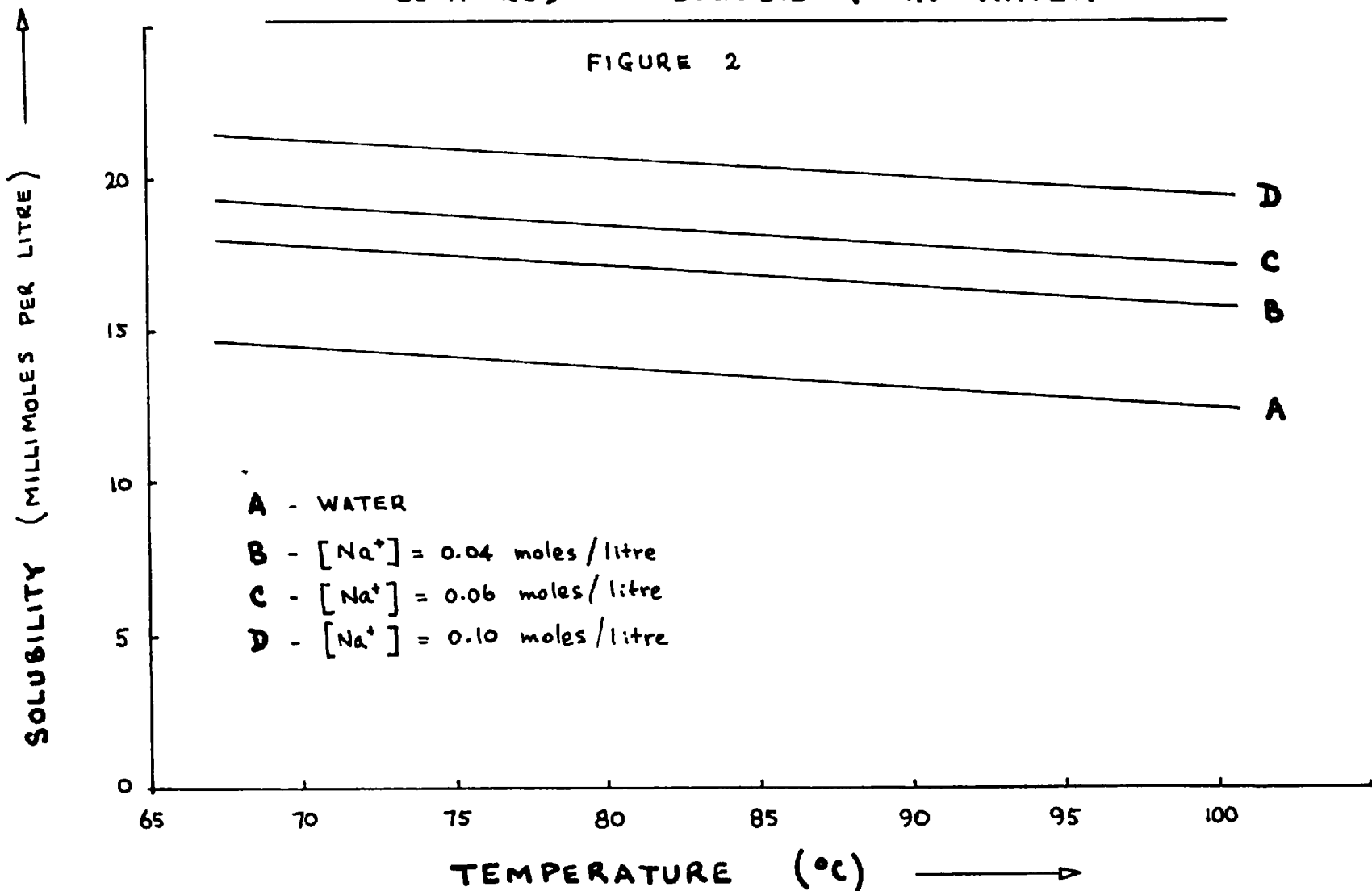
As figure 1 illustrates, the hemihydrate is unstable with respect to the other forms of calcium sulphate at all temperatures. At temperatures below about 40°C, the dihydrate is the most stable form; above this temperature insoluble anhydrite is the most stable form. However,

metastable forms can exist for quite appreciable periods in contact with solution. For example, Power and Fabuss³⁰ found that the dihydrate was stable in solutions up to 105°C for at least 72 hours. Also, the stability of the hemihydrate was found to vary with the difference between its solubility and that of the dihydrate, becoming more stable as this difference decreased. Thus, as the temperature increased, so did the stability until at 100°C no change in water content was detected after 48 hours in solution.

The solubility of calcium sulphate is often affected by the presence of other salts in the solution. In the present work, many of the solutions were prepared by mixing equimolar solutions of calcium chloride and sodium sulphate, producing two moles of sodium chloride for each mole of calcium sulphate. Although several studies on the solubility of calcium sulphate in sodium chloride solutions have been made, most of these were carried out at a few temperatures below 60°C, which was below the range of interest in the present work. However, Power and Fabuss³⁰ have reported solubilities at 10°C intervals in the range, 25°-95°C, and these have been used to calculate supersaturations in the present work. Power and Fabuss reported that the presence of sodium chloride in solution increased the solubility of all forms of calcium sulphate but that

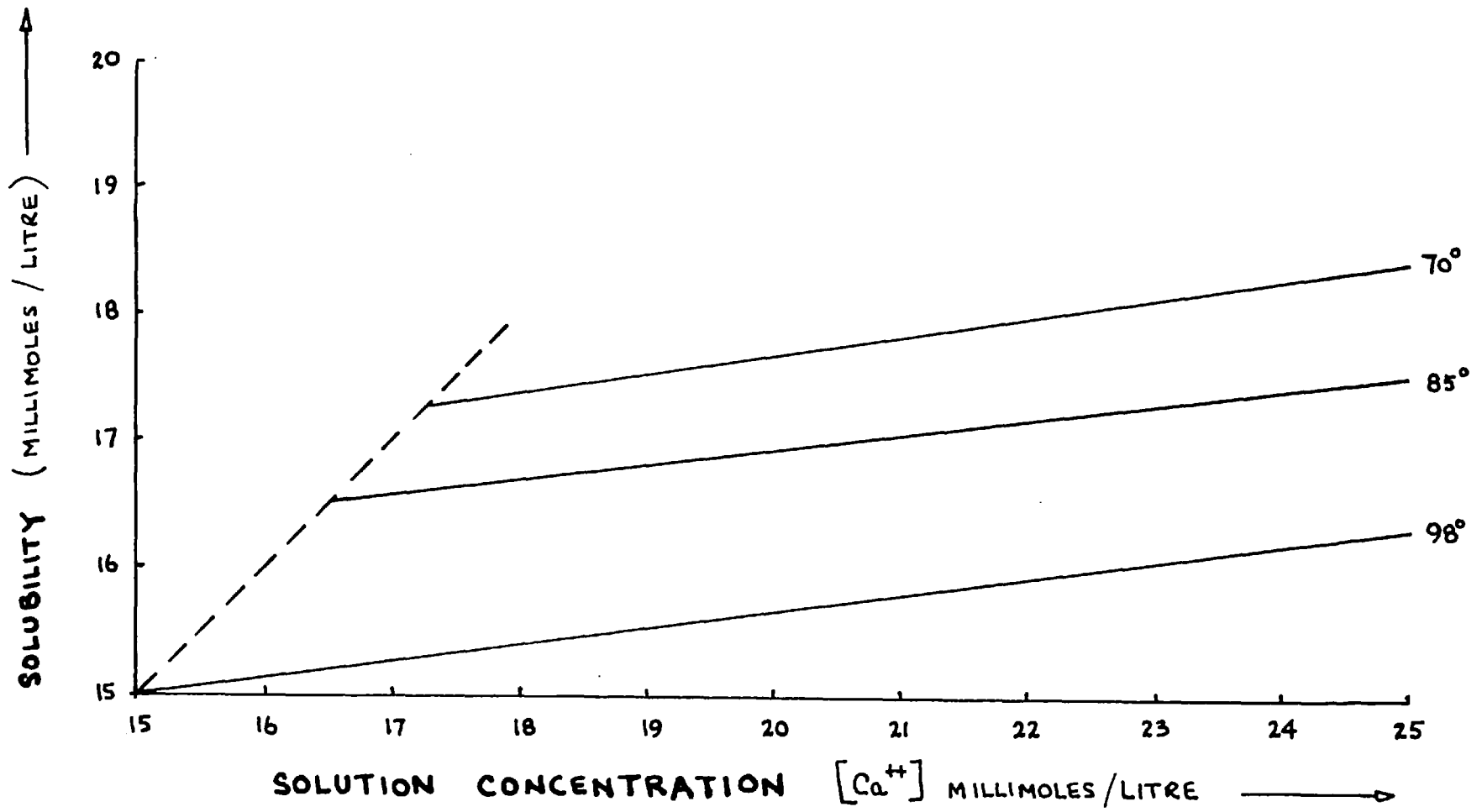
SOLUBILITY OF THE DIHYDRATE IN MIXED CALCIUM CHLORIDE AND
SODIUM SULPHATE SOLUTIONS (CALCULATED FROM REFERENCE 30)
COMPARED TO SOLUBILITY IN WATER

FIGURE 2



SOLUBILITY OF THE DIHYDRATE IN MIXED CALCIUM CHLORIDE AND SODIUM SULPHATE SOLUTIONS (CALCULATED FROM REFERENCE 30)

FIGURE 3



the temperatures at which the curves intersected were unchanged from those in figure 1. The solubility of the dihydrate calculated from these data is illustrated in figures 2 and 3. In figure 2, the solubility is plotted against temperature for three sodium chloride concentrations in the range of those in the present work, and this is compared to the solubility in water. In figure 3, the increase in solubility with solution concentration is illustrated at three temperatures.

2.3 Apparatus

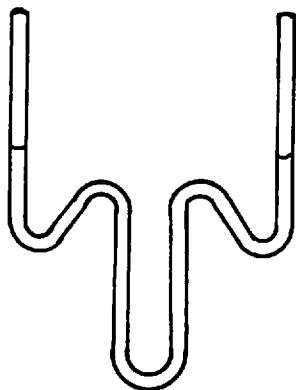
Most of the experiments in the present work were carried out in one of two similar constant temperature baths. The well-insulated glass tank contained about 12.5 litres of liquid paraffin and heat was supplied by a 1 kilowatt immersion heater in series with a variable resistance. The heater was regulated by an electronic relay actuated by a mercury-toluene thermoregulator. The bath was well-stirred so that temperature control was within ± 0.1 C^o under experimental conditions.

2.4 The Effect of Temperature and Supersaturation on the Relative Amounts of Dihydrate and Hemihydrate Formed in Solution.

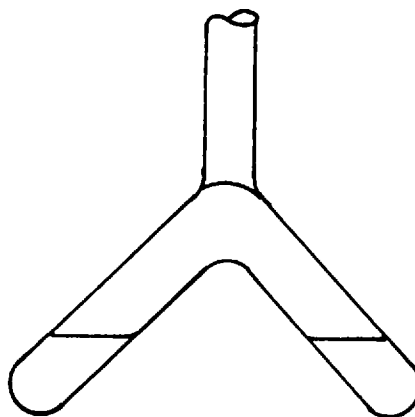
Although at temperatures above 40^oC, the most stable form of calcium sulphate in pure solutions is the

TUBES USED IN NUCLEATION EXPERIMENTS

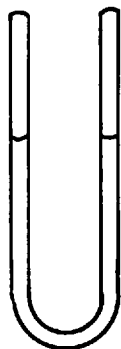
FIGURE 4



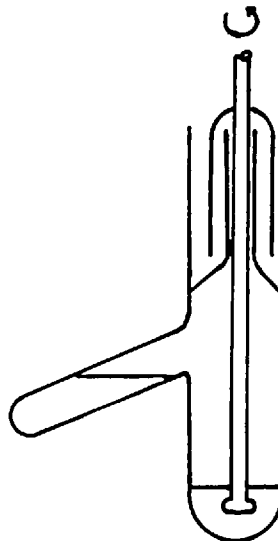
TYPE A TUBE



TYPE B TUBE



TYPE C TUBE



TYPE D TUBE

insoluble anhydrite, both hemihydrate and dihydrate can form in supersaturated solutions at these temperatures and remain relatively stable for long periods. A series of experiments was carried out in order to determine which hydrate(s) form under various conditions of temperature and supersaturation.

EXPERIMENTAL

From time to time throughout the present work, stock solutions of calcium chloride and sodium sulphate were prepared by dissolving the appropriate Analar reagent in distilled water. The concentration of the calcium chloride solution was determined by titration for calcium ion with EDTA, using Eriochrome Black T indicator. The concentration of the sodium sulphate solution was determined gravimetrically by precipitation of the sulphate ion as barium sulphate. Then equimolar solutions of calcium chloride and sodium sulphate of the desired concentration were prepared for each series of runs by dilution of a small volume of stock solution.

A number of glass tubes of two types, A and B (see figure 4), were prepared for use in these experiments, each tube being used only once. In A tubes, which were a minor modification of C tubes used in later experiments, any crystals forming on the solution surface were prevented from settling into the solution under observation in the

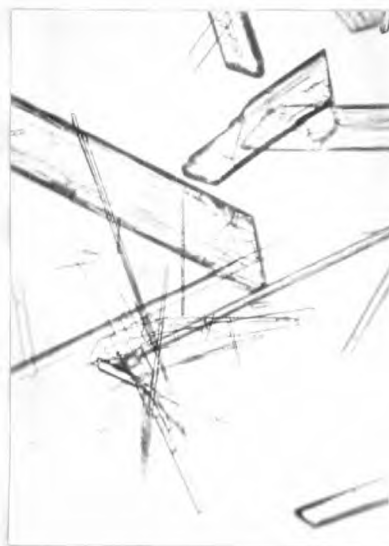
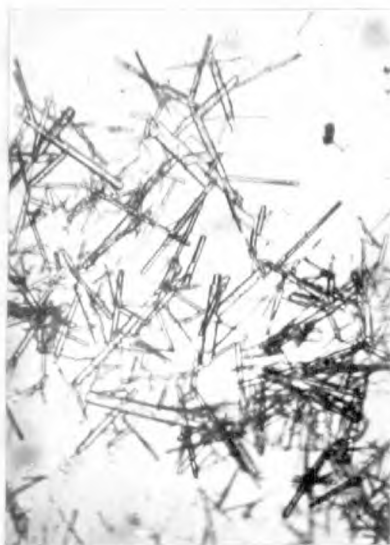
central arms of the tube. For this type of tube, equimolar solutions of calcium chloride and sodium sulphate were mixed at room temperature to give a calcium sulphate solution supersaturated with respect to the dihydrate, and in some cases to the hemihydrate also, at the temperature of the experiment. The solution was added to the tube which was then sealed and placed in the constant temperature bath. After a number of crystals had formed, the tube was removed from the bath and the contents were examined under a microscope. For B tubes, the equimolar solutions were added to separate legs of the tube which was then sealed and placed in the bath. After the solutions had reached bath temperature, the tube was tipped to mix them. Again, when a number of crystals had been observed to form, the tube was removed from the bath and the contents examined under a microscope.

The crystals produced in these runs were identified by general appearance and extinction angle between crossed polaroids. Some of the properties of hemihydrate and dihydrate are listed in Appendix 2. By observing up to a few hundred crystals in each sample, the relative amounts of each hydrate were estimated.

In these runs, temperatures were between 52° and 100°C , solution concentrations between 20 and 50 millimoles per litre, and the times at which the crystals were examined ranged from 7 to 195 minutes.

DIHYDRATE AND HEMIHYDRATE CRYSTALS

Figure 5



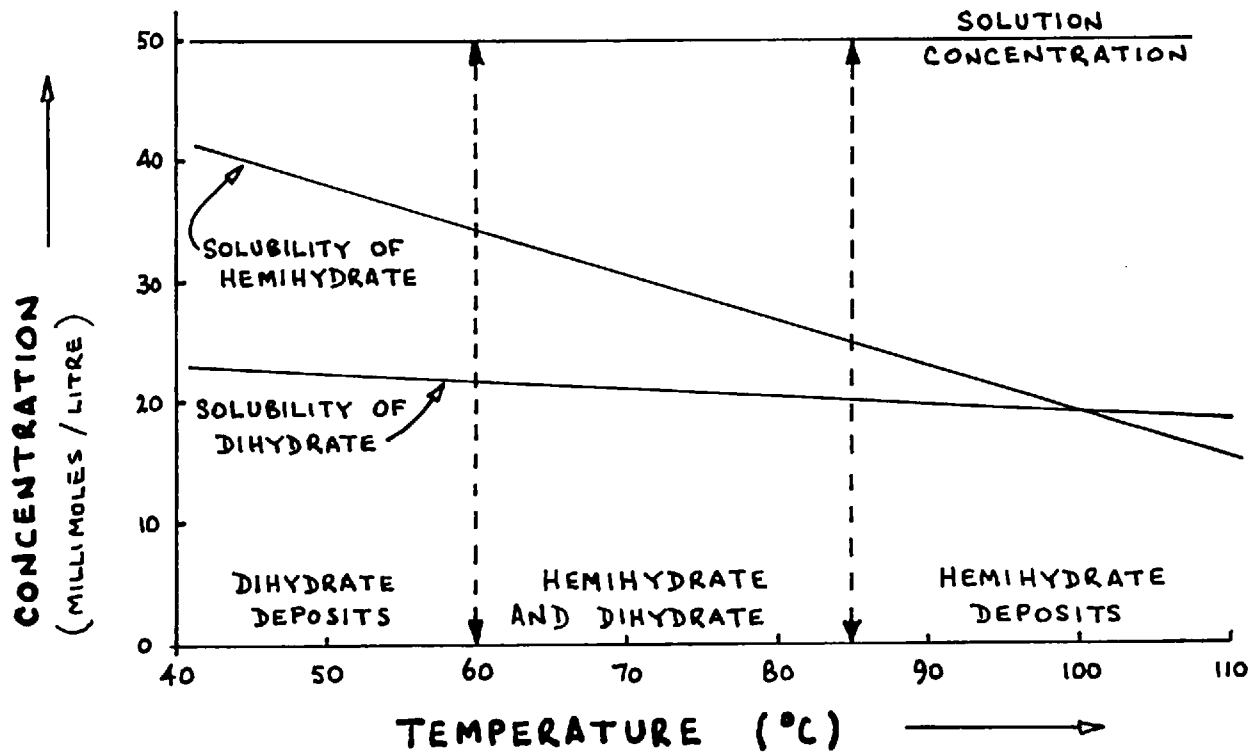
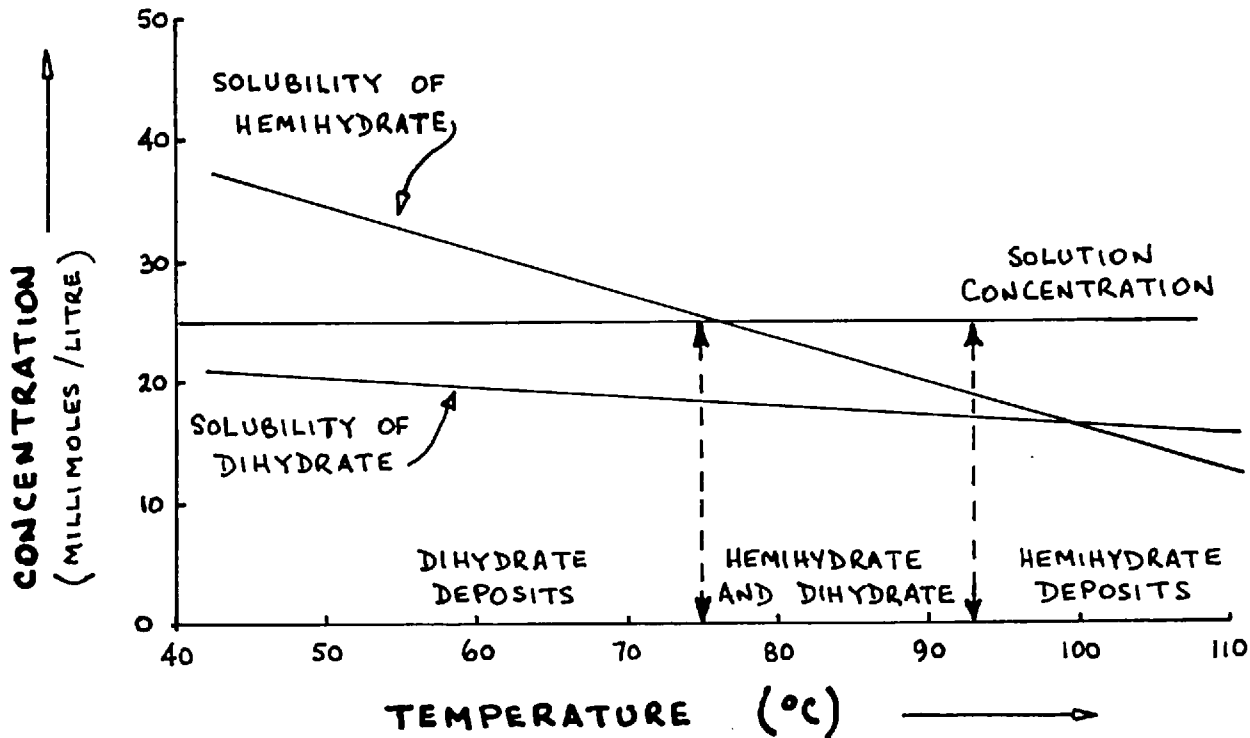
DIHYDRATE CRYSTALS (50x)



HEMIHYDRATE CRYSTALS (50x)

EFFECT OF SUPERSATURATION ON THE HYDRATE FORMED
 IN SOLUTIONS OF 25.0 AND 50.0 MILLIMOLES / LITRE

FIGURE 6



RESULTS

Photographs of some dihydrate and hemihydrate crystals produced in these and other experiments are shown in figure 5. It is evident from these that on the basis of general appearance alone, well-formed dihydrate and hemihydrate crystals can be readily distinguished. Also, since the extinction angle of the dihydrate is oblique and that of hemihydrate is parallel, even the most irregular crystals could be identified.

The results of these runs are listed in Table 1, Appendix 1. At high solution concentrations, there is a tendency to a higher proportion of dihydrate in A tubes. This is undoubtedly due to the occurrence of nucleation in these solutions before or during heat-up to the temperature of the experiment.

The results in B tubes indicate that for a particular solution concentration, there is a temperature range over which the form of calcium sulphate produced changes from the dihydrate to the hemihydrate. It appears that this change corresponds, to a certain extent, to the temperature at which the solution becomes supersaturated with respect to the hemihydrate. In figure 6, the hydrate produced is compared to the solubilities in these sodium chloride solutions as calculated from reference 30. In the 25 millimoles/litre solutions, it is apparent that when

the solution becomes even slightly supersaturated with respect to the hemihydrate, small amounts of this hydrate begin to form. At higher temperatures, the supersaturation with respect to the hemihydrate increases as does the proportion of hemihydrate in the deposit. When this supersaturation approaches that with respect to the dihydrate, the crystals formed are entirely hemihydrate.

In the 50 millimoles/litre solutions, this effect is less marked and the solution must be somewhat more than slightly supersaturated with respect to the hemihydrate before any is found in the deposit. However, at these lower temperatures, the hemihydrate is very unstable³⁰ and transformation to the dihydrate is likely.

Thus, in the temperature range of these runs, the dihydrate forms when the solution is supersaturated with respect to this hydrate only, and a mixture of the hemihydrate and the dihydrate forms when the solution is supersaturated with respect to both hydrates. In the latter case, the proportion of the mixture which is hemihydrate increases as the supersaturation with respect to hemihydrate increases until only the hemihydrate forms when the supersaturation with respect to both hydrates is approximately equal.

2.5 The Rate of Nucleation in Unstirred Calcium Sulphate Solutions

A study of the rate of nucleation of calcium sulphate was made in order to determine how quickly and at what supersaturations crystals of hemihydrate and dihydrate can be expected to form in the 70° to 110°C range. The formation of crystal nuclei is usually detected either by direct observation or by measuring the change in concentration of the solution during nucleation. In this study, the induction time, the time to produce visible crystals at a given supersaturation, was measured. The induction time is composed of two parts: the time for crystals to nucleate and the time for these crystals to grow to a visible size, and so is not strictly a measure of the nucleation rate alone. However, it is one of the simplest methods of defining the conditions of supersaturation under which crystals can be expected to form and, in this sense, the results are likely to be useful. This method is at least as good a measure of the rate of nucleation as that of measuring the decrease in solution concentration as nucleation occurs. A simple calculation shows that a decrease of only 10^{-6} moles per litre corresponds to about 40 gypsum crystals of length 10^{-2} cm. in the test volume of 0.5 cc. This size could be detected in the present experiments. In this connection, Lurie et al.¹⁵ observed

that a supersaturated calcium sulphate solution became cloudy with gypsum crystals before any concentration change was measured.

The induction time, ϕ_I , can be related to the rate of nucleation, the number of crystal nuclei produced per unit volume of solution per unit time, if we assume that approximately equal numbers of crystals have been produced in each run by the time the first crystal is detected and that the time for the nuclei to grow to visible size is proportional to the time for the formation of the nuclei. Then, equation 7 can be rewritten as:

$$\phi_I = B \exp \left[\frac{16\pi\sigma^3 M^2}{3kR^2 T^3 \rho^2 (\ln S)^2} \right] \quad (8)$$

$$\text{Since } \phi_I \propto \frac{1}{N} \quad (9)$$

It follows that:

$$\log \phi_I \propto \frac{1}{T^3 (\log S)^2} \quad (10)$$

Ideally in a nucleation study, it would be desirable to be able to produce a solution at the desired concentration and temperature precisely at the beginning of each run and to maintain these conditions until nucleation has been detected. In practice, however, this is not easy and generally either the temperature or the concentration must be altered suddenly at the beginning of the run, necessitating a transition period during which the unstable system attains the conditions of the experiment.

In the nucleation studies reported here, two methods were used. In the first, a solution of the desired concentration was prepared at room temperature and then heated rapidly to the temperature of the experiment. In the second, solutions of calcium chloride and sodium sulphate were heated separately to the temperature of the experiment and then mixed. Thus in these two methods, the temperature and the supersaturation respectively were suddenly changed at the beginning of the experiment.

2.5.1 Induction Times in Heated Solutions

EXPERIMENTAL

In these experiments, a solution was prepared at the desired concentration and rapidly heated to the temperature of the experiment. The solutions were prepared by heating Anelar calcium sulphate dihydrate at 300°C for 10 minutes, dissolving the hemihydrate so formed in distilled water, and immediately filtering the solution to remove the undissolved salt. In this way, it was possible to prepare a solution supersaturated with respect to the dihydrate which would remain stable for several hours, providing the supersaturation was not too great.

A number of glass tubes of two types, A and C (see figure 4) were prepared, each tube being used only once. As explained in the previous section, the A tubes

were slightly modified C tubes in which any crystals forming on the solution surface were prevented from settling into the solution under observation in the central arms of the tube. Both types of tubes were prepared from 0.2 cm. diameter pyrex glass tubing which was previously cleaned with chromic acid cleaning mixture.

Before each run, a volume of solution was filtered through a sintered glass filter. For solutions in C tubes, a porosity 3 filter was used. This removed particles larger than 30 microns. For solutions in A tubes, a porosity 4 filter removed particles larger than 10 microns. The concentration of the solution was determined by an EDTA titration for calcium ion.

About 0.5 ml. of solution was placed in the tube, the ends were sealed and the tube placed in the constant temperature bath. The tubes, illuminated with a 150 watt light source, were observed by means of a travelling microscope so that crystals of 10^{-2} cm. in length could be easily detected. The time of detection of the first crystal was recorded for solution concentrations between 12.3 and 30.0 millimoles per litre and temperatures in the range, 70°-110°C.

In a few runs, a copper-constantin thermocouple was inserted into the tube to determine the time required for heat-up of the solution.

RESULTS

In all of these experiments, the crystals deposited were acicular, becoming increasingly so at high supersaturations. Also at high supersaturations, there was a tendency to form random clusters of crystals radiating from a common point. Generally, the crystals were first observed in the bulk of the solution, later settling to the tube bottom and walls and becoming loosely attached there. Only occasionally, when the supersaturation was low, were they observed initially on the tube walls and it is not clear whether the nucleation actually occurred on the wall or elsewhere because of the very few crystals present.

Although both types of tubes were completely sealed before immersion in the constant temperature bath, crystals were frequently produced in the thin film of solution on the glass wall just above the solution surface, because of a slight amount of evaporation from the film into the air space during heat-up. Occasionally, some of these crystals broke away from the solution surface and settled down through the solution. In type C tubes, these crystals, when they formed, interfered with measurements of the induction time. In type A tubes, any such crystals were trapped in the side arms and therefore did not affect the induction times.

Measurement of the temperature of the solution at various stages of heat-up indicated that it rose from room temperature to within 1 C° of the bath temperature in about 45 seconds after immersion of the tube in the bath. A heat balance on the system indicated that the change in temperature during heat-up could be represented by the following equation:

$$\ln \frac{T_B - T_0}{T_B - T} = \frac{U A_H}{c_s \rho_s V} \phi \quad (11)$$

where T is the temperature of the solution ($^{\circ}\text{K}$) at time ϕ (seconds); T_0 is the initial solution temperature at $\phi = 0$; T_B is the bath temperature; U is the overall heat transfer coefficient ($\text{cal. cm}^{-2} \cdot \text{sec}^{-1} \cdot ^{\circ}\text{C}^{-1}$); A_H is the surface area for heat transfer (cm^2); c_s is the specific heat of the solution ($\text{cal. gm}^{-1} \cdot ^{\circ}\text{C}^{-1}$); ρ_s is the density of the solution (g. cm^{-3}) and V is the volume of the solution (cm^3). Substitution into equation 11 of the temperatures measured at various times during heat-up allowed calculation of U ($2.6 \times 10^{-3} \text{ cal. cm}^{-2} \cdot \text{sec}^{-1} \cdot ^{\circ}\text{C}^{-1}$). Equation 11 then becomes for these tubes:

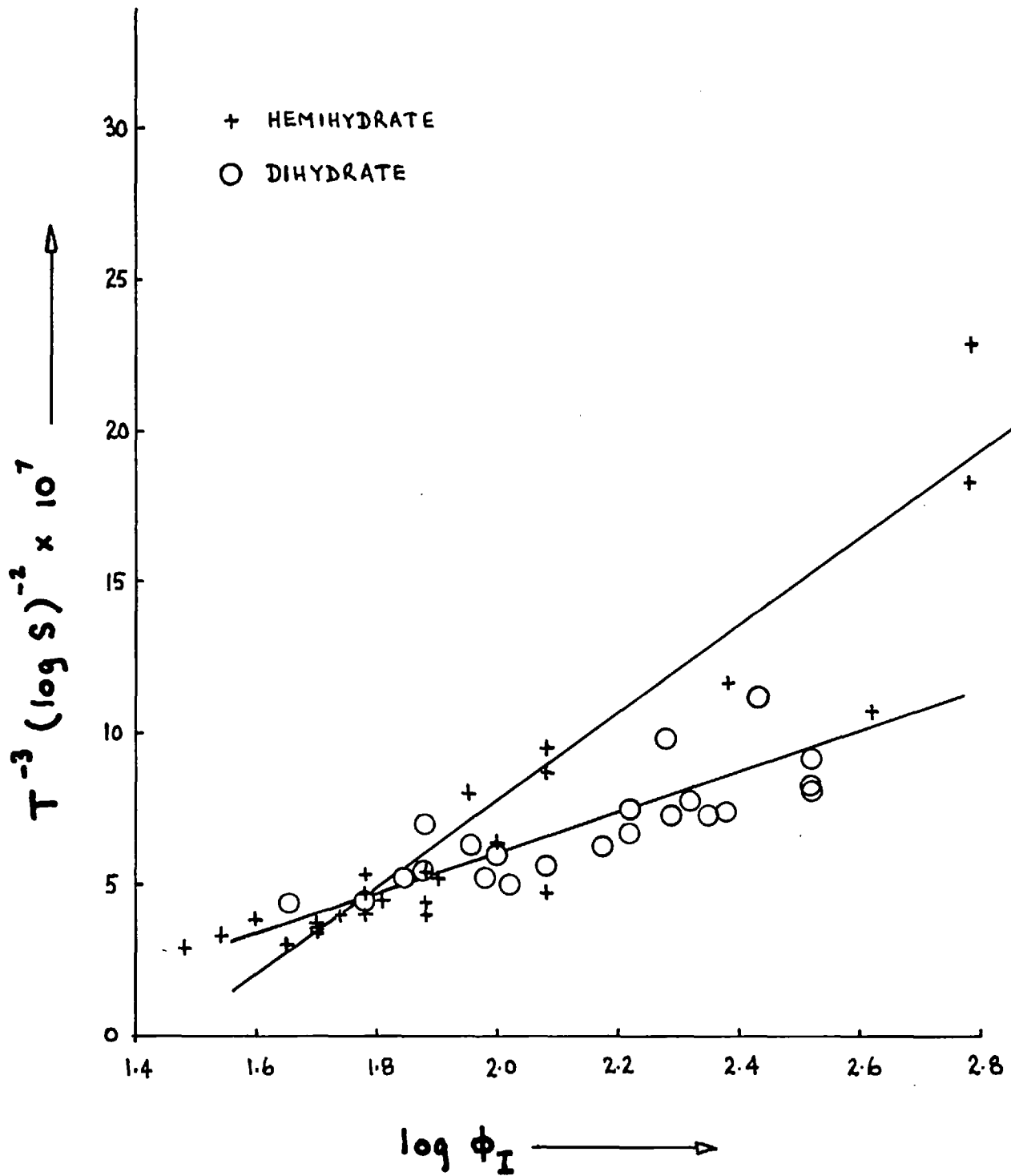
$$\phi = 10.8 \ln \frac{T_B - T_0}{T_B - T} \quad (12)$$

$$\text{or } T = T_B - (T_B - T_0) e^{-0.09 \phi} \quad (13)$$

Although this time for heat-up was a small fraction of the induction time in most of the runs, it was certainly

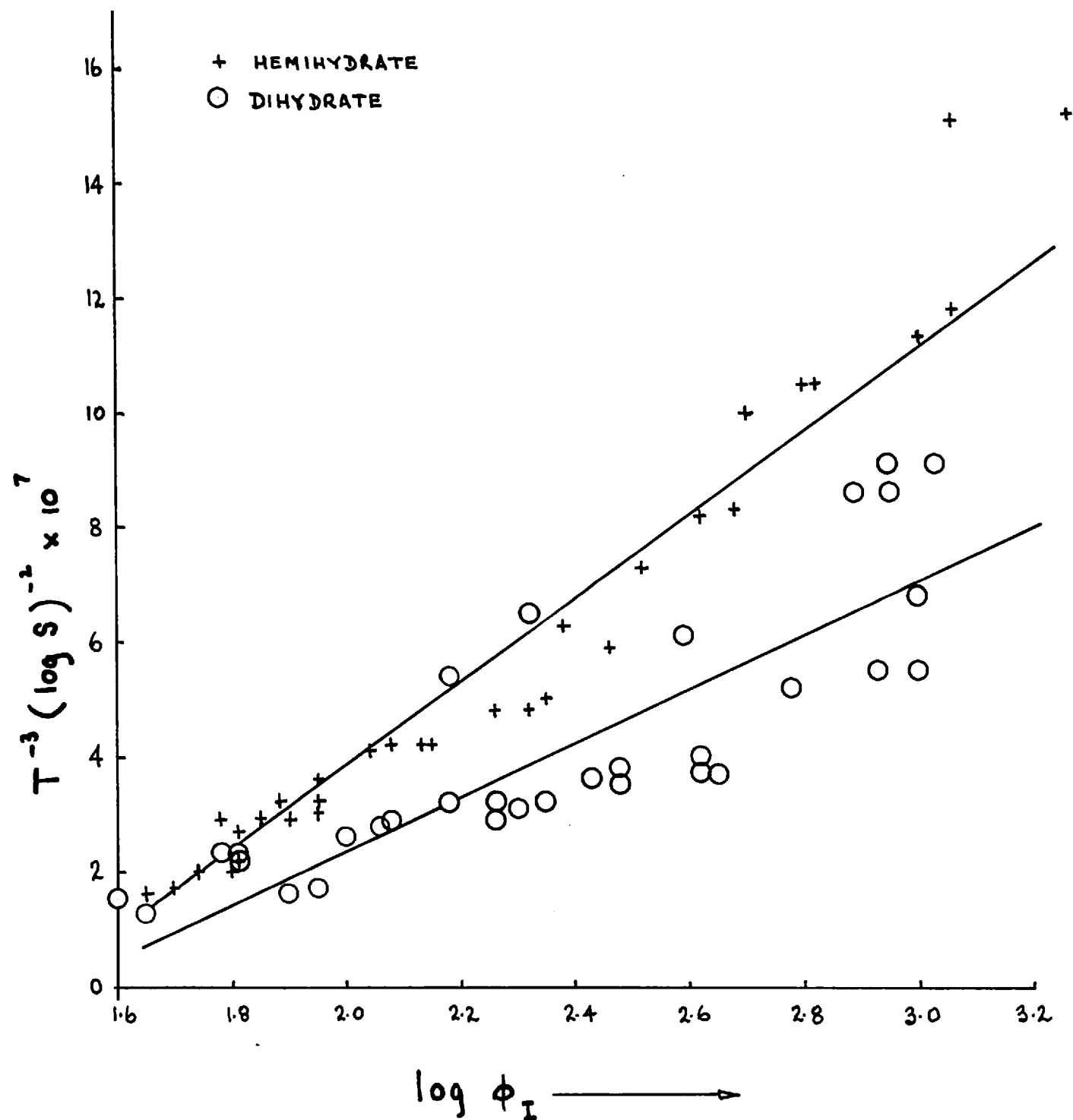
INDUCTION TIMES IN C TUBES

FIGURE 7



INDUCTION TIMES IN A TUBES

FIGURE 8



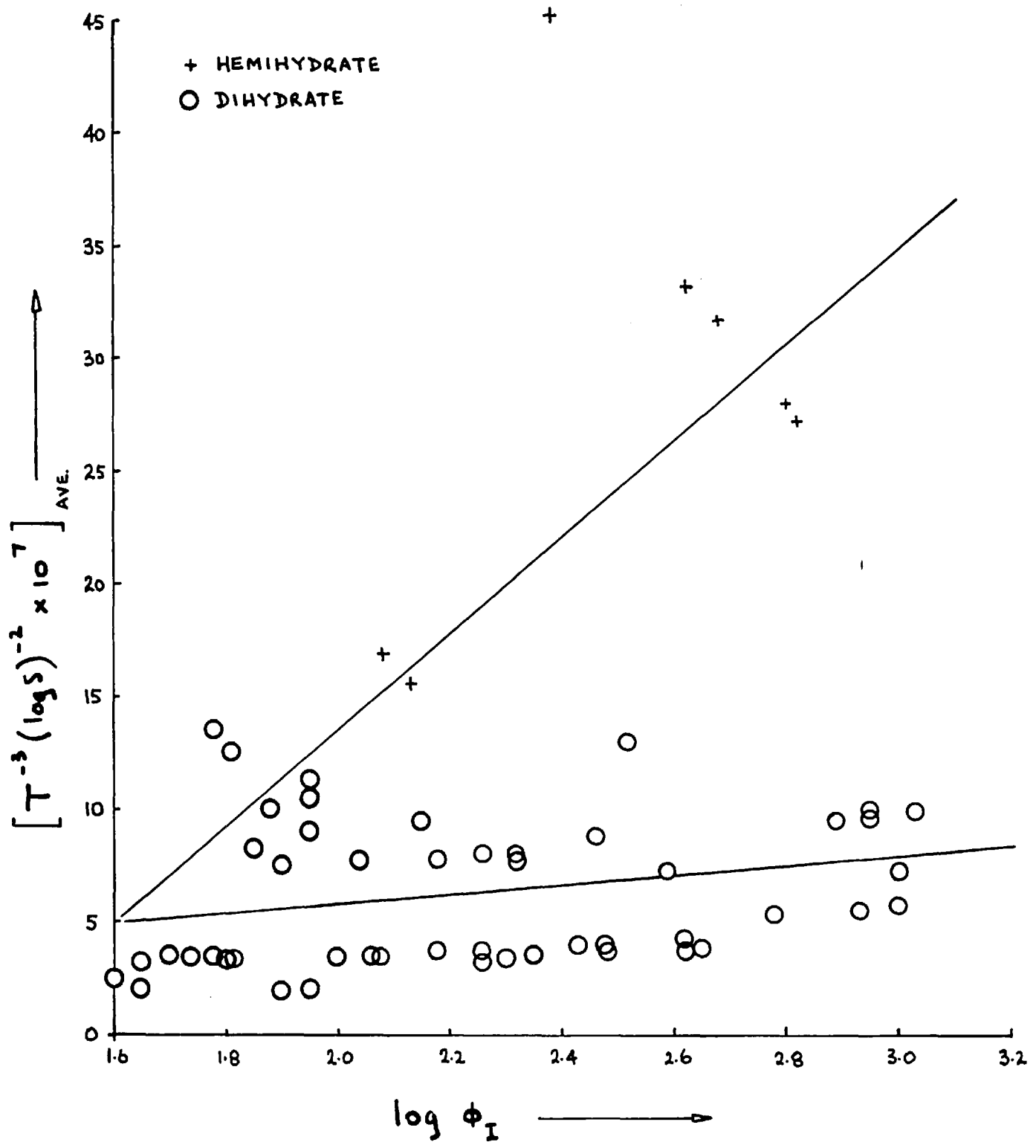
appreciable at the higher supersaturations and, because of the changing supersaturation during heat-up, it had to be taken into account in the analysis of the results.

The solubilities of the dihydrate and the α hemihydrate from figure 1 were used in the analysis of the results. For any particular solution temperature, the lower of the two solubilities was used. Thus, the solubility of the dihydrate was used at temperatures below 98°C (the intersection of the two solubility curves) and the solubility of the hemihydrate above this temperature.

The results of these experiments in C and A tubes are listed in tables 2 and 3 respectively. In figures 7 and 8, $T^{-3}(\log S)^{-2}$ is plotted against $\log \phi_I$ (see equation 10) assuming that the solution was at the bath temperature throughout the run. However, since this was not the case, an attempt at taking the heat-up period into account was made. Firstly, for each of the runs in A tubes, the value of $T^{-3}(\log S)^{-2}$ was calculated for various times during heat-up, using equation 13 with the solubility of the dihydrate below 98° and that of the hemihydrate above 98° . These values were plotted against ϕ and a graphical integration was performed between $\phi = 0$ and $\phi = \phi_I$ to give an average value of $T^{-3}(\log S)^{-2}$ for the run. Secondly, an average solution temperature was calculated for the run by combining equation 13 with the following equation:

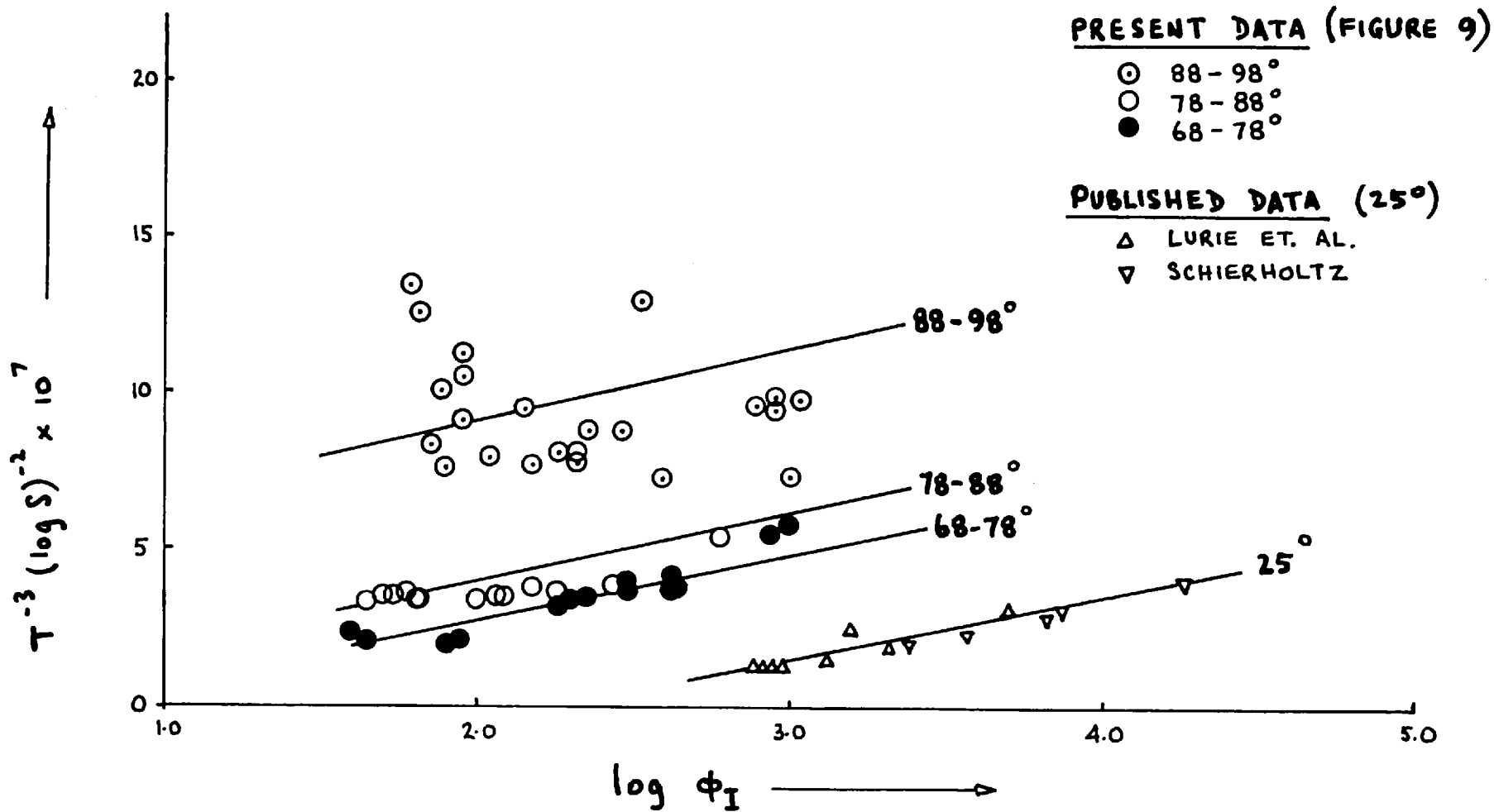
INDUCTION TIMES IN A TUBES WITH HEAT-UP CORRECTION

FIGURE 9



COMPARISON OF DIHYDRATE INDUCTION TIMES
AT VARIOUS TEMPERATURES

FIGURE 10



$$T_{\text{ave}} = \frac{1}{\Phi} \int_0^{\Phi_I} T d\Phi \quad (14)$$

resulting in the following equation:

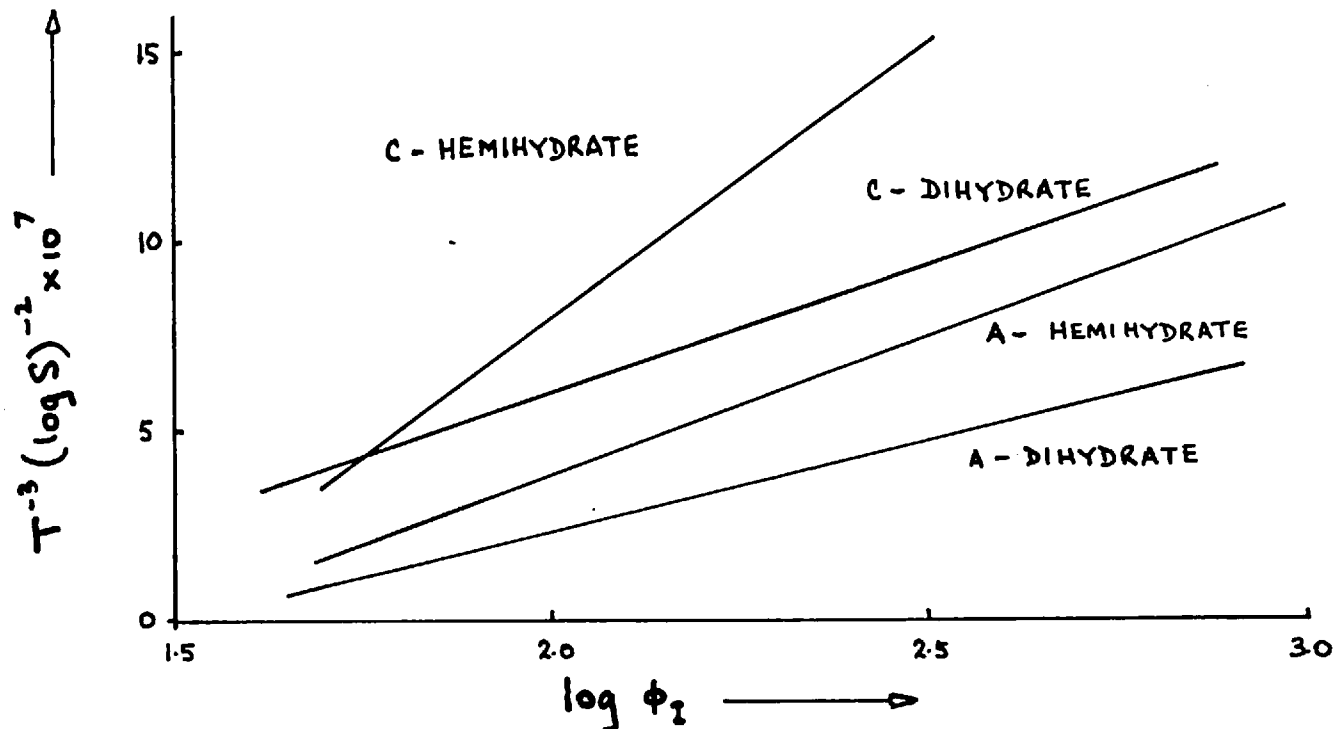
$$T_{\text{ave}} = T_B - \frac{10.8(T_B - T_0)}{\Phi_I} \left[1 - e^{-0.09\Phi_I} \right] \quad (15)$$

This equation indicates that not until about 10 minutes after immersion is the average solution temperature within 1 C° of the bath temperature. The results of these two calculations for the runs in A tubes are listed in table 4 and illustrated in figure 9.

Figures 7, 8 and 9 indicate that the induction times can be reasonably well represented by an equation of the form of equation 10, although it appears that the effect of temperature is not completely accounted for by an equation of this type. For instance, the induction times for the dihydrate illustrated in figure 9 show some scatter and when these were divided into three groups according to the average solution temperature: 68°-78°, 78°-88° and 88°-98°, the results illustrated in figure 10 were obtained. (The induction times obtained by Lurie et al.¹⁵ and Schierholz¹⁶ for the dihydrate in stirred simple calcium sulphate solutions at 25°C are also included in this figure for comparison.) It is apparent from this figure that the induction time is still dependent on temperature, but it can be described by an equation of the form of equation 10 over a relatively short temperature range.

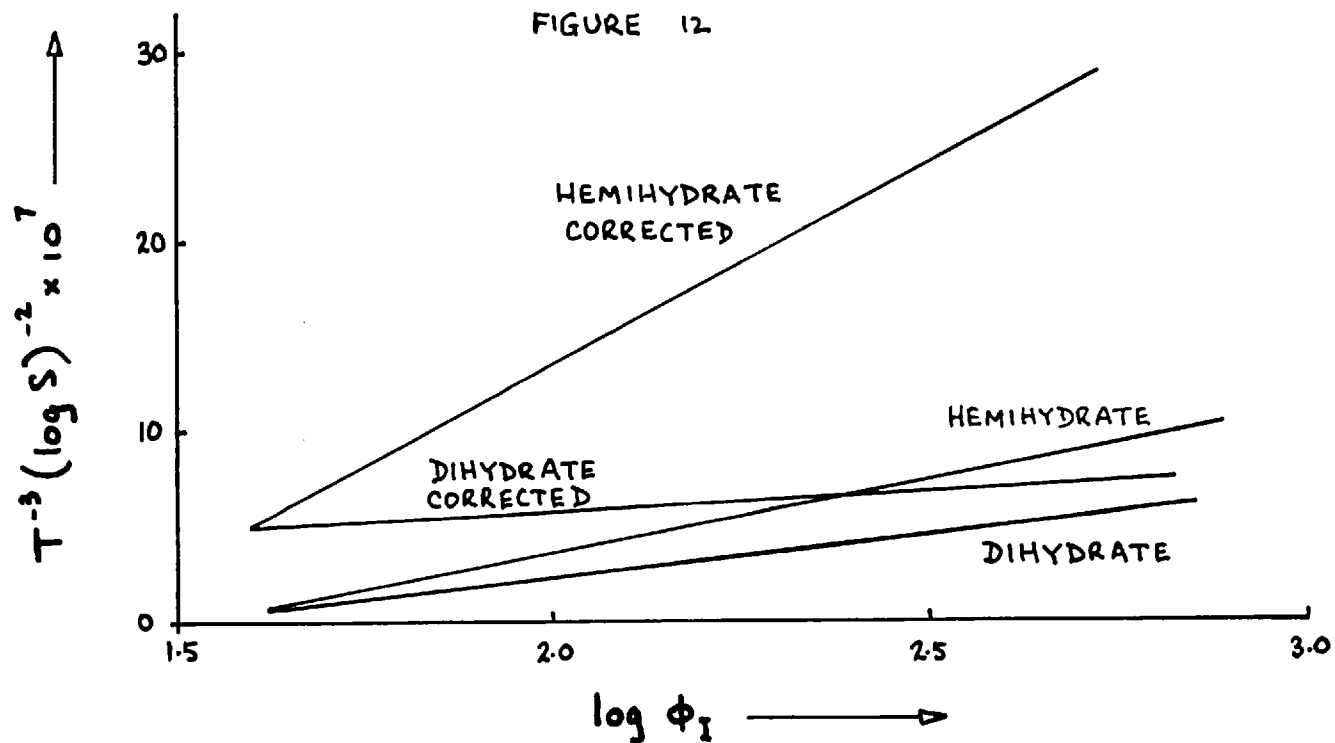
COMPARISON OF INDUCTION TIMES IN A AND C TUBES

FIGURE 11



COMPARISON OF INDUCTION TIMES IN A TUBES WITH AND WITHOUT HEAT-UP CORRECTION

FIGURE 12



Figures 7, 8 and 9 show that the induction times for the hemihydrate (temperature greater than 98°) are less than those for the dihydrate (temperature less than 98°) for comparable supersaturations. This may be due in part to the faster growth rate of the hemihydrate (see Chapter 4).

In figure 11, the results in C and A tubes are compared and it is evident that the induction times in the former tubes are much shorter. There are two possible reasons for this. In the first place, the solutions prepared for A tubes were filtered with a finer filter (porosity 4) than that used for the solutions prepared for C tubes (porosity 3). This may have resulted in the removal from the former solutions of a greater number of foreign particles which could induce nucleation. Secondly, the A tubes were designed to prevent crystals from the solution surface settling into the solution and interfering with the measurement of the induction time. This too would tend to give longer induction times in the A tubes.

In figure 12, the results in A tubes with and without correction for heat-up are compared. Since during heat-up, the solution temperature and supersaturation are less than the bath temperature and corresponding supersaturation, the results corrected for heat-up lie above the uncorrected results in this figure.

The results of these experiments indicate that in this temperature range, small degrees of supersaturation are sufficient to cause nucleation. When the supersaturation S is about 2, nucleation occurs almost instantaneously; at a supersaturation of 1.2, the induction time is 30 minutes or less. Thus, in order to prevent nucleation, the supersaturation of the solution must be kept well below this value.

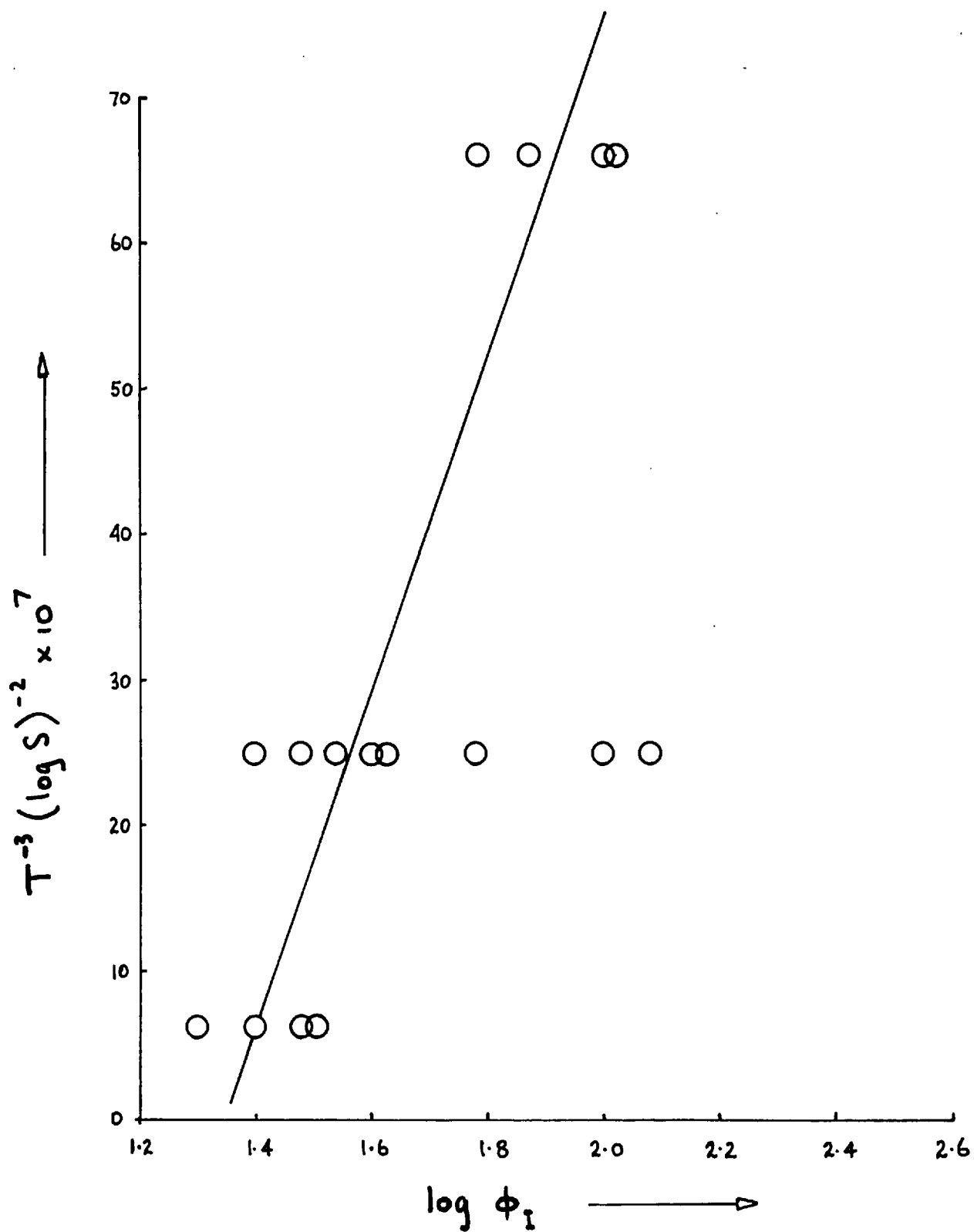
2.5.2 Induction Times in Mixed Solutions

EXPERIMENTAL

In these experiments, equimolar solutions of calcium chloride and sodium sulphate were heated separately to 100°C and then mixed. The solutions were prepared by dilution of the appropriate stock solutions which were prepared as outlined in section 2.4. A number of type B glass tubes (see figure 4) were constructed from 0.7 cm. diameter pyrex glass tubing which had been cleaned with a chromic acid cleaning mixture, and 0.5 ml. of each of the solutions was introduced into the separate legs of the tube using a pipette with a long tip. The opening in the tube was sealed and the tube placed in the constant temperature bath. Temperature measurement during heat-up indicated that the solution required 5 minutes to reach bath temperature and therefore, a 10 minute period was

INDUCTION TIMES IN B TUBES

FIGURE 13



allowed for heat-up in these experiments. The tube was then tipped to mix the solutions in one leg and the solution was observed with a travelling microscope. The time of detection of the first crystal was recorded. In these experiments, solution concentrations were between 17.5 and 25.0 millimoles per litre and the temperature was 100°C.

When a number of crystals had formed, the tube was removed from the bath and the contents examined under a microscope. The form of calcium sulphate was identified by refractive index and extinction angle.

RESULTS

The crystals deposited at all solution concentrations at 100°C were entirely hemihydrate needles. Again, as in section 2.5.1, the crystals were usually observed first in the bulk of the solution, later settling to the glass walls. Crystals also tended to form at the solution surface as noted in the previous section, but these did not appear to settle into the bulk of the solution during the induction time.

The results of these experiments are listed in table 5 and illustrated in figure 13. It is evident that the induction times in these experiments are much shorter than those for solutions of similar supersaturations reported in section 2.5.1. For example, at an S of 1.5, the induction time in mixed solutions was about 25 seconds

compared to about 46 seconds in the simple calcium sulphate solutions; at an S of 1.3, the corresponding induction times were 30 seconds (mixed) and 115 seconds (simple).

The reason for such a large difference between the two sets of results is not clear. Filtering of the calcium chloride and sodium sulphate solutions does not appear to have an effect on the induction time. A porosity 3 sintered glass filter was used to filter the solutions for all of these runs except run 183. In this run, a porosity 4 filter was used but no significant difference in the induction time was observed. Nor can the difference be attributed to insufficient correction for heat-up time in the previous results since any correction applied would primarily affect the shorter induction times and give a flatter, rather than a steeper line.

It might be argued that the technique of mixing calcium chloride and sodium sulphate solutions to prepare the calcium sulphate solutions for these runs could have temporarily produced abnormally high supersaturations in some regions of the solution (because of non-uniform mixing), thus causing premature nucleation. However, this would not be expected to occur in all of the runs especially in those at the lower supersaturations, and since the induction times were invariably shorter in these runs than in those reported in the previous section it seems that

non-uniform mixing belongs to the class of possible but not probable causes of reduced induction times.

It appears more likely that the sodium chloride present in these solutions is responsible for the reduced induction times of the hemihydrate. In this connection, Lurie et al.¹⁵ have reported that the induction time for the dihydrate in mixed calcium chloride and sodium sulphate solutions is shorter than that in simple calcium sulphate solutions at the same supersaturation. An equivalent result has also been obtained by Schierholtz¹⁶ who found that the addition of sodium chloride to a supersaturated calcium sulphate solution at 25° had negligible effect on the induction time for dihydrate even though the solubility had been increased by the addition. If sodium chloride does in fact induce the nucleation of calcium sulphate, this suggests that very slight supersaturations would be sufficient to cause nucleation in sea water brines.

2.6 The Rate of Nucleation in Stirred Calcium Sulphate Solutions

EXPERIMENTAL

In order to determine the effect of agitation on the rate of nucleation of calcium sulphate, a few experiments were carried out at 100°, in which the solution was stirred. Type D tubes, illustrated in figure 4, were used

in these experiments and the calcium chloride and sodium sulphate solutions were prepared and added to the separate legs of the tube as described in section 2.5.2. A glass stirring rod with small paddles was inserted into the tube and connected to a small stirring motor. The tube was then immersed in the constant temperature bath and after a 10 minute heat-up period, stirring at about 200 r.p.m. was started in the solution in the main tube. The tube was tipped to mix the two solutions, the stirring being continued during mixing and until the first crystal was detected with a travelling microscope.

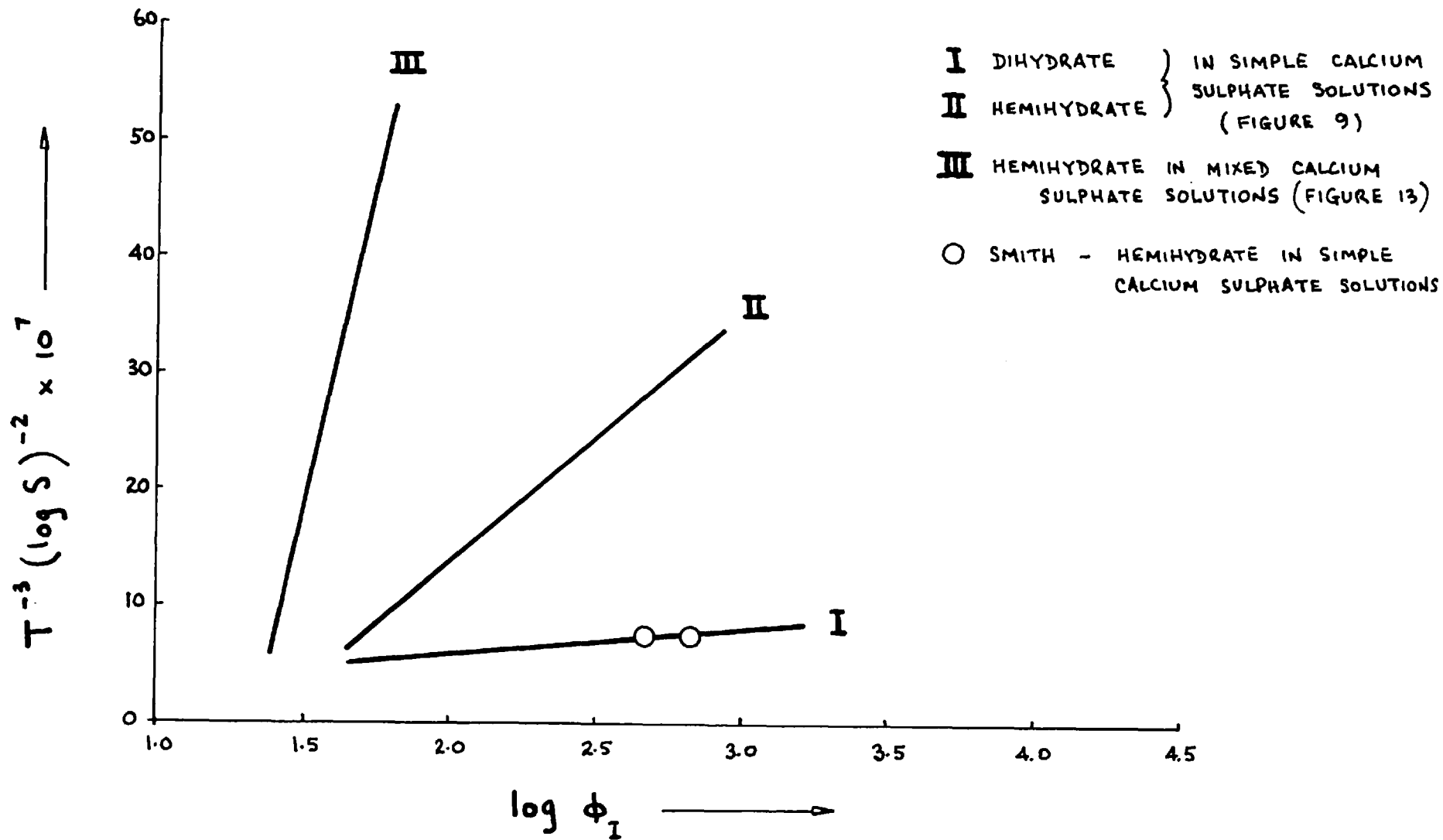
Of the four types of tubes used in the nucleation experiments, only the D tubes were used for more than one run. After each run, the solution was removed and the tube was filled with distilled water for several hours to dissolve any crystals of calcium sulphate present. Then the tube was cleaned with a chromic acid mixture, rinsed and dried ready for reuse.

RESULTS

The results of these experiments, all of which were carried out at a single solution concentration of 22.0 millimoles per litre, are listed in table 6. Although a few other runs were carried out at lower concentrations, the results were inconclusive because of the difficulty of preventing crystals, which formed at the solution surface,

COMPARISON OF INDUCTION TIMES TO PUBLISHED DATA

FIGURE 14



from becoming entrained in the stirred solution and interfering with the measurement of the induction time. In the experiments listed in table 6, crystals were observed in the solution before any were detected on the solution surface. These induction times are generally shorter than those reported for unstirred solutions in section 2.5.2, indicating that stirring increases the rate of nucleation.

In figure 14, the induction times reported in the previous sections are compared to the published data for the hemihydrate. Several studies on the nucleation of the dihydrate at 25° have also been reported in the literature^{15,16,40}; on a plot of this type, these induction times are about 100 times longer than those obtained for the dihydrate in the present work (see figure 10) but since figure 10 indicates that the effect of temperature on induction time is not completely eliminated in such a plot (the time increases as the temperature decreases), the published data for the dihydrate have little relevance to the present results. In figure 14, the data of Smith⁴¹ for the nucleation of hemihydrate in unstirred simple calcium sulphate solutions at 105°C are plotted. These induction times are seen to be about 10 times those for the hemihydrate in the present work, as represented by line II. Since the solution temperature was approximately the same in the two cases, the difference cannot be ascribed to

this factor. In addition, the filtering procedure used for the solutions in the present work appears to be at least as good as that employed by Smith and therefore it is unlikely that the relatively longer induction times obtained in the latter investigation can be attributed to a more complete removal of foreign particles from the solutions. While in the present work, no definite conclusions could be reached on the effect of filtering simple calcium sulphate solutions, the use of a finer filter for mixed solutions apparently had no effect on induction time.

At least part of the difference between the published data and the present results may be due to the methods used to detect the onset of nucleation. In the present work, crystals 0.01 cm. long could be easily detected and it is probable that in many runs, the crystals were even smaller when first observed. The sighting of the first crystal was taken as evidence of nucleation although in most runs, several crystals were observed at the induction time. The detection method used by Smith involved measurement of the solution concentration and, as discussed in section 2.5, a considerable number of crystals would be produced by the time the solution concentration had dropped appreciably. It seems then that the longer induction times reported by Smith may be partly attributed to a later detection of crystals in the solution.

Although the present work has raised several questions on the factors affecting the formation of calcium sulphate nuclei in a solution, it was not possible to make an exhaustive study of them and measurements of the growth rate of calcium sulphate dihydrate and hemihydrate were begun.

2.7 Summary

In a solution supersaturated with respect to all forms of calcium sulphate, a mixture of dihydrate and hemihydrate crystals was observed to form after some time. The composition of this mixture depended largely on the relative supersaturation with respect to each hydrate. Relatively slight degrees of supersaturation with respect to the hemihydrate were sufficient to cause its deposition and as this supersaturation approached that with respect to the dihydrate (as the temperature approached 100°), the fraction of the mixture as hemihydrate became unity.

In measurements of the rate of formation of calcium sulphate crystals, dihydrate and hemihydrate were detected at times ranging up to 30 minutes for supersaturations down to 1.2. In these experiments, the hemihydrate had a lower induction time than the dihydrate for solutions of the same supersaturation. In mixed calcium chloride and sodium sulphate solutions, the induction time for

hemihydrate was much shorter being less than 2 minutes for supersaturations of 1.1, and stirring the solution reduced this time even further. These results provide information on the rate of nucleation in calcium sulphate solutions in the temperature range, 70° - 110° C, for which little data has previously been published.

In these experiments, the crystals almost invariably appeared first in the bulk of the solution, later settling to the walls of the container. Both the dihydrate and the hemihydrate formed needle-like crystals which deposited individually or in clusters depending on the supersaturation.

CHAPTER 3THE GROWTH RATE OF DIHYDRATE CRYSTALS3.1 Introduction

Once a crystal greater than the critical size has nucleated in a supersaturated solution, it will begin to grow. Having reported measurements on the rate of formation of nuclei of calcium sulphate dihydrate and hemihydrate in Chapter 2, the next two chapters will be concerned with a study of the rates of growth of single crystals of these two hydrates.

The deposition of solute from a supersaturated solution onto a crystal surface is generally considered to occur in two consecutive steps. In the first, dissolved solute is transported from the bulk of the solution to the surface of the growing crystal (mass transfer) and in the second, the solute atoms become incorporated into the lattice of the crystal (surface reaction). The rate of mass transfer can be expressed in an equation of the form:

$$\frac{dn}{dt} = k_m A (c - c_i) \quad (16)$$

where n is the number of moles of solute transferred in time t ; k_m is the coefficient of mass transfer; A is the surface area of the crystal; c is the concentration of solute in the bulk of the solution and c_i is the concentration of solute at the crystal-solution interface. Although complex expressions for the rate of the surface

reaction have been proposed, it can be most conveniently approximated to an expression in terms of a simple power of the concentration difference, $c_i - c^*$:

$$\frac{dn}{dt} \sim k_r A (c_i - c^*)^p \quad (17)$$

where k_r is the surface reaction coefficient; c^* is the solubility of the solute in solution and p is a constant.

In connection with mass transfer, equation 16 states that the rate varies linearly with the concentration difference, $c - c_i$, providing k_m is constant with respect to supersaturation. A number of theories have been advanced on the mechanism of mass transfer of solute to the crystal surface and from these, expressions for k_m have been derived. Nernst⁴² suggested that there was a thin laminar film of solution next to the crystal surface which provided the major resistance to mass transfer by diffusion. In this case, the value of k_m was given by:

$$k_m = \frac{D}{\delta} \quad (18)$$

where D is the diffusion coefficient of the solute and δ is the thickness of the laminar film. On the other hand, Higbie⁴³ proposed the penetration theory, later modified by Danckwerts⁴⁴, in which elements of solution from the bulk approached the crystal-solution interface and remained there for some time interval, during which mass transfer from the solution element to the crystal surface took place

and after which the element was replaced by a fresh element of solution from the bulk. The value of k_m in this case was given by:

$$k_m = (D.f)^{\frac{1}{2}} \quad (19)$$

where f is the fractional rate of surface renewal. More recently, a film-penetration theory combining the elements of both theories has been proposed by Toor and Marchello⁴⁵. A more complicated expression has been derived for k_m in this case, but at short contact times this reduces to equation 19 (penetration theory) and at long contact times to equation 18 (film theory). Whichever of these theories is assumed to apply, D and δ (or f) must be constant with respect to supersaturation in order for k_m to be a constant in equation 16.

When the solute atoms have reached the crystal surface, they may then attach themselves and become a part of the crystal lattice. Volmer⁴⁶ suggested that this surface reaction step involves adsorption of solute atoms to the crystal surface and migration of these adsorbed atoms to positions where the attractive forces to the atoms of the crystal lattice are greatest. When each layer of the lattice is completed, a new layer is begun by a process of two-dimensional nucleation of the solute atoms on the completed layer. Further atoms adsorb to the surface and migrate to this nucleus and thus begin to build a new layer

onto the crystal lattice.

If growth proceeds by this mechanism, a considerable degree of supersaturation would be required for the creation of the nucleus of each new layer. However, it has been suggested by Frank⁴⁷ that for many crystals, it is unlikely that this two-dimensional nucleation is necessary because of the presence of imperfections in the crystal lattice. One example of these is the screw dislocation which provides a continuous imperfection through the lattice as the crystal grows. The adsorbed atoms can migrate to this imperfection and as the layer is never actually completed, there is no need for two-dimensional nucleation. Growth can therefore proceed at a lower supersaturation.

When steady state conditions are reached in crystal growth, the rate of mass transfer from the solution to the interface equals the rate of the surface reaction. The overall rate of solute transfer from the bulk solution to the crystal lattice must also be equal to the rates of the individual processes, and can be written:

$$\frac{dn}{dt} = KA(c - c^*) \quad (20)$$

where K is the overall coefficient for solute transfer. K is generally not a constant with respect to supersaturation, as is shown below. Combining equations 16, 17 and 20 gives:

$$K(c - c^*) = k_m(c - c_i) = k_r(c_i - c^*)^p \quad (21)$$

$$\text{Setting } (c_i - c^*)^{p-1} = Z \quad (22)$$

$$k_m(c - c_i) = k_r Z (c_i - c^*)$$

$$\text{Therefore, } c_i = \frac{k_m c + Z k_r c^*}{k_m + Z k_r}$$

Substituting this expression for c_i into equation (21)

$$k_m(c - c_i) = \frac{c - c^*}{\frac{1}{k_m} + \frac{1}{Z k_r}} = K(c - c^*)$$

which gives on rearranging:

$$\frac{1}{K} = \frac{1}{k_m} + \frac{1}{k_r(c_i - c^*)^{p-1}} \quad (23)$$

This is the mathematical expression for the statement that the overall resistance to solute transfer equals the sum of the resistance to mass transfer and the resistance to surface reaction. Assuming that k_m , k_r and p are constant with respect to supersaturation, then a number of conclusions can be drawn from this equation.

(1) The value of K will be constant with respect to supersaturation only if the surface reaction is first order ($p = 1$) or if the overall rate is completely mass transfer controlled

$$(k_m \ll k_r(c_i - c^*)^{p-1}).$$

(2) If K varies with supersaturation, then the overall rate is not completely mass transfer

controlled and the surface reaction is not first order ($p \neq 1$).

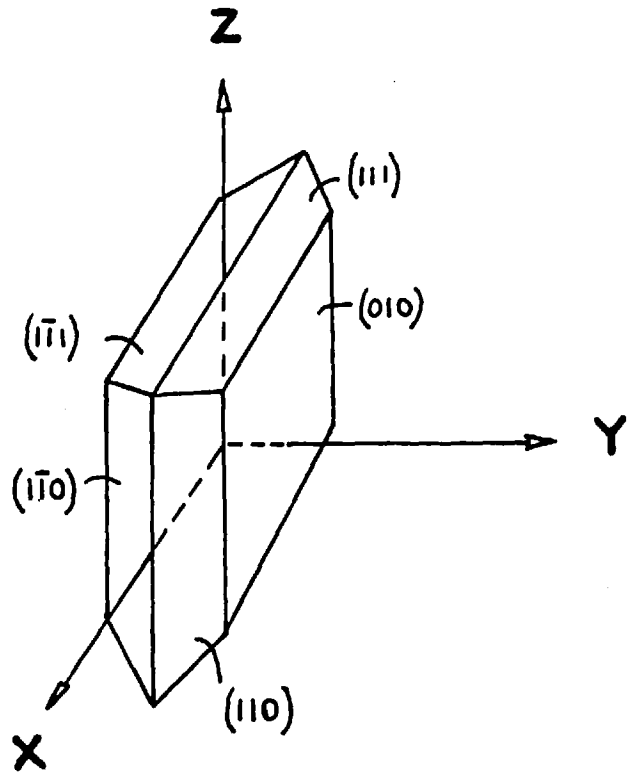
- (3) If K increases with supersaturation, $p > 1$;
if K decreases with supersaturation, $p < 1$.

Because of the difficulty of measuring the interfacial concentration c_i , the relative contributions of mass transfer and surface reaction to the overall growth process are generally found indirectly. This is done by determining the effect on the overall rate of altering some variable which primarily affects one or other of the two steps. One such variable is the degree of agitation in the solution. The value of k_m is dependent to some extent on v , the relative velocity between the crystal surface and the solution. An increase in v would tend to decrease the laminar film thickness δ in equation 18, or increase the fractional rate of surface renewal f in equation 19, and hence increase the value of k_m . As the value of k_m increases, the resistance to mass transfer decreases (by equation 23) and the overall resistance to solute transfer approaches the resistance to the surface reaction, allowing c_i to be approximated to c .

In this chapter, measurements of the rate of growth of single crystals of calcium sulphate dihydrate are reported. These measurements were made under isothermal conditions in solutions of known and constant

DIAGRAM OF AN IDEAL DIHYDRATE CRYSTAL

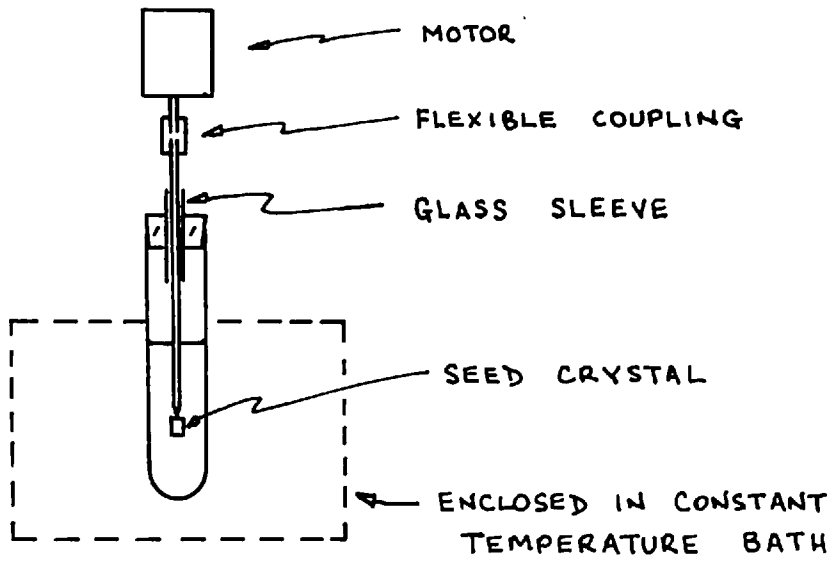
FIGURE 15



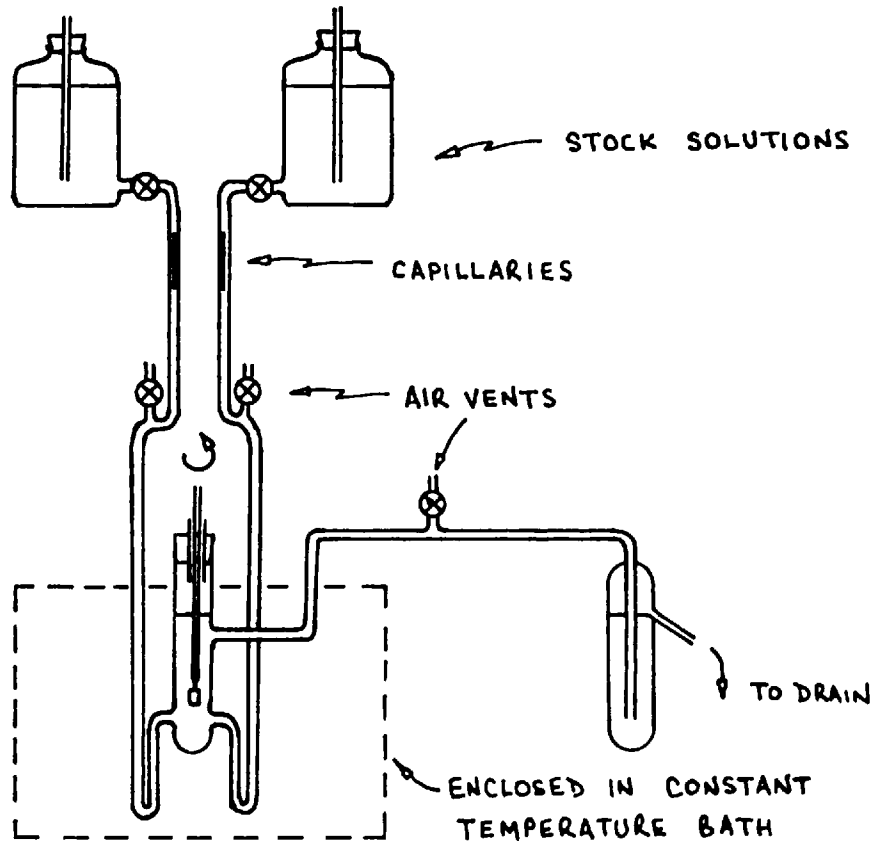
APPARATUS FOR GROWTH RATE MEASUREMENTS

FIGURE 16

BATCH SYSTEM



FLOW SYSTEM



supersaturations in the temperature range, 70°-98°C. The growth rates of both stirred and unstirred crystals were determined in order to show the relative contributions of mass transfer and surface reaction to the overall rate.

3.2 Growth Rates of Unstirred Crystals

The dihydrate crystallizes in the monoclinic form. A diagram of an ideal crystal is shown in figure 15. In these experiments, the displacement of the fast-growing edge which is bounded by the (111) and ($1\bar{1}1$) planes was measured and the growth rate R_1 obtained. Also, in a few runs, the growth rate R_2 was obtained for the slower-growing edge bounded by the (110) and ($1\bar{1}0$) planes.

EXPERIMENTAL

For each run, a dihydrate seed crystal was fixed on a glass rod with Araldite adhesive, with the c direction of the crystal parallel to the length of the rod. The seed crystals which were generally up to 1 mm. in length were selected from some produced in previous nucleation studies. Examination of the seed crystals showed them to be either single or twinned along the (100) plane and in all cases, free of any visible surface crystals.

The apparatus used for these growth rate measurements is illustrated in figure 16. For the batch system, the calcium sulphate solution was prepared at the start of

each run by mixing equal volumes of equimolar solutions of calcium chloride and sodium sulphate. About 30 ml. of mixed solution was added to the 60 ml. test tube, the seed crystal immersed in solution, and the tube placed in the constant temperature bath for heat-up to the temperature of the experiment.

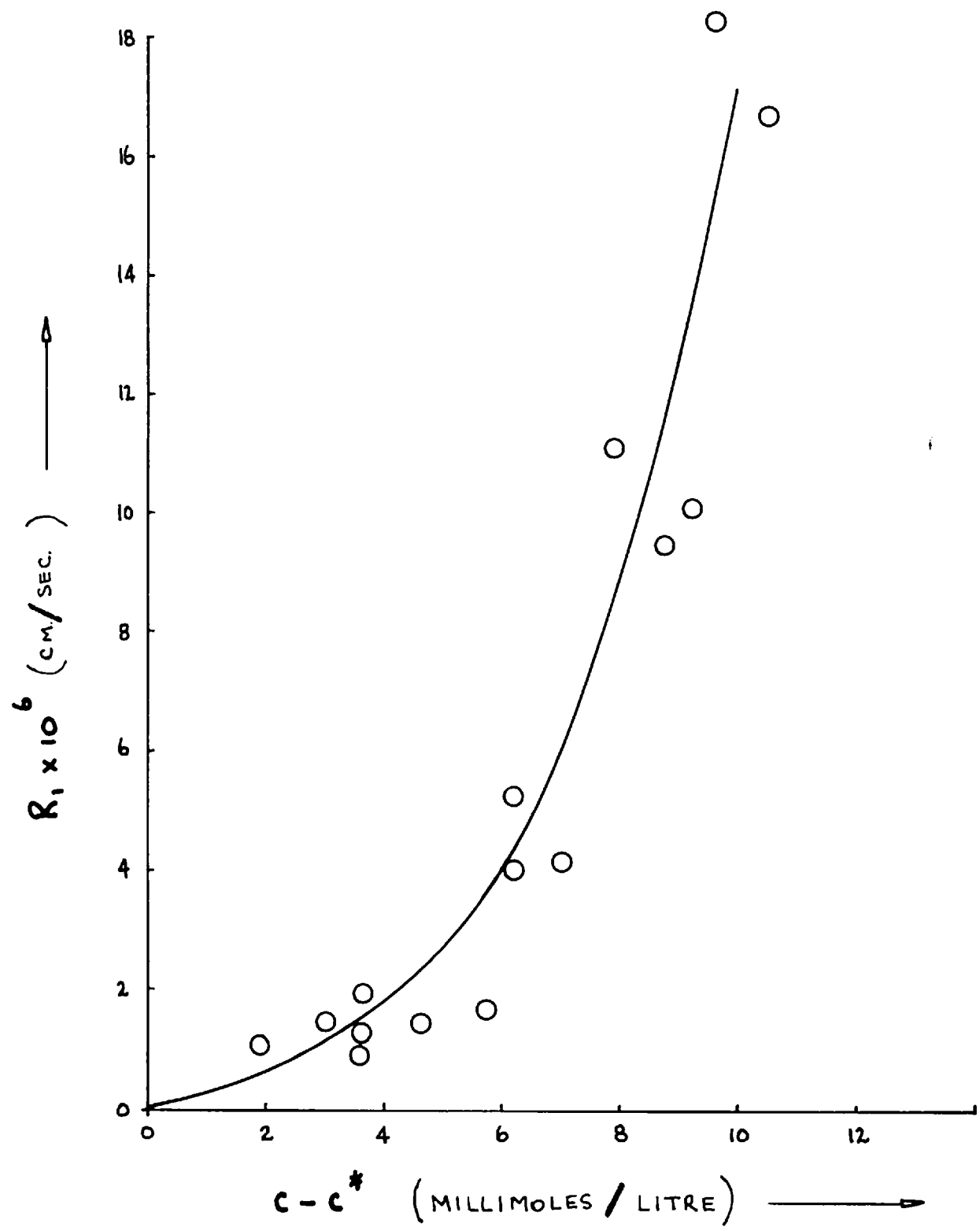
In the flow system, the calibrated capillaries in the solution feed lines ensured equal delivery rates of the two stock solutions (350 ml. per hour each) to the 100 ml. tube. Mixing of the calcium chloride and sodium sulphate solutions occurred continuously at the point where the feed lines joined the tube. The seed crystal was immersed in the solution and the tube placed in the bath as before.

After allowing sufficient time for heat-up of the solution to bath temperature, the growth of the crystal was followed by measuring the displacement with a travelling microscope. The eyepiece of the microscope was fitted with a graticule so that displacements of 0.04 mm., corresponding to 1 division on the graticule, could be easily measured. The growth rate of the crystal was then obtained from a displacement-time plot.

Measurements were made at three temperatures: 70°, 85° and 98°C. The solution concentration was constant for the duration of each run, with a value in the range,

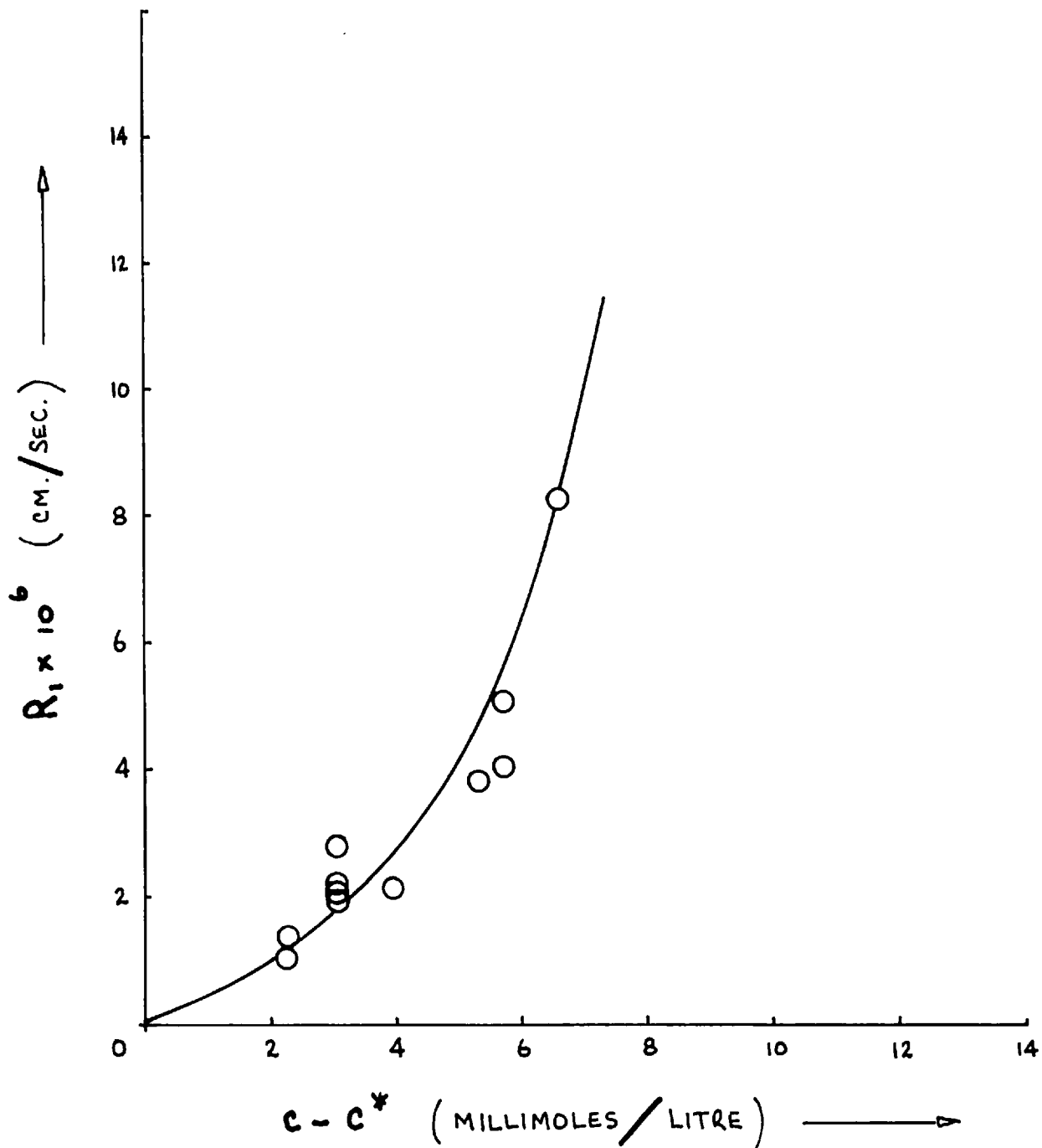
UNSTIRRED DIHYDRATE GROWTH RATE (R_1) AT 70°C

FIGURE 17



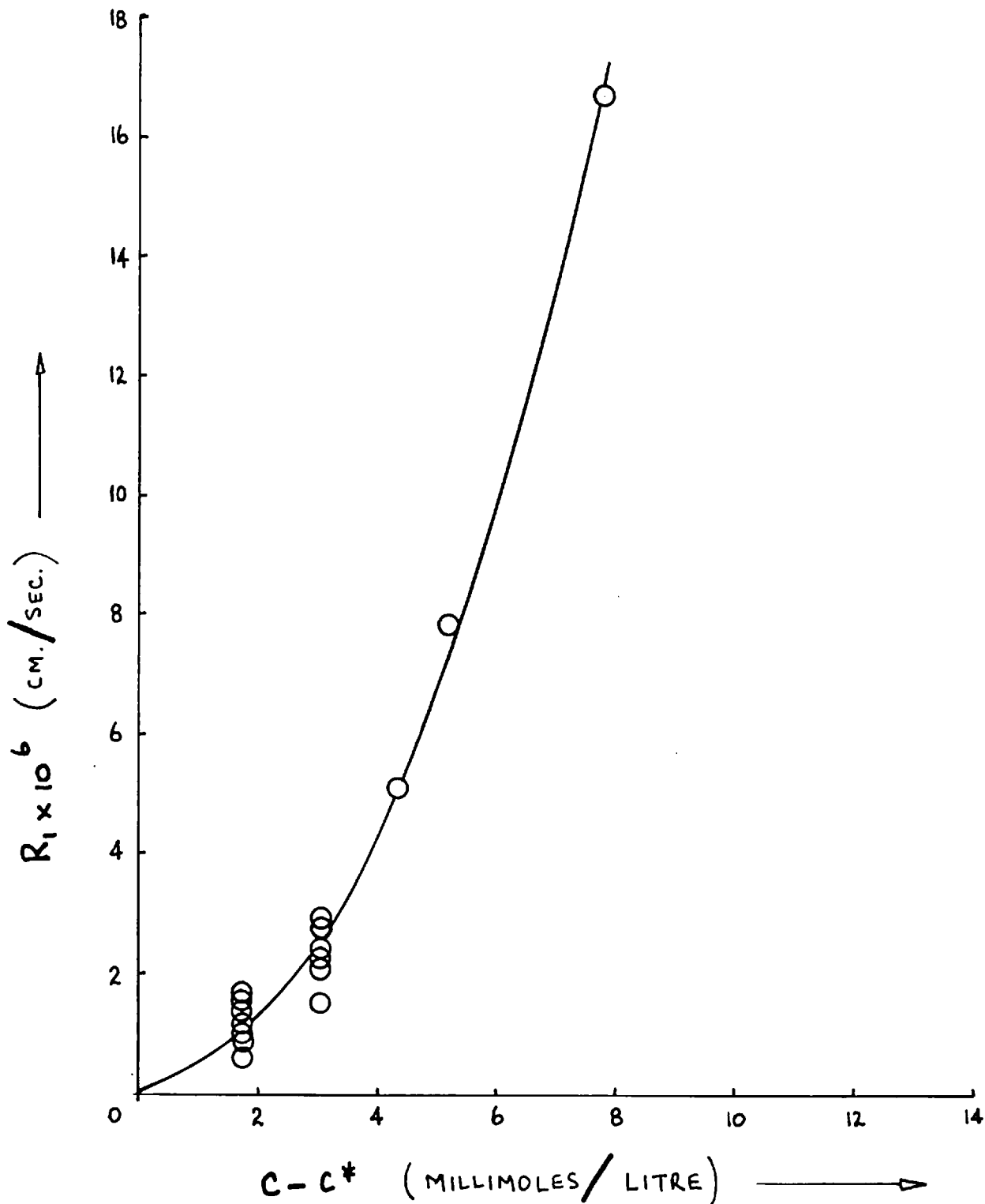
UNSTIRRED DIHYDRATE GROWTH RATE (R_1) AT 85°C

FIGURE 18



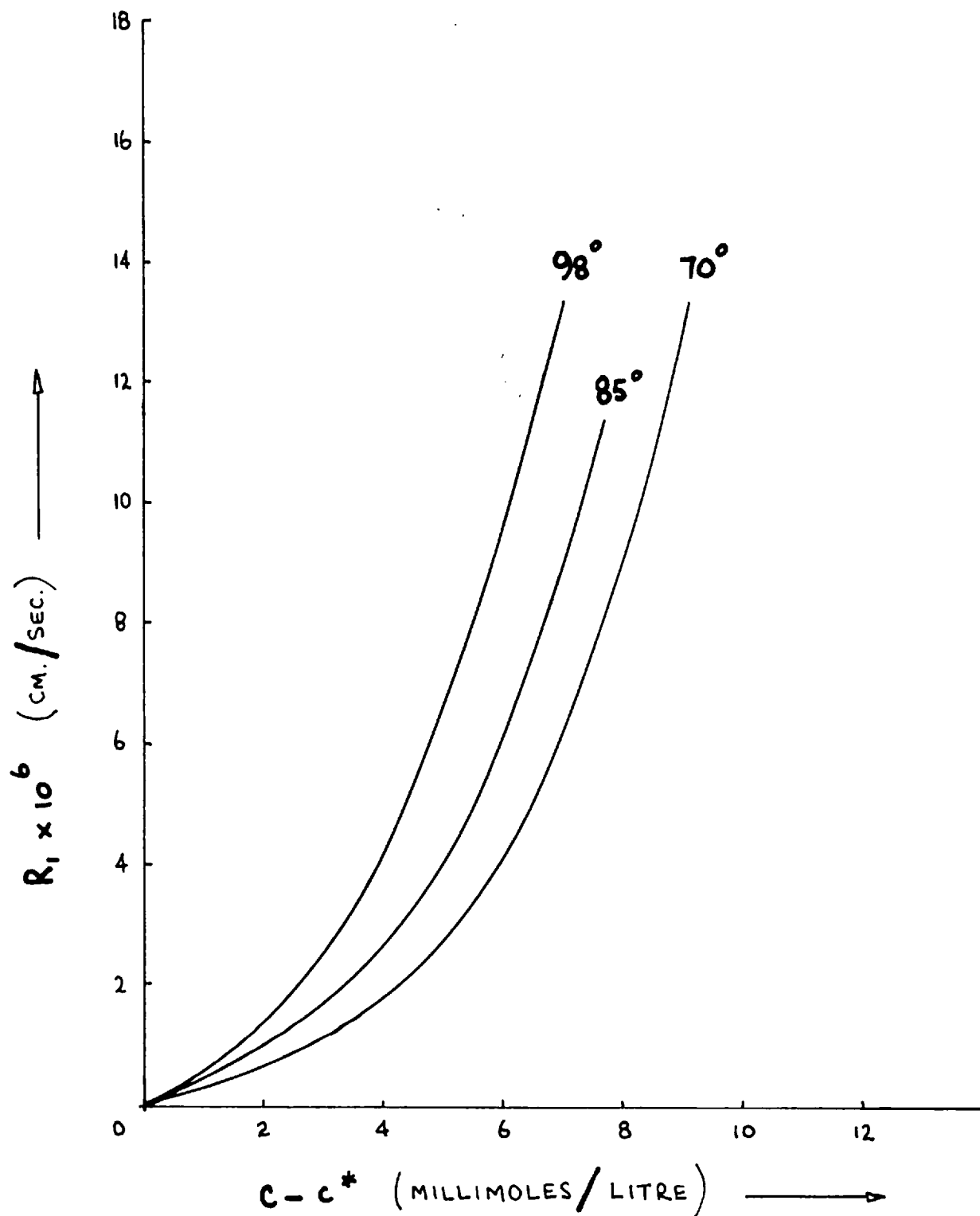
UNSTIRRED DIHYDRATE GROWTH RATE (R_1) AT 98°C

FIGURE 19



UNSTIRRED DIHYDRATE GROWTH RATE (R_1) AT 70°, 85° AND 98°

FIGURE 20



17.0 to 29.55 millimoles per litre. The duration of the runs varied from 0.5 to 7 hours and the total displacement from 0.1 mm. to 1 mm.

RESULTS

In these experiments, the growth rate was constant during the period of measurement, suggesting that no appreciable nucleation had occurred. This view was supported by the observation that the growth rates obtained in the flow system were not noticeably different from those obtained in the batch system.

The results of these measurements are listed in tables 7, 8 and 9. Although the actual magnitude of the unstirred growth rate may, by itself, be of limited theoretical value, it does allow certain conclusions to be drawn on the relative rates of mass transfer and surface reaction and serves as a basis to which the stirred growth rates reported in the next section can be compared.

The effect of the overall supersaturation $c - c^*$ on the growth rate R_1 is illustrated for the three temperatures in figures 17, 18 and 19, and in figure 20 the three growth rate curves are compared. It is apparent that the growth rate R_1 increases more than linearly with supersaturation and thus the value of K as defined by equation 20 increases with respect to supersaturation. If k_m is taken to be a constant, it follows that the overall growth

rate is not completely mass transfer controlled, and also that the surface reaction must depend on supersaturation to a power greater than unity ($p > 1$).

The overall growth rate can be expressed in terms of a power of the supersaturation. A linear regression of $\log R_1$ on $\log(c - c^*)$ was carried out for these unstirred growth rates, resulting in the three empirical equations shown below, where Δc is the overall supersaturation $c - c^*$ in millimoles per litre. These equations give 95% confidence limits on the rate.

$$70^\circ \quad R_1 = (1.88 \pm 1.36) \times 10^{-7} (\Delta c)^{1.96 \pm 0.43} \text{ cm. sec}^{-1}$$

$$85^\circ \quad R_1 = (6.13 \pm 4.17) \times 10^{-7} (\Delta c)^{1.38 \pm 0.51} \text{ cm. sec}^{-1}$$

$$98^\circ \quad R_1 = (4.97 \pm 2.24) \times 10^{-7} (\Delta c)^{1.62 \pm 0.25} \text{ cm. sec}^{-1}$$

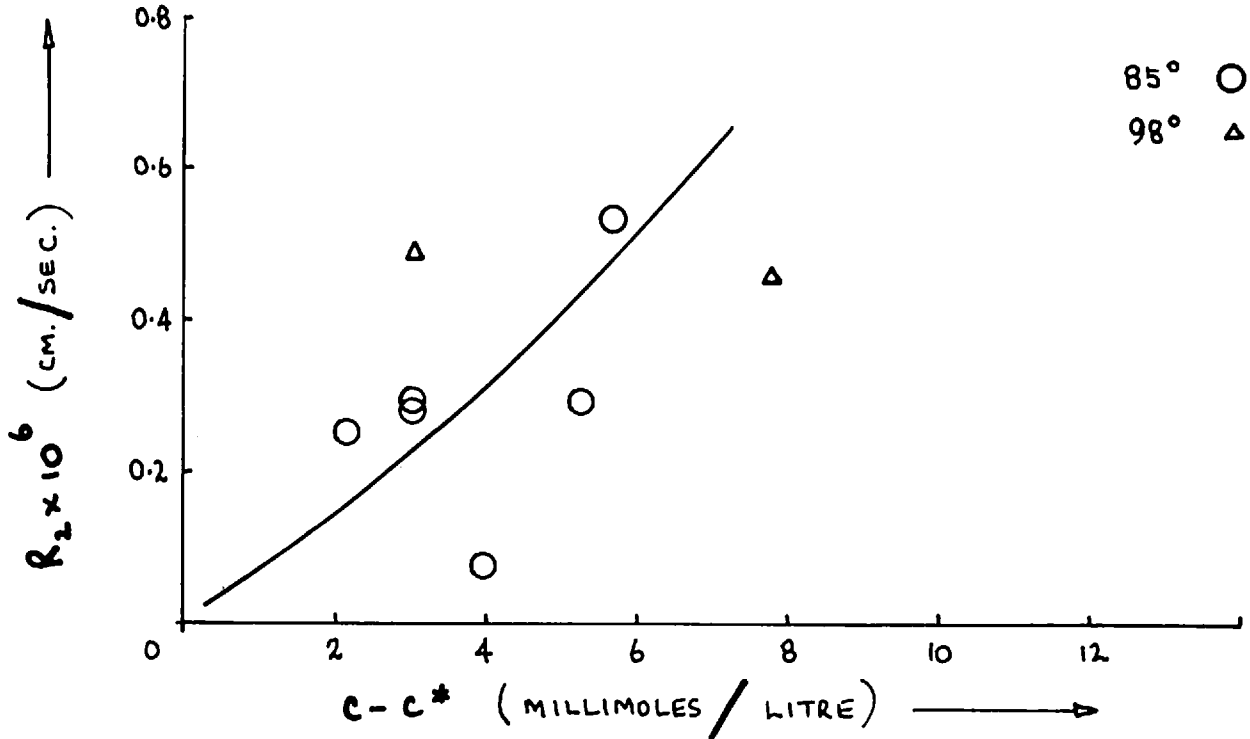
In figure 20, the growth rates at the three temperatures are compared. The effect of temperature on the unstirred growth rate can be expressed in the form of an Arrhenius reaction rate equation:

$$K = K' e^{-E/RT} \quad (24)$$

where K' is a constant, R is the gas constant, T is the absolute temperature and E is the energy associated with the process, usually called the activation energy. The results as described by the above equations yielded an activation energy for unstirred growth of about 6.1 kilocalories per mole.

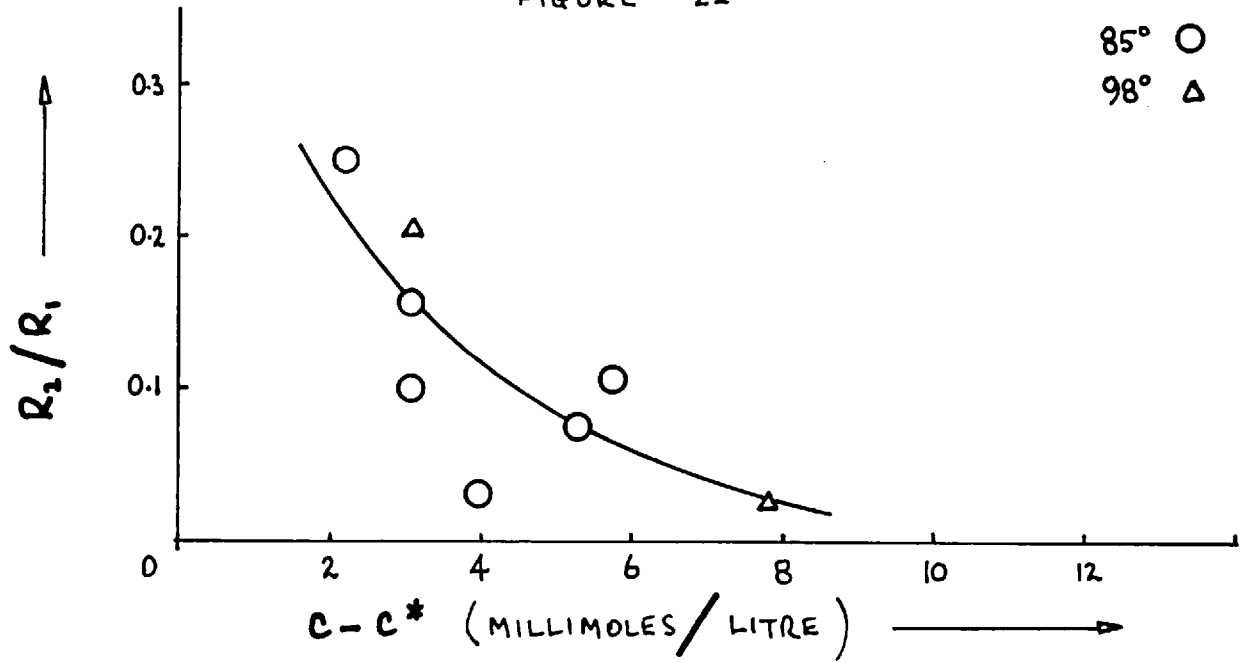
UNSTIRRED DIHYDRATE GROWTH RATE (R_2) AT 85° AND 98°

FIGURE 21



RATIO OF UNSTIRRED DIHYDRATE GROWTH RATES (R_2/R_1) AT 85° AND 98°

FIGURE 22



The growth rate R_2 was measured in a few runs and the effect of supersaturation on the rate is illustrated in figure 21. Although there is considerable scatter in the results, it is evident that R_2 is less than R_1 for the same supersaturations. In figure 22, the ratio of the growth rates, R_2/R_1 , is plotted against supersaturation. This figure shows that an increase in supersaturation has a greater effect on R_1 than on R_2 for unstirred crystals. This is in agreement with the observation that longer and thinner crystals are usually produced in highly supersaturated solutions.

3.3 Growth Rates of Stirred Crystals

An increase in v , the relative velocity between the solution and the crystal surface, frequently causes an increase in the growth rate of the crystal by reducing the resistance to mass transfer. Hixson and co-workers^{48,49} have applied a form of the Chilton-Colburn analogy between heat and mass transfer to the growth and dissolution of crystals in agitated solutions. Using an equation of the form:

$$\text{Sh} = \text{constant} (\text{Re})^a (\text{Sc})^b \quad (25)$$

where

$$\text{Sh} = \text{Sherwood number} = \frac{k_m d}{D}$$

$$\text{Re} = \text{Reynolds number} = \frac{dv \rho_s}{\mu}$$

$$\text{Sc} = \text{Schmidt number} = \frac{\mu}{\rho_s D}$$

STIRRED DIHYDRATE GROWTH RATE (R_1) AT 70°

FIGURE 23

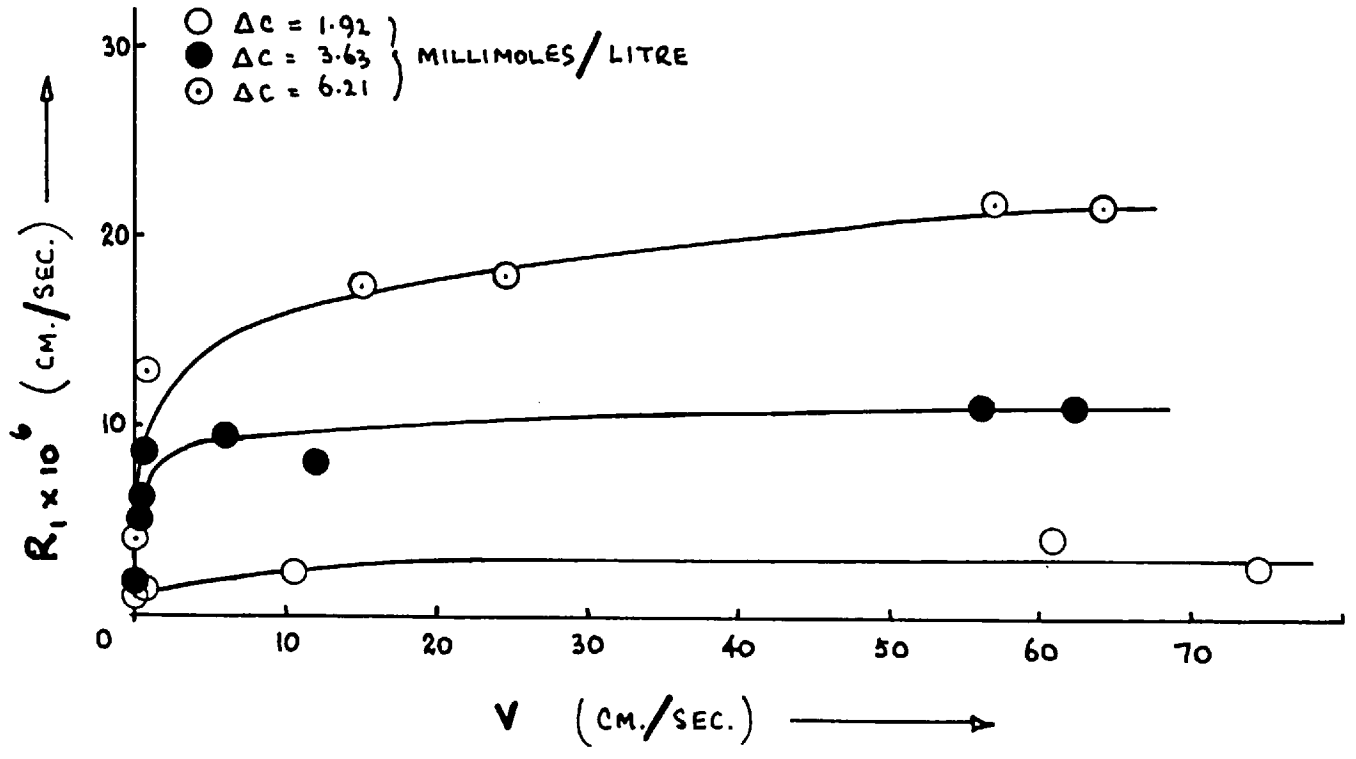
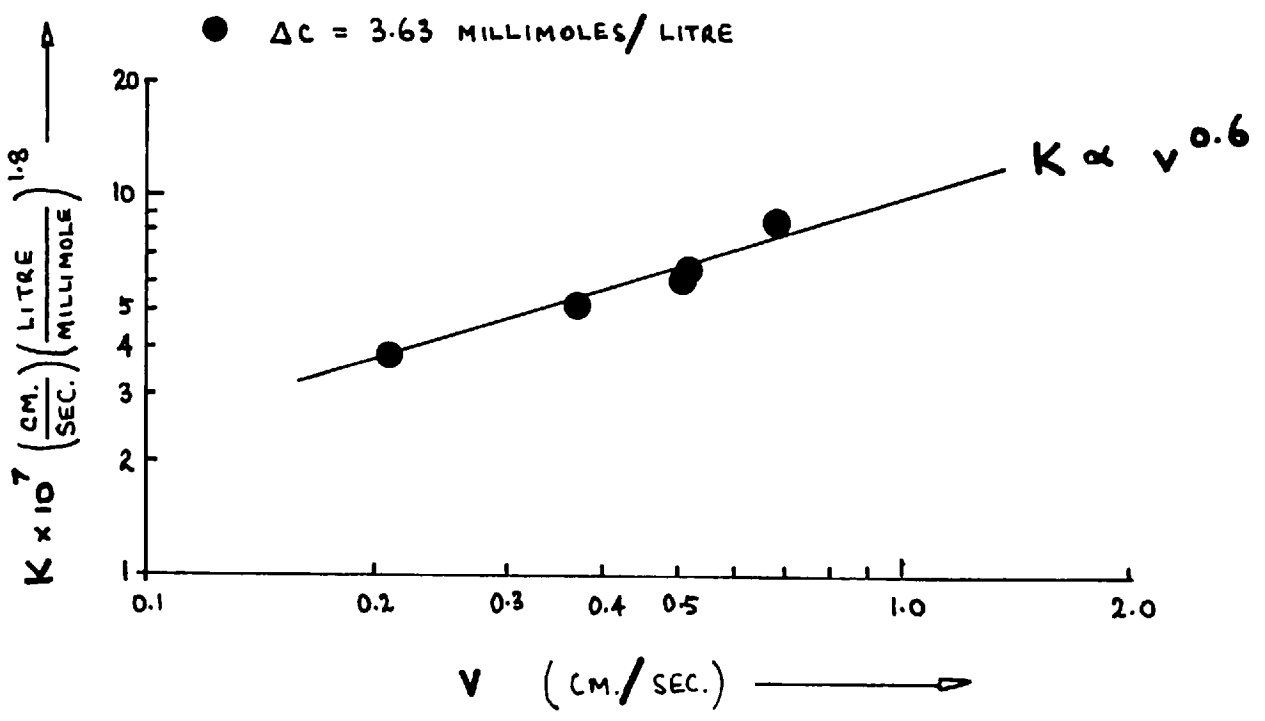


FIGURE 24



STIRRED DIHYDRATE GROWTH RATE (R_1) AT 85°

FIGURE 25

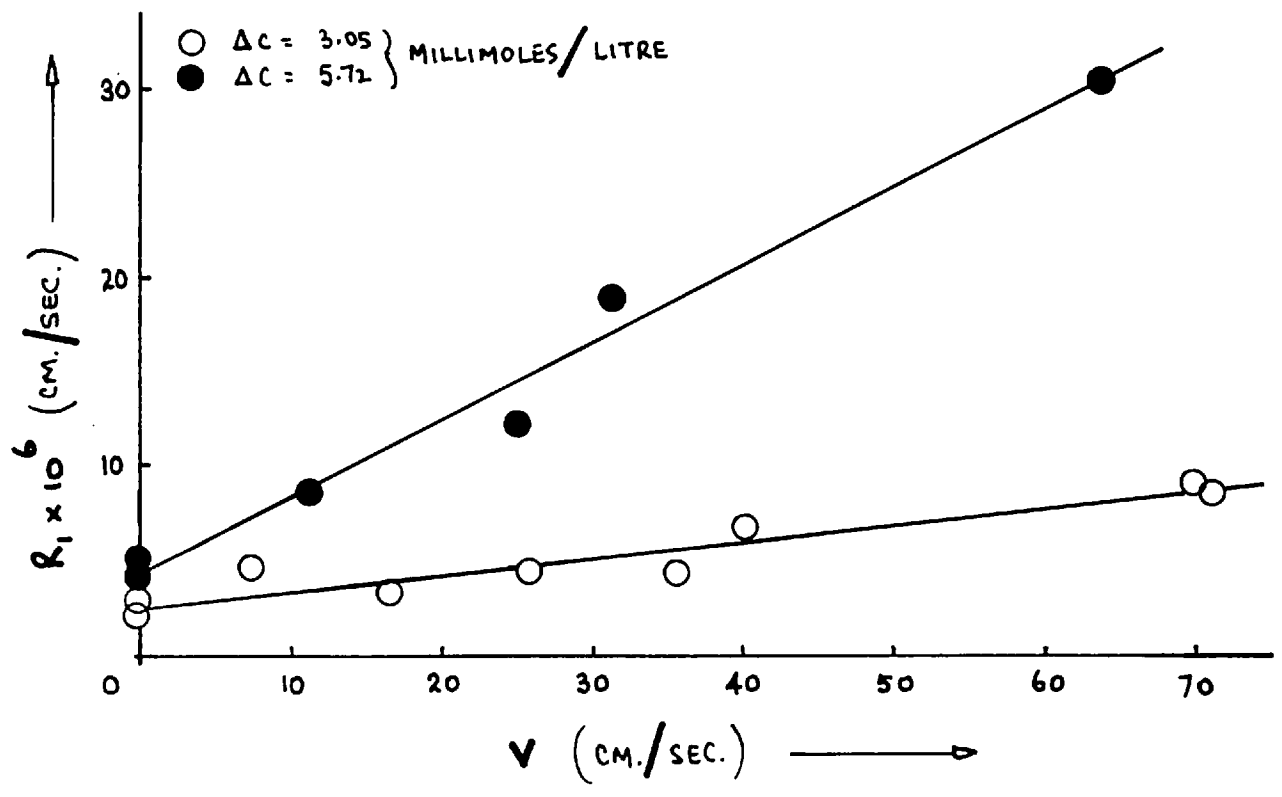
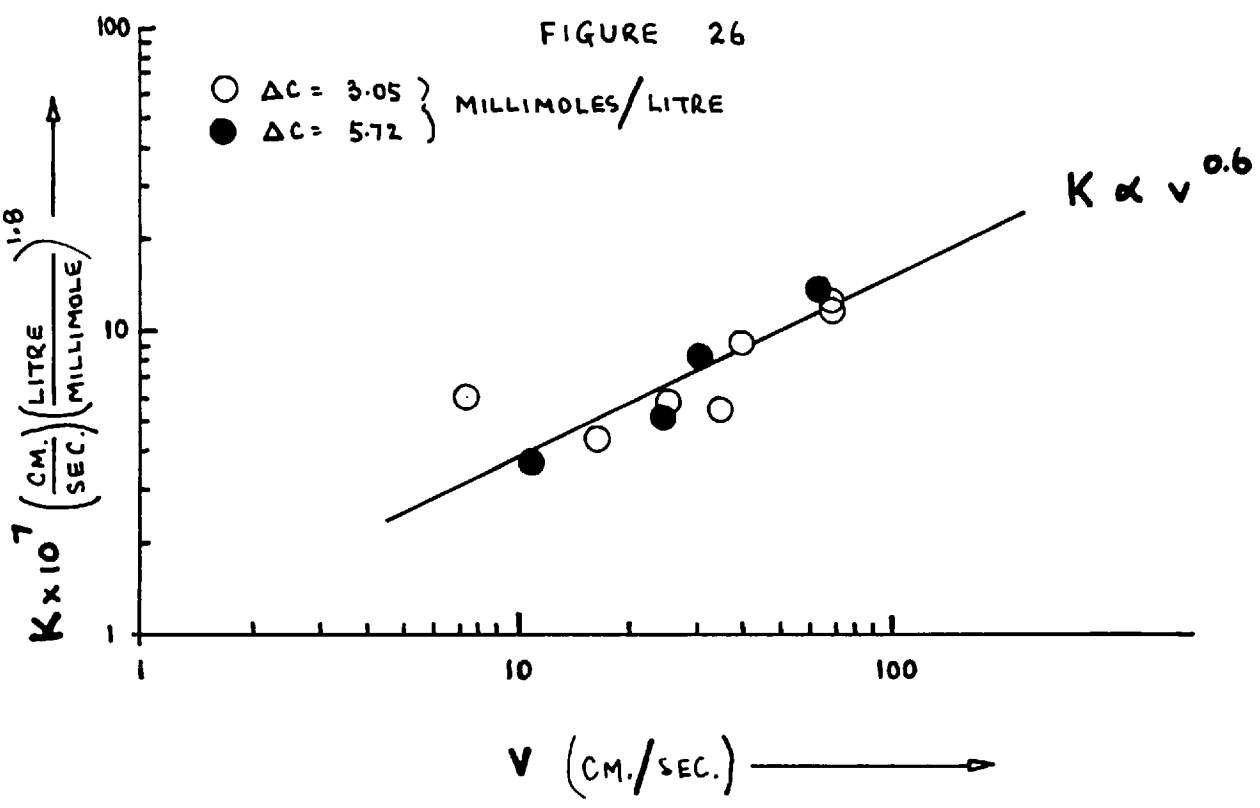


FIGURE 26



STIRRED DIHYDRATE GROWTH RATE (R_1) AT 98°

FIGURE 27

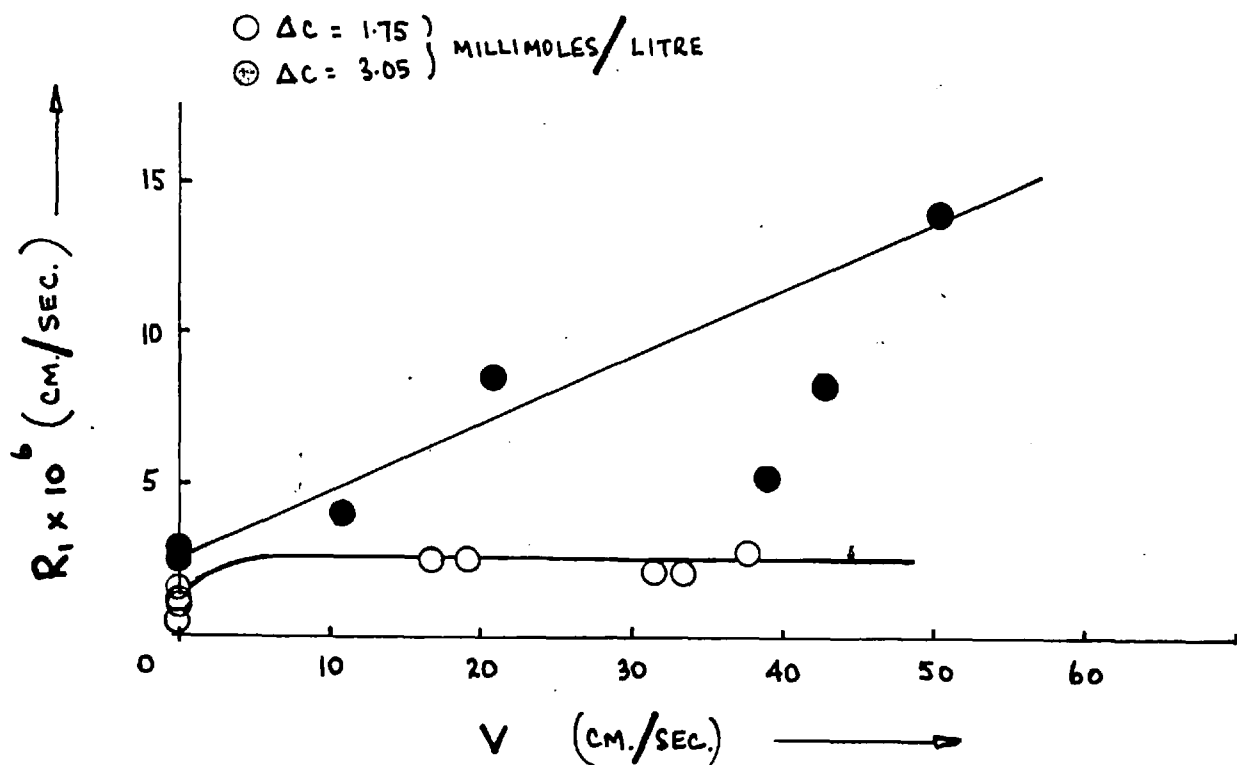
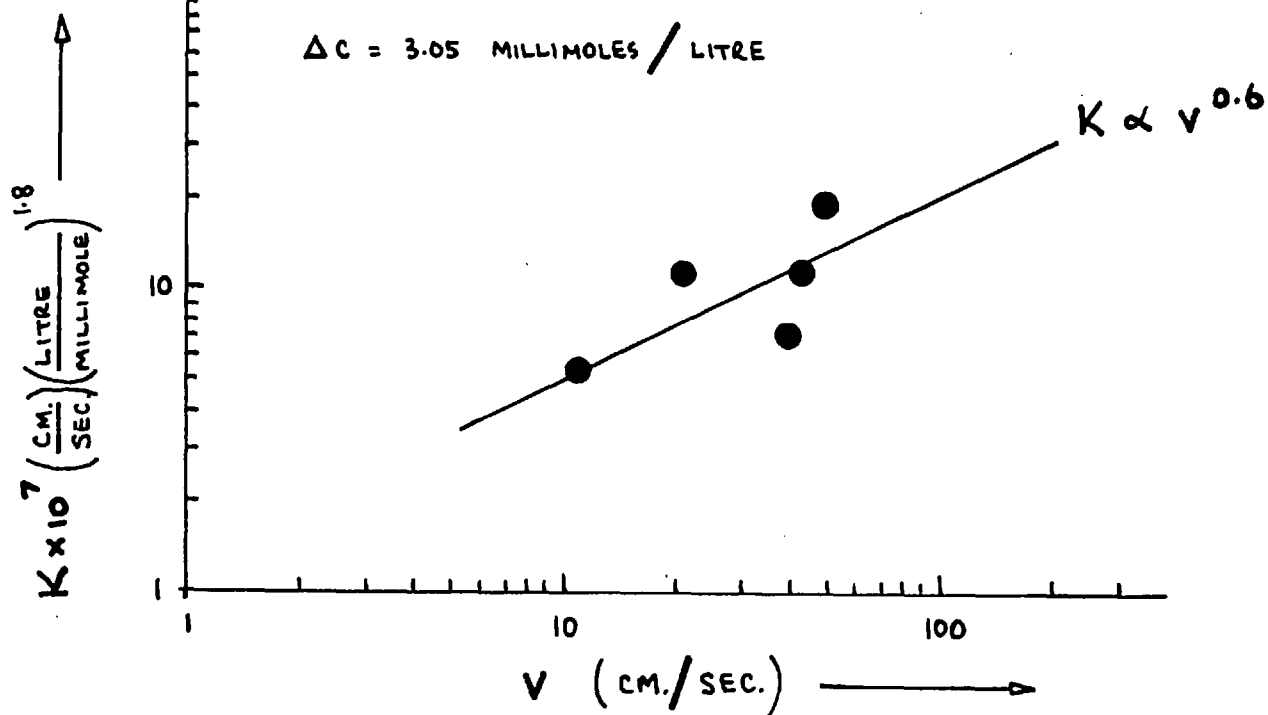


FIGURE 28

 $\Delta C = 3.05$ MILLIMOLES / LITRE


they found that $a = 0.6$ for the growth of $\text{MgSO}_4 \cdot 7\text{H}_2\text{O}$ and $\text{CuSO}_4 \cdot 5\text{H}_2\text{O}$ crystals. On the other hand, for the dissolution of various salts in water, the value of a was found to be between 0.6 and 1.4 depending on the velocity.

In order to determine to what extent the rate of mass transfer controls the overall growth rate of calcium sulphate dihydrate, measurements of the growth rate of stirred crystals were made.

EXPERIMENTAL

The apparatus and procedure used in these experiments was similar to that described in section 3.2. The relative velocity of the crystal in the solution was calculated from the diameter of revolution of the crystal and the rpm of the glass support rod, the former being measured with the travelling microscope and the latter with a stroboflash.

The measurements were again made at 70° , 85° and 98°C . The solution concentration which was constant for the duration of each run had a value between 17.0 and 24.6 millimoles per litre. Crystal velocities ranged from 0.2 to $75 \text{ cm}\cdot\text{sec}^{-1}$.

RESULTS

The growth rates obtained for stirred dihydrate crystals are listed in tables 10, 11 and 12. In figures 23, 25 and 27, the effect of the relative velocity v on

the growth rate R_1 is illustrated. At all temperatures and supersaturations, the growth rate increased to some extent with stirring indicating that the overall growth rate of unstirred crystals is at least partly mass transfer controlled. At 70° , for all the supersaturations investigated, the stirred growth rate approached a constant value as the stirring rate was increased, suggesting that the rate of surface reaction becomes increasingly the controlling rate at high stirring velocities. At the higher temperatures, however, the growth rate continued to increase over the range of stirring rates investigated, except for solutions of low supersaturation. This indicates that the overall rate becomes increasingly controlled by the rate of mass transfer as the temperature is increased, and that only at very low supersaturations and high stirring velocities can the control by mass transfer be removed.

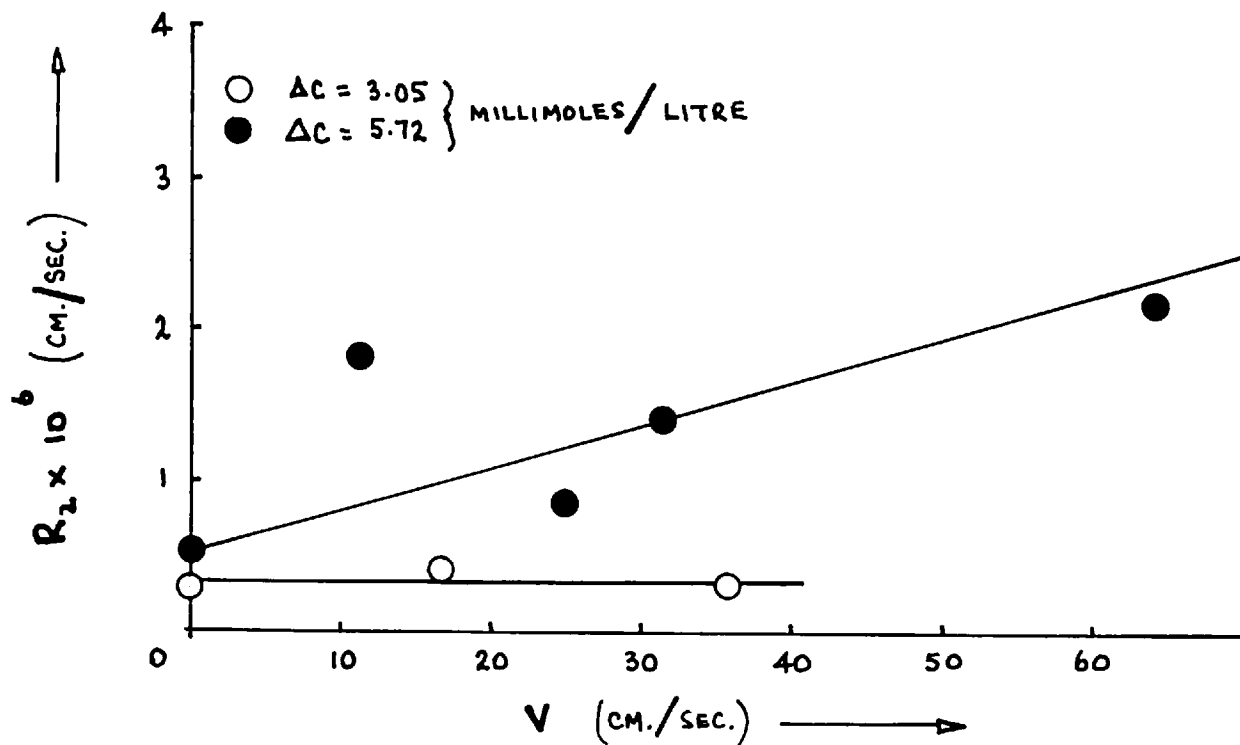
When the growth rate is largely mass transfer controlled, the effect of v on K might be expected to be similar to that on k_m . Assuming a rate equation of the form found in section 3.2,

$$R_1 = K(\Delta c)^{1.8} \text{ cm. sec}^{-1}$$

values of K were calculated for the measured growth rates on the steep portions of the curves in figures 23, 25 and 27 (the portions of the curves where the growth rate is not yet approaching a constant value with increasing

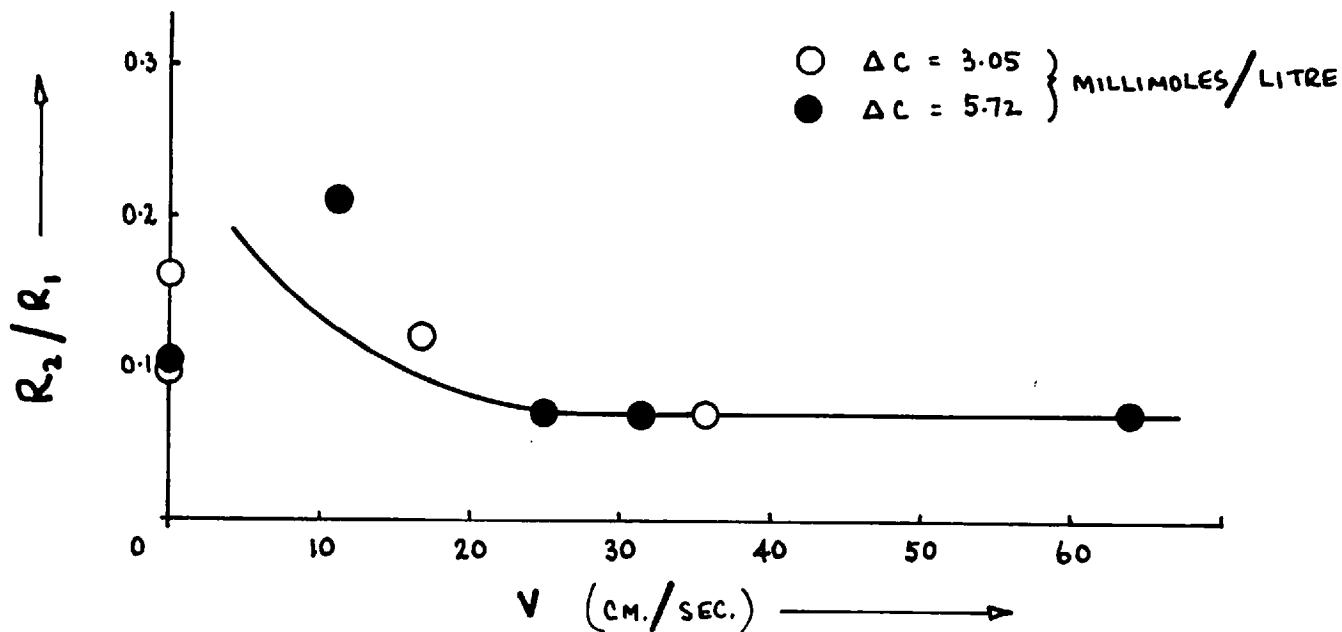
STIRRED DIHYDRATE GROWTH RATE (R_2) AT 85°

FIGURE 29



RATIO OF STIRRED DIHYDRATE GROWTH RATES (R_2/R_1) AT 85°

FIGURE 30



stirring velocity). These values of K which are listed in tables 10, 11 and 12 are plotted against v in figures 24, 26 and 28. The lines in these figures correspond to the relationship:

$$K \propto v^{0.6}$$

It appears that this empirical relationship, which is similar to that described by equation 25, adequately describes these results.

In figure 29, the effect of the rate of stirring on the growth rate R_2 at 85° is illustrated. These results again indicate that only at low supersaturations and high stirring rates is a maximum growth rate reached.

In figure 30, the ratio of the growth rates, R_2/R_1 , is plotted against the stirring velocity. This figure indicates that an increase in the stirring rate tends, if anything, to have a greater effect on R_1 than on R_2 , thus producing longer and thinner crystals. This is contrary to what one would expect if the formation of needle-like crystals in unstirred solutions is to be attributed to mass transfer limitations. It has often been stated that needle-like crystals form because of a stagnant layer of solute-depleted solution along the sides of the unstirred crystal, while the faster-growing tip is exposed to fresh solution because of convection and its faster growth rate. If this were actually the case, then needle

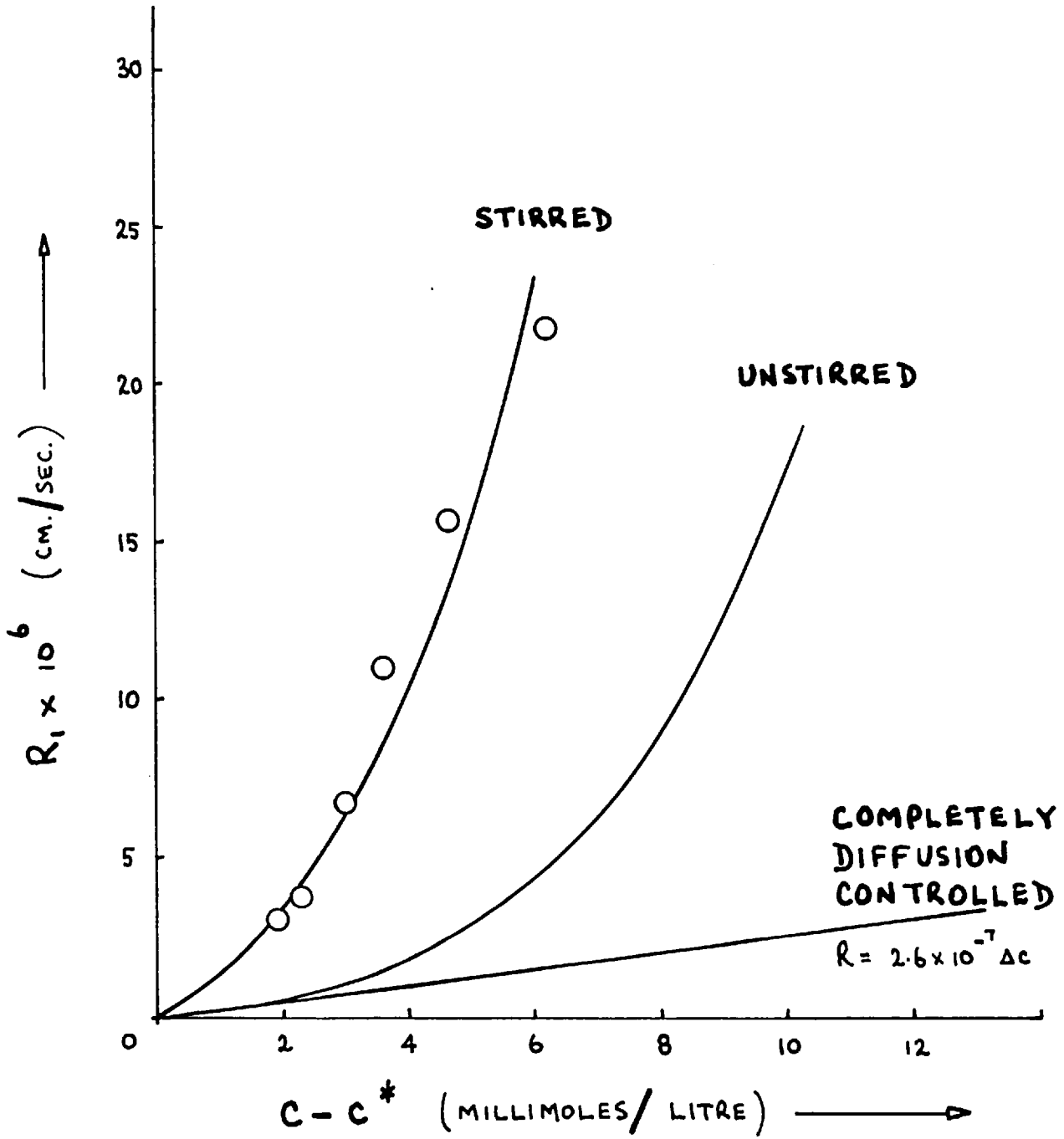
growth should be abolished altogether when the crystal is well stirred. Instead, these dihydrate crystals became rather more needle-like when stirred.

Another cause of needle growth that has been proposed involves the dissipation of the heat of crystallization. If heat is more readily dissipated from a crystal tip than from the sides, an unstirred crystal with a positive solubility would be exposed to solution with a greater supersaturation at the tip. Stirring the crystal would again tend to equalize the supersaturation around the crystal and remove the cause of needle growth. However, the dihydrate, which liberates a small heat of crystallization, has a negative solubility and although the more ready dissipation of heat from the tip of an unstirred crystal might account for the relatively higher R_2/R_1 values in this case, it certainly does not explain why needle-like crystals should form at all in unstirred solutions.

Since at 70° the growth rate R_1 approached a constant maximum value when the stirring rate was above 10 to 15 cm. sec^{-1} , this suggests that the resistance to mass transfer was reduced to such an extent that the overall growth rate was controlled by the rate of the surface reaction, and the supersaturation at the crystal-solution interface was very nearly that in the bulk of the solution.

STIRRED AND UNSTIRRED GROWTH RATES OF DIHYDRATE AT 70°

FIGURE 31



In figure 31, these growth rates of well-stirred crystals (from table 10) are compared to the corresponding growth rates of unstirred crystals at 70° from section 3.2. A linear regression of $\log R_1$ on $\log \Delta c$ for the stirred results gave the following empirical equation, with 95% confidence limits on the rate:

$$R_1 = (1.03 \pm 0.45) \times 10^{-6} (\Delta c)^{1.80 \pm 0.29} \text{ cm. sec}^{-1}$$

If the rate of the surface reaction is assumed to be independent of the stirring velocity, then unstirred and stirred crystals having similar growth rates must have similar supersaturations, $c_i - c^*$ at the crystal interface. Using this estimate of the interfacial concentration, one can then calculate the rate of mass transfer to the unstirred crystals at 70°. For example, from figure 31, when the growth rate is $3.2 \times 10^{-6} \text{ cm. sec}^{-1}$ ($4.3 \times 10^{-5} \text{ millimoles. cm}^{-2} \cdot \text{sec}^{-1}$), $c - c^* = 2$ millimoles per litre for well-stirred crystals and 5.2 millimoles per litre for unstirred crystals. From the solubility data illustrated in figure 3, the corresponding bulk solution concentrations are respectively 19.7 and 23.4 millimoles per litre. Assuming that $c_i = c$ for the stirred crystals, then $c_i - c^* = 2$ millimoles per litre for the unstirred crystals. Using this value along with the solubility data, c_i for unstirred crystals is calculated to be 20.8 millimoles per

litre. Therefore, $c - c_i$ for unstirred crystals is 2.6 millimoles per litre and $k_m = 0.017 \text{ cm. sec}^{-1}$. The results of a few of these calculations are listed in Table 13.

These results indicate that the value of k_m increases with increasing supersaturation. Although there may have been a slight error introduced into the calculations by assuming that for the stirred crystals, the interfacial concentration equalled the bulk solution concentration, this could account for only part of the increase. It is more probable that some factor, such as convection, caused k_m or c_i (or both) to increase from the value corresponding to mass transfer in still solutions, and that this effect was more pronounced in the more concentrated solutions.

An estimate has been obtained for the growth rate of unstirred crystals under conditions of complete mass transfer control without convection. Using Fick's law and assuming a diffusion layer of infinite thickness, an expression for the rate of diffusion to the hemispherical tip of a crystal was found. Fick's law gives at steady state:

$$\frac{J}{A} = \frac{D}{10^3} \cdot \frac{dc}{dr} \quad \text{millimoles. cm}^{-2} \cdot \text{sec}^{-1}$$

where J is the molar flux in millimoles per second passing through the hemispherical area $A = 2\pi r^2 \text{ cm}^2$; D is the diffusion coefficient in $\text{cm}^2 \cdot \text{sec}^{-1}$; c is the solution concentration in millimoles per litre at r , the radial distance from

the centre of the hemispherical tip in cm. Integrating this equation with the boundary conditions:

$$(1) \quad r = r_t \quad \text{the radius of the crystal tip at} \\ c = c^*$$

$$(2) \quad r = \infty \quad \text{at } c = c_\infty$$

results in the following equation:

$$\frac{J}{A} = R_1 = \frac{D}{10^3} \cdot \frac{(c_\infty - c^*)}{r_t} \quad \frac{\text{millimoles}}{\text{cm}^2 \text{sec}} \quad (26)$$

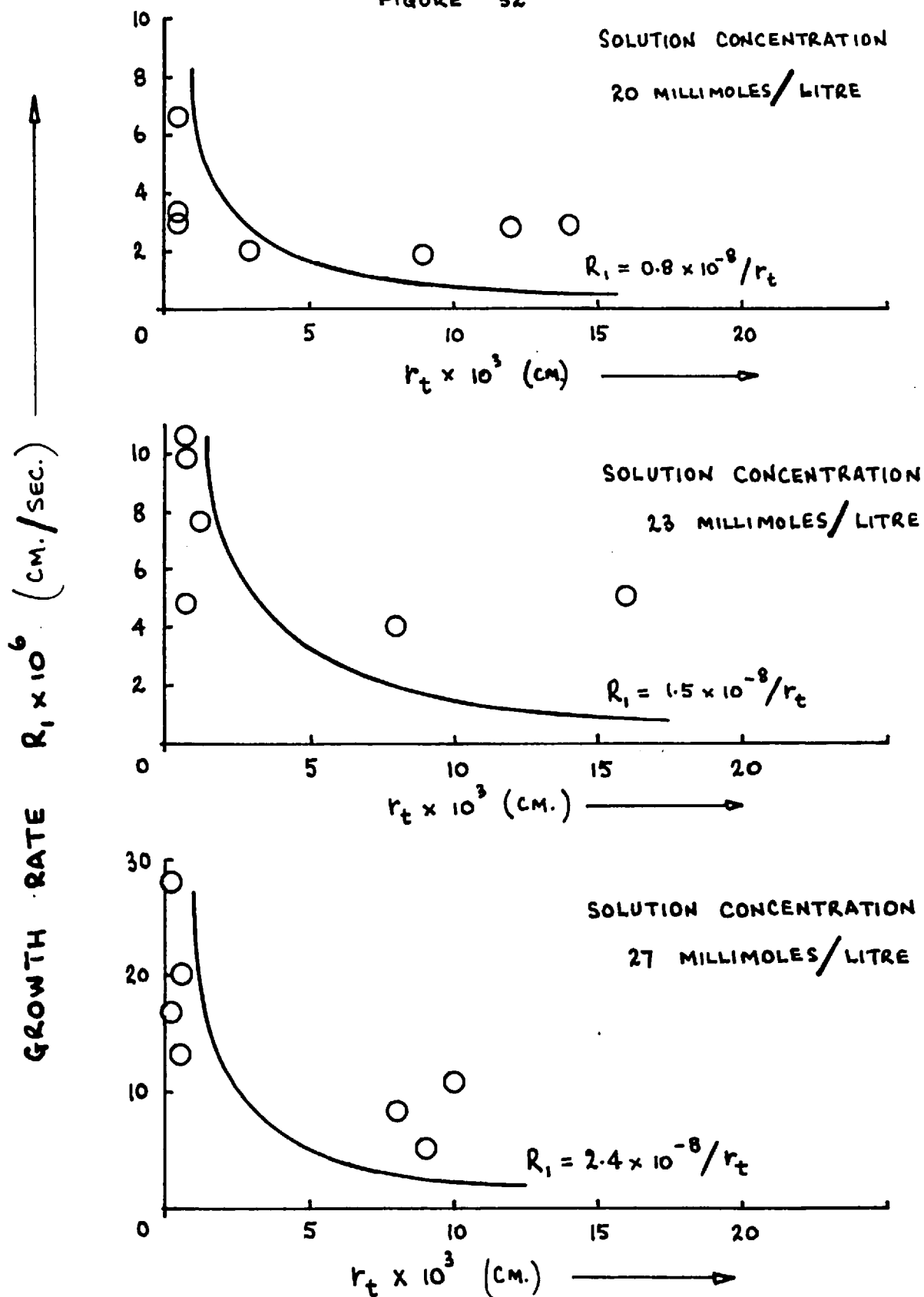
The dihydrate crystals used in the present growth rate measurements had an r_t of approximately 10^{-2} cm., and with $D = 3.5 \times 10^{-5} \text{ cm}^2 \cdot \text{sec}^{-1}$, equation 26 reduces to:

$$R_1 = 3.5 \times 10^{-6} (c_\infty - c^*) \text{ millimoles} \cdot \text{cm}^{-2} \cdot \text{sec}^{-1} \\ = 2.6 \times 10^{-7} (c - c^*) \text{ cm} \cdot \text{sec}^{-1}$$

The rate given by this equation is compared to the measured unstirred growth rate in figure 31. At low supersaturations, the rate calculated from this equation agrees well with the observed growth rate. At higher supersaturations, however, the predicted rate is much lower than the measured rate presumably because, as discussed previously, convection comes into play and under these conditions, the above equation would not be applicable.

THE EFFECT OF CRYSTAL SIZE ON UNSTIRRED DIHYDRATE GROWTH RATES

FIGURE 32



3.4 The Effect of Crystal Size on Growth Rate

The equation derived for the rate of growth under complete diffusion-control:

$$R_1 = \frac{D}{10^3 r_t} (c_\infty - c^*) \frac{\text{millimoles}}{\text{cm}^2 \text{ second}}$$

predicts that the rate increases as the radius of the crystal tip, r_t , decreases. To determine whether crystal size affects the growth rate in these conditions, measurements were made of the growth rate R_1 of smaller unstirred dihydrate crystals.

EXPERIMENTAL

The apparatus and procedure used in these experiments were the same as described in section 3.1 for the batch system. The value of r_t was taken as half the width of the crystal and varied from 2×10^{-4} cm. to 160×10^{-4} cm. The growth rate was measured in solutions at 85°C with concentrations of 20, 23 and 27 millimoles per litre.

RESULTS

The results of these measurements are listed in table 14 along with the appropriate results from table 8, and illustrated in figure 32. The curves drawn in these graphs were obtained by substitution in the above equation.

The measured growth rates agree reasonably well with the predicted rate over the range of crystal sizes investigated, although the effect of crystal size is not

quite as pronounced as that calculated from the equation. For example, the observed rates do not increase indefinitely as $r_t \rightarrow 0$, nor do they decrease indefinitely as $r_t \rightarrow \infty$, as predicted by the equation. In the former case, the growth rate approaches the rate obtained for well-stirred crystals where the rate of the surface reaction becomes the controlling rate. In the latter case, the growth rate is probably not completely diffusion-controlled for larger crystals because of convection in the solution. However, the approximate agreement of the measured rates with the equation indicates that the growth rate of unstirred dihydrate crystals is to a large extent diffusion-controlled and dependent on the size of the crystal.

3.5 Summary

The growth rate of the fast-growing edge of both stirred and unstirred calcium sulphate dihydrate crystals has been measured as a function of supersaturation in mixed calcium chloride and sodium sulphate solutions at temperatures between 70° and 98°C . The empirical equations derived indicate that the rate is approximately second order with respect to supersaturation.

A quite considerable increase in growth rate was obtained by stirring the crystals, suggesting that the rate

is partly, if not wholly, controlled by the rate of mass transfer at these temperatures. At 70°, for supersaturations up to about 6 millimoles per litre, mass transfer effects were virtually eliminated at high stirring rates, but at higher temperatures a constant maximum stirred growth rate could be obtained only at very low supersaturations. This indicates that as might be expected, mass transfer becomes increasingly the rate controlling step at higher temperatures.

The calculated mass transfer coefficient for unstirred growth at 70° increased with solution concentration. This is believed to be due to convection which becomes increasingly important at higher solution concentrations.

The dihydrate crystals produced at these temperatures and supersaturations were needle-like and became longer and thinner at higher supersaturations. The formation of needle-like crystals cannot be attributed to mass transfer limitations since the effect of stirring was to produce even longer and thinner crystals.

The size of unstirred crystals has been shown to affect their growth rates, and the increase in rate with decreasing crystal size agrees reasonably well with the predicted values for complete mass transfer control of the growth rate.

CHAPTER 4

THE GROWTH RATE OF HEMIHYDRATE CRYSTALS4.1 Introduction

In this chapter, measurements of the rate of growth of calcium sulphate hemihydrate are reported. Hemihydrate, or subhydrate as it is sometimes called because of its variable water content, is unstable with respect to the other forms of calcium sulphate over the entire temperature range (see figure 1). However, in the 90° - 130°C range, hemihydrate is frequently formed and can remain in apparent equilibrium with solution for long periods.

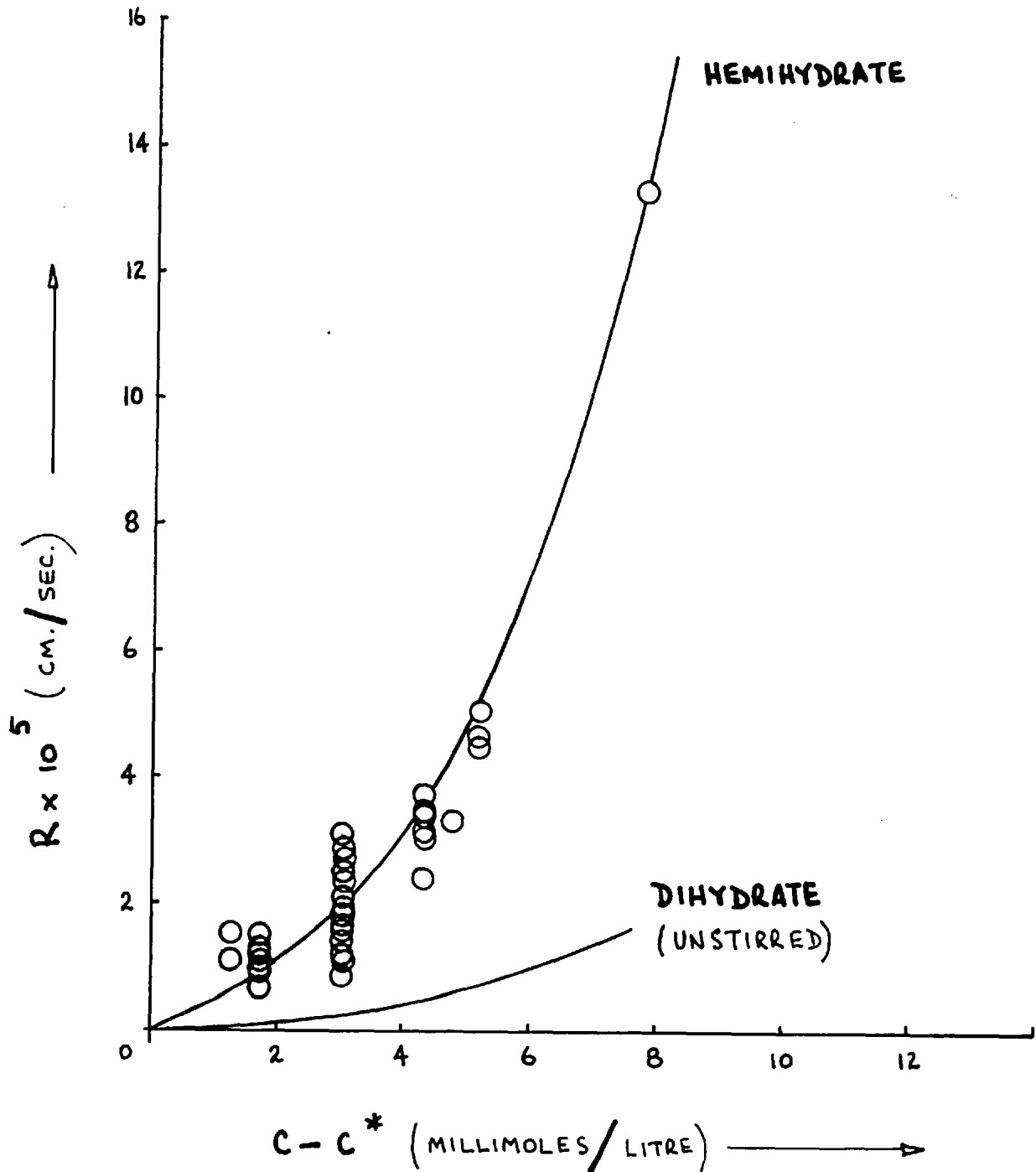
Hemihydrate is normally encountered as long, thin needles and in these experiments the displacement in the lengthwise or fast-growing direction of the needle was measured. The rates of growth of both unstirred and stirred crystals were obtained in solutions of known and constant supersaturations at 98°C .

4.2 Growth Rates of Unstirred CrystalsEXPERIMENTAL

The apparatus and procedure used to obtain hemihydrate growth rates was similar to that used for the dihydrate as described in section 3.2. The seed crystals were taken from some produced in previous nucleation runs

GROWTH RATE OF UNSTIRRED HEMIHYDRATE AT 98°

FIGURE 33



and mounted on glass rods as before. The crystals were generally less than 0.001 cm. in width as compared to 0.02 cm. or more for the dihydrate seed crystals in section 3.2.

The solution concentration which was constant for the duration of each run ranged from 16.5 to 24.0 millimoles per litre. Measurements of displacements from 0.1 mm. to 1 mm. were made over periods of up to 2 hours.

RESULTS

The results of these runs are listed in table 15 and illustrated in figure 33 where they are compared to the unstirred dihydrate growth rate at 98°. The solubilities of hemihydrate and dihydrate at this temperature are equal and hence the data of reference 30 for the dihydrate were used.

A linear regression of $\log R$ on $\log \Delta c$ gave the following empirical equation, with 95% confidence limits on the rate:

$$R = (5.01 \pm 1.23) \times 10^{-6} (\Delta c)^{1.32 \pm 0.18} \text{ cm/sec}$$

It is apparent from figure 33 that the growth rate of unstirred hemihydrate is somewhat higher than that of unstirred dihydrate at 98°. However, the difference in the size of the seed crystals should be noted. It was found that the growth rate of unstirred dihydrate crystals increased with decreasing crystal size. Considering the

magnitude of the increase indicated in figure 32, dihydrate crystals of a size similar to these hemihydrate crystals would be expected to have growth rates approximately equal to the hemihydrate growth rates.

4.3 Growth Rates of Stirred Crystals

In order to determine to what extent the rate of mass transfer controls the overall growth rate of the hemihydrate, measurements of the growth rates of stirred crystals were made. The results are reported below in two parts: preliminary measurements of the growth rate and factors affecting the rate.

4.3.1 Preliminary Measurements of the Stirred Growth Rate

EXPERIMENTAL

In the preliminary stirred runs, the apparatus and procedure was similar to that used for the stirred dihydrate growth rate measurements in section 3.3. As for the unstirred hemihydrate crystals, the measurements were made at 98°. Solution concentrations were 17.0 and 18.5 millimoles per litre and crystal velocities ranged from 4.2 to 65 cm/sec.

RESULTS

The results of these measurements are listed in

THE EFFECT OF STIRRING ON GROWTH OF HEMIHYDRATE (RUN 573)

FIGURE 34

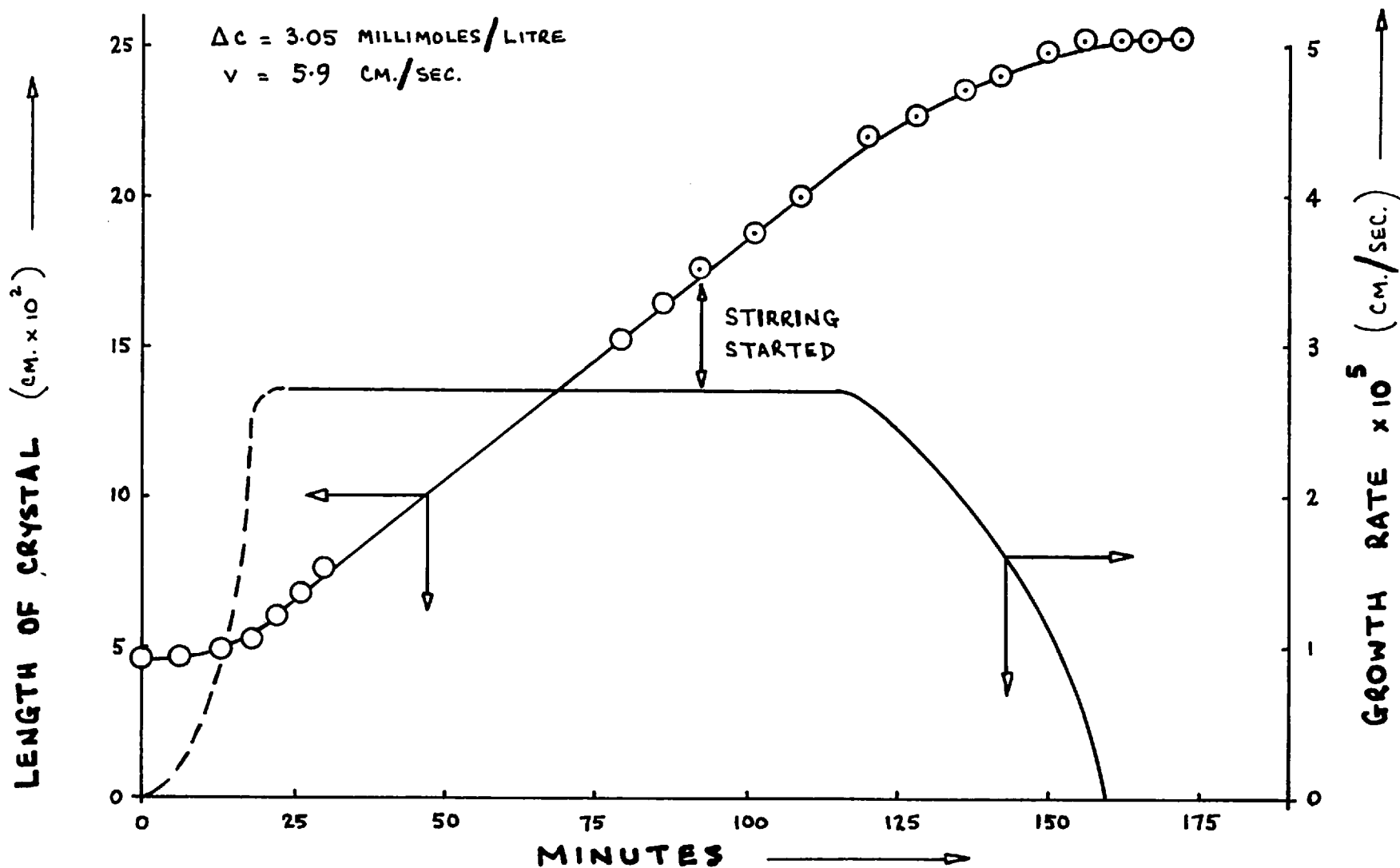


table 16. In most of these runs, the rate continually decreased over the period of stirring and eventually growth ceased altogether. A typical run is illustrated in figure 34 where the displacement and corresponding growth rate of the crystal are plotted against time. In this run, the crystal was unstirred for about 90 minutes and a constant growth rate was observed. Stirring was then begun and this rate of growth was maintained for a further 25 minutes after which it decreased sharply to zero.

The time elapsed between the beginning of stirring and the cessation of growth varied widely in these runs, as indicated in table 16. In some, growth stopped in a few minutes and in a few, no growth whatsoever was measured after stirring was begun. It was also observed that in both batch and flow systems, crystals which had stopped growing during stirring often did not resume growth when stirring was stopped.

Analysis of the solution concentration in several runs showed no significant difference between growth and non-growth conditions. Nor were there any heat of crystallization effects detected in temperature measurements of the solution at points up to 1 mm. from the crystal tip.

Although the hemihydrate crystals were long, thin needles, breakage during stirring was uncommon and

easily recognized by a sudden change in crystal length, after which growth resumed.

In a very few of these runs, it was observed that the solution became progressively cloudy when the crystal was stirred. This cloudiness was caused by the glass dust produced when the crystal support rod rotated at high speeds in the glass sleeve. Gradually, the dust fell into the solution and settled out on the surfaces in contact with the solution. This same cloudiness was occasionally observed in the stirred dihydrate experiments reported in section 3.3, but no effect on the growth rate was detected in that case.

4.3.2 Effect of Impurities on the Growth of Hemihydrate

In crystal growth, the surface reaction is often affected by the presence in solution of impurities which may become attached to the crystal surface. Growth may then be inhibited by the reduction in the number of sites available for solute adsorption, and may stop altogether if all the sites are covered by the impurity. In this section, experiments are described in which the effect on the hemihydrate growth rate of the glass dust observed in the previous section was investigated.

EXPERIMENTAL

Four types of experiments are reported in this section and the procedure for each is described below.

(1) The growth rates of stirred dihydrate and hemihydrate crystals were measured simultaneously. One seed crystal of each of the two hydrates was mounted on the same glass rod so that the growth rates could be obtained under identical conditions for comparison.

(2) The effect on the unstirred hemihydrate growth rate of a visible deposit of glass dust on the crystal tip was investigated. Some glass dust was added to the solution either by stirring the glass rod for some time or by crushing and grinding a piece of glass rod and adding the dust to the solution. The crystal was then observed for a visible deposit as the growth rate was measured.

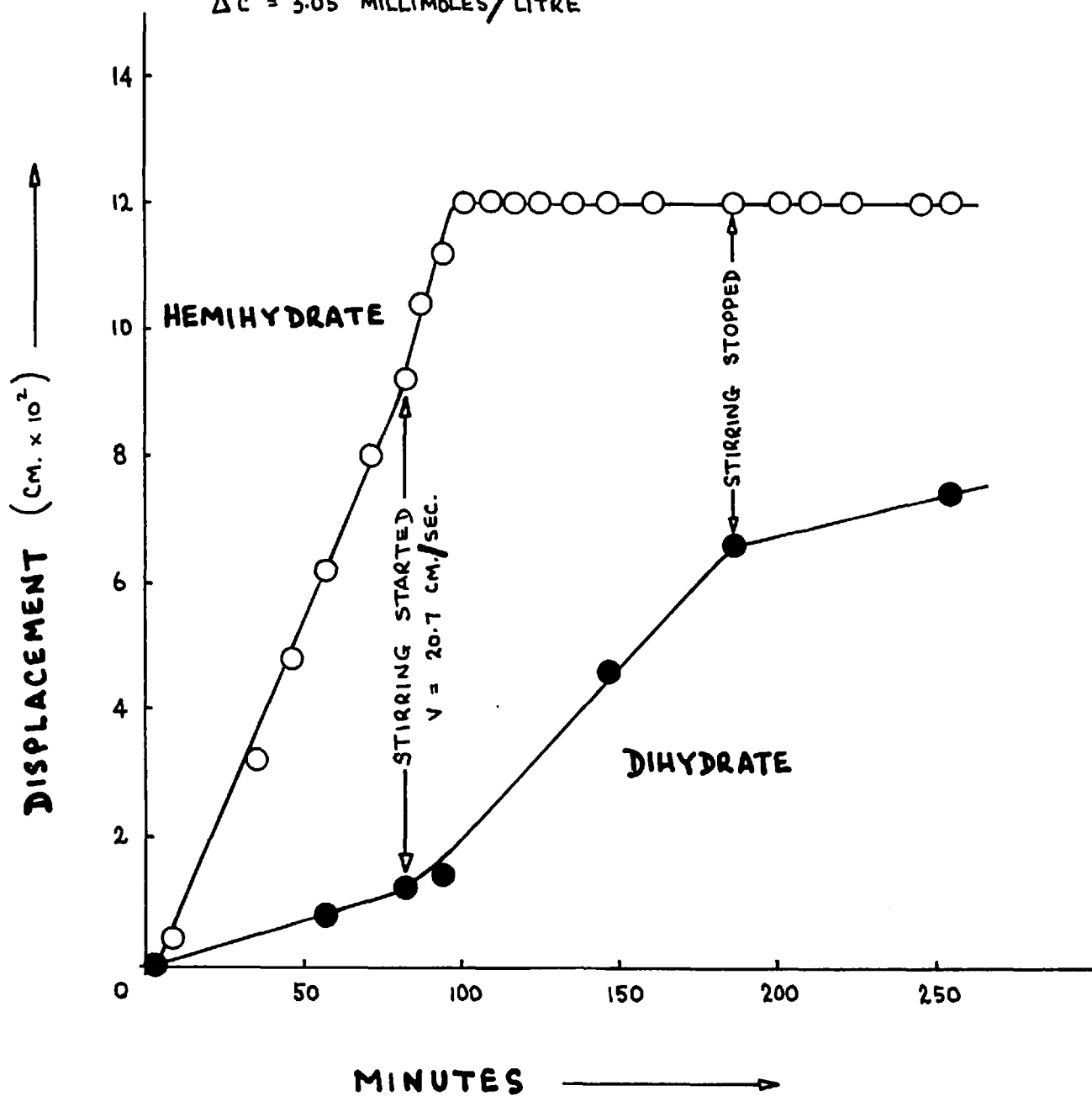
(3) The effect of partial dissolution on subsequent growth of hemihydrate was investigated. Crystals that had stopped growing were removed from the solution and immersed in distilled water for a few minutes. The crystal was then returned to the solution and the growth rate measured.

(4) The formation of glass dust was prevented in a few stirred runs either by using a brass crystal support rod in a brass sleeve or by using a rigid coupling, without sleeve, between the glass support rod and the motor.

SIMULTANEOUS GROWTH OF DIHYDRATE AND HEMIHYDRATE

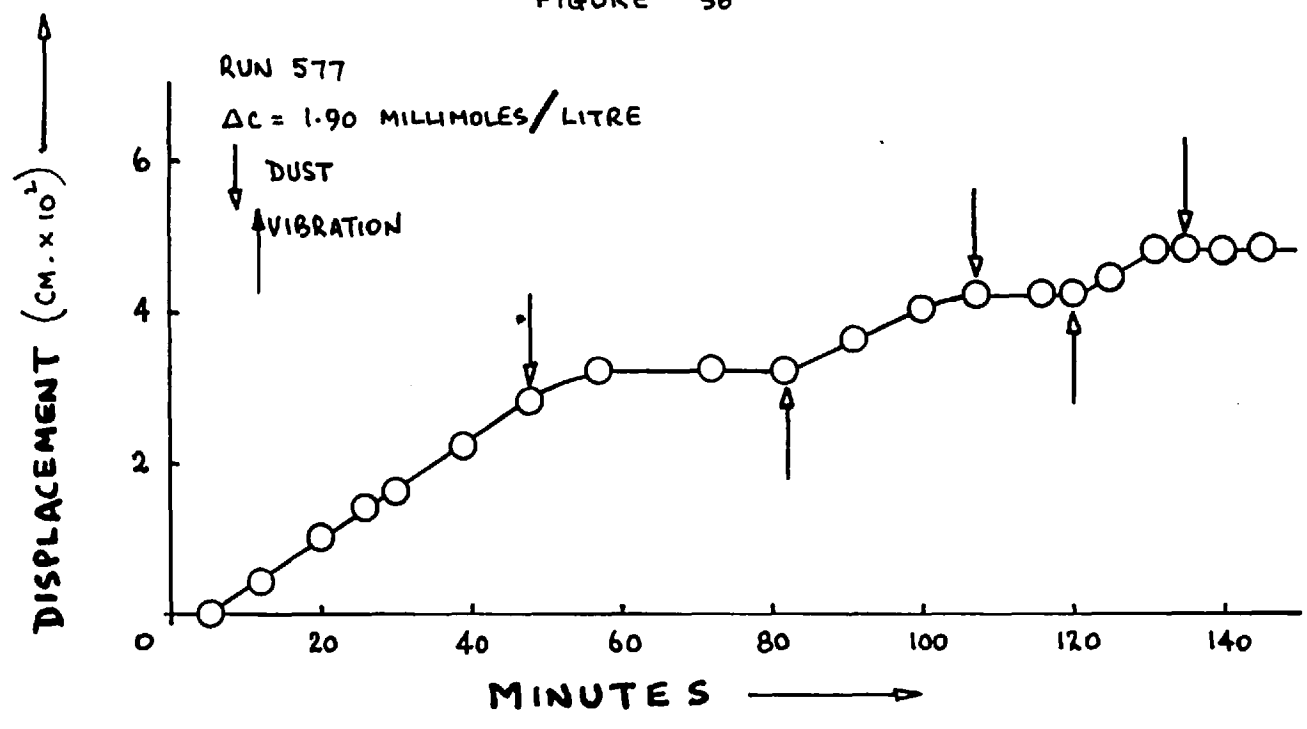
FIGURE 35

RUN 571

 $\Delta C = 3.05$ MILLIMOLES/LITRE

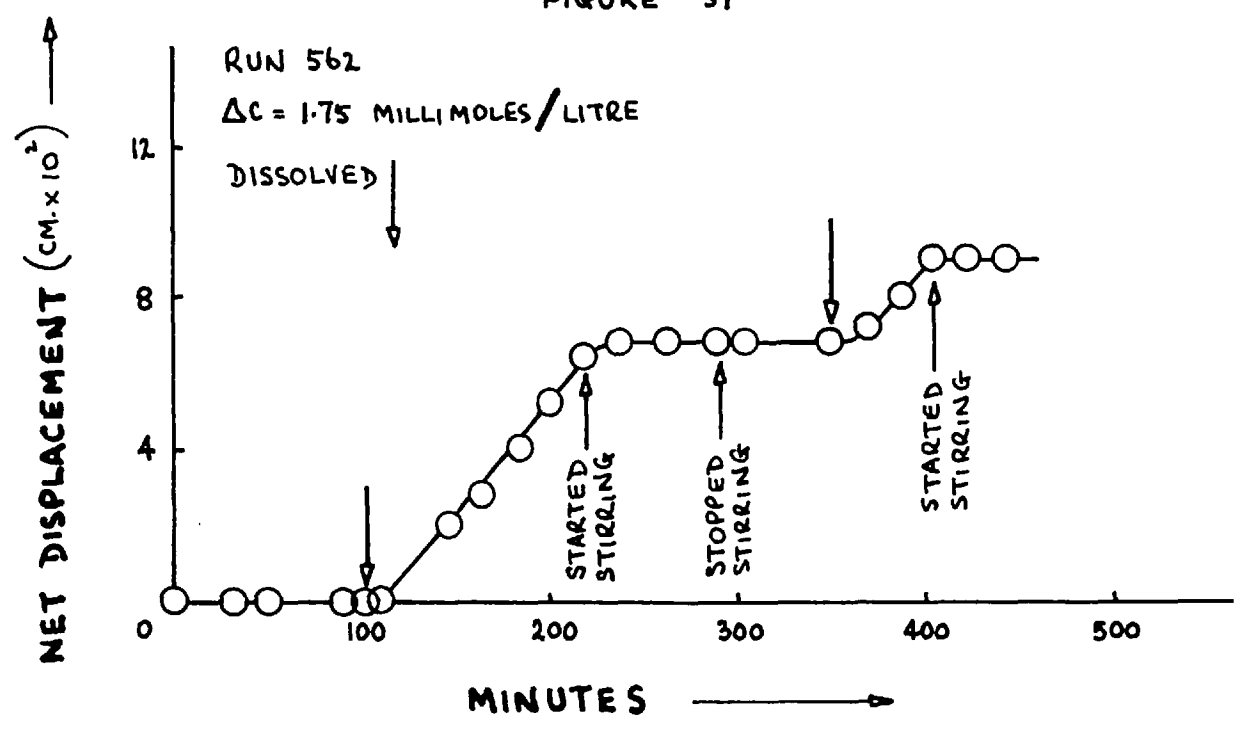
EFFECT OF GLASS DUST ON UNSTIRRED GROWTH RATE

FIGURE 36



EFFECT OF SURFACE DISSOLUTION ON GROWTH RATE

FIGURE 37



RESULTS

The results of the simultaneous growth rates of hemihydrate and dihydrate are listed in table 17. In figure 35, the displacement-time plot for a typical run is illustrated. This shows that the dihydrate, unlike the hemihydrate, does not have any tendency to grow at a reduced rate when stirred. Rather, the stirred rate is higher than the unstirred rate as reported in section 3.3. This provides further evidence that the solution concentration is not affected by stirring. It is evident from figure 35 that the hemihydrate grows at an increased rate just after stirring is begun, but this rate soon drops to zero and remains there even after stirring is stopped.

The effect of a visible deposit of glass dust on the unstirred growth rate of hemihydrate is indicated in table 18. In figure 36, a time-displacement plot of one of the runs is illustrated. The growth was observed to stop at about the same time as the presence of dust was detected on the growing crystal tip. That the crystal had in fact stopped growing and was not merely growing through the deposit was shown by lightly tapping the crystal support rod to remove the adhered dust. When this was done, the crystal length was found to be unchanged. However, growth resumed immediately after the dust had

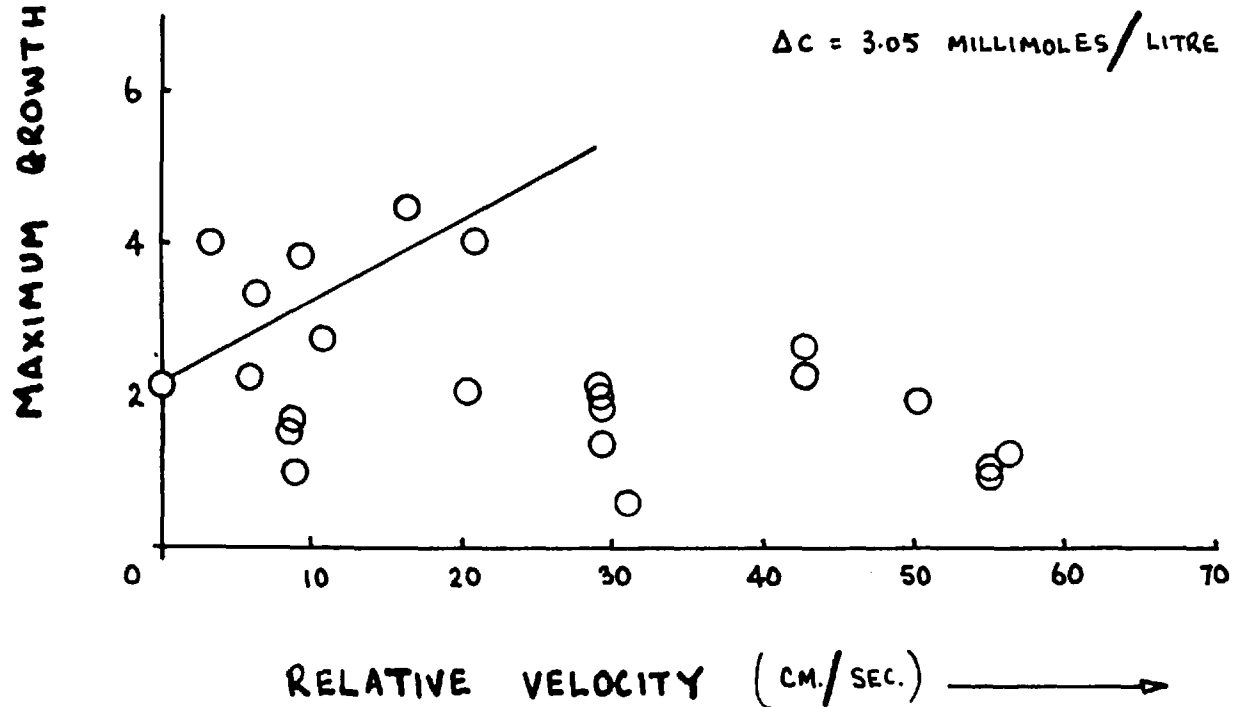
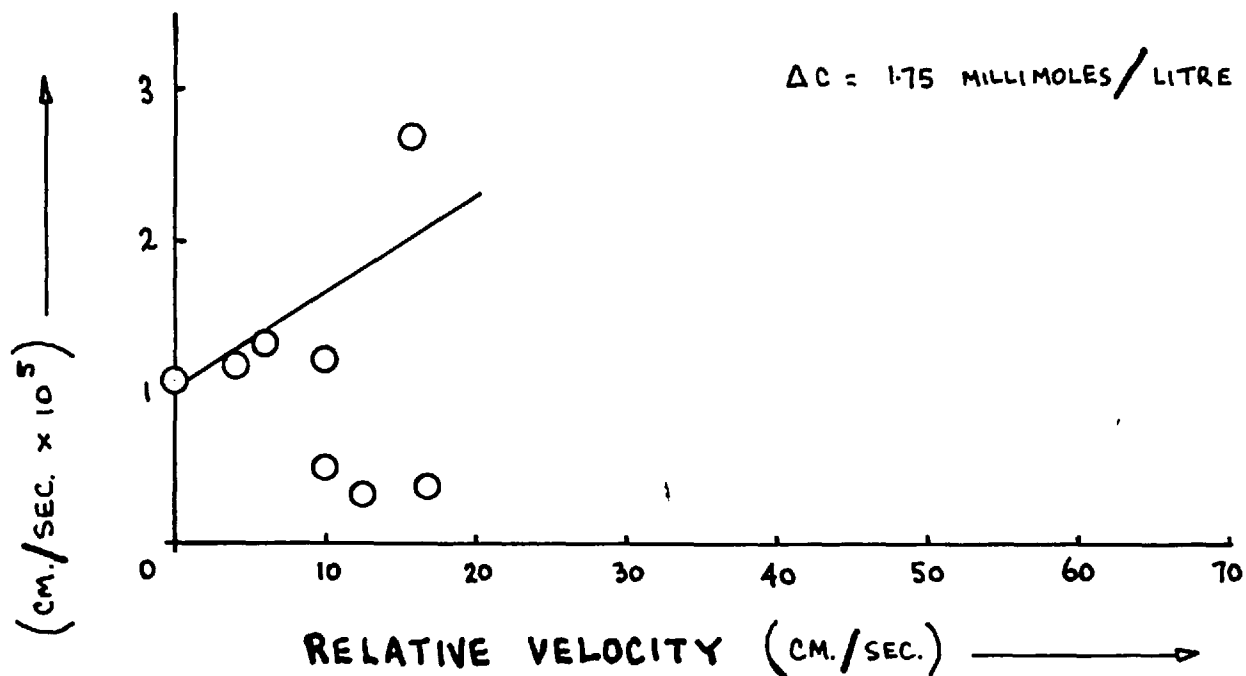
been removed. Clearly, a visible deposit of glass dust was sufficient to prevent growth of unstirred hemihydrate crystals.

Partial dissolution of a hemihydrate crystal that had stopped growing, only occasionally activated the crystal for growth. The results of these dissolution runs are listed in table 19, and a run in which activation occurred is illustrated in figure 37. If the growth stoppage of hemihydrate can be attributed to adhering impurities, dissolution would be expected to remove these and allow growth to proceed. It is not clear why growth resumed in only a few cases unless the freshly dissolved surface quickly picked up impurities when replaced in the solution.

When the formation of glass dust was prevented by using a brass support rod or a rigid coupling, stirred hemihydrate crystals with only one exception continued to grow for periods of up to 2 hours without any decrease in growth rate, as indicated by the results listed in table 20. Since the stirred growth rate was generally constant in the absence of glass dust this, together with the fact that visible deposits of glass dust have been shown to inhibit the growth of unstirred hemihydrate crystals, strongly suggests that the cause of the decrease in growth rate of stirred hemihydrate crystals in the

MAXIMUM STIRRED HEMIHYDRATE GROWTH RATE

FIGURE 38



present work is a coating of glass dust on the growing tip of the crystal. If this is so, a very small deposit appears to be sufficient since in the previous runs, none was visible on stirred crystals that had stopped growing in solutions containing glass dust, when the crystals were examined at 150x magnification. Although the presence of glass dust may not be the sole cause of the growth rate decrease in these experiments (growth stopped in one of these runs with a rigid coupling and has also been observed to stop in the experiments described in the following chapter where a brass rod was rotated in a brass sleeve), it clearly is a factor which affects the growth rate.

In figure 38, the maximum stirred hemihydrate growth rates are plotted against stirring velocity, excluding runs where no growth occurred. The rates are also listed in table 21. These rates were generally obtained just after stirring was started and they subsequently decreased to zero. It is probable, therefore, that many are below the true stirred growth rate of the hemihydrate since the rate decrease set in very rapidly in some runs. Nevertheless, it appears that at the low stirring velocities an increase in the rate is brought about by stirring the crystal, suggesting that the growth of hemihydrate may be partly mass transfer controlled under these

conditions. However, it should also be noted that the stirred growth rates obtained in the absence of glass dust were not significantly higher than the unstirred rate.

4.4 The Growth Rates of Hemihydrate and Dihydrate in 1.0 Molar Sodium Chloride Solutions

EXPERIMENTAL

A few measurements of growth rates of stirred and unstirred hemihydrate and dihydrate crystals were made in 1 M NaCl solutions in order to determine if their growth behaviour in these solutions was similar to that found in mixed calcium chloride and sodium sulphate solutions. The solutions were prepared by adding equal volumes of equimolar calcium chloride and sodium sulphate solutions to a volume of NaCl solution so that the total concentration of NaCl was 1 M. The apparatus and procedure for growth rate measurement was similar to that used previously. The crystals were mounted on glass rods and glass dust was produced on stirring. Solution temperature was again 98° and concentrations of 45.0 and 46.0 millimoles per litre were used.

RESULTS

The results of these measurements are listed in table 22. The solubility data of reference 30 were used.

These growth rates of hemihydrate and dihydrate are approximately equal in value to the growth rates measured previously in mixed calcium chloride and sodium sulphate solutions at corresponding supersaturations. As before, the growth rate of the dihydrate increased when the crystal was stirred, and the hemihydrate stopped growing after about 20 minutes of stirring.

A visible deposit of glass dust on an unstirred hemihydrate crystal in run 577 was again observed to affect the growth rate. The results of this run were therefore included in table 18.

It is apparent then that the growth behaviour of dihydrate and hemihydrate is largely unaffected by the sodium chloride present in the solution.

4.5 Summary

The growth rate of hemihydrate needles in the lengthwise direction has been measured in mixed calcium chloride and sodium sulphate solutions at 98° . The rate of growth of unstirred crystals was found to be dependent on the supersaturation to the power, 1.3, and was higher than the unstirred dihydrate growth rate, R_1 , at the same temperature. Differences in seed crystal sizes in the two cases, however, does not allow a direct comparison of the rates.

The rate of growth of stirred hemihydrate crystals was found to decrease with time until, in many cases, growth stopped altogether. The cause of this decrease is believed to be the presence in the solution of glass dust produced at high rates of stirring by abrasion of the glass stirring rod in the glass sleeve. Dihydrate crystals grown simultaneously in the same solution were not so affected and showed an increase in rate when stirred, as was found previously in section 3.3. Also, it was shown that the growth rate of an unstirred hemihydrate crystal could be inhibited by a visible deposit of glass dust on the growing tip. When the formation of glass dust in solution was prevented, stirred hemihydrate crystals generally grew at a constant rate.

An increase in the growth rate with stirring appears to be indicated, suggesting that the overall growth rate may be to some extent mass transfer controlled.

The growth rates of hemihydrate and dihydrate measured in 1 M NaCl solutions were similar to those in mixed calcium chloride and sodium sulphate solutions for similar supersaturations. Stirring and the presence of glass dust had an effect on the growth rates similar to that found in previous experiments.

CHAPTER 5

THE FORMATION OF MASSIVE DEPOSITS OF
DIHYDRATE AND HEMIHYDRATE5.1 Introduction

Up to this point, the present work has been concerned with the kinetics of formation and growth of single crystals in the bulk of the solution. With this as a basis, the following work investigates the mechanism and the rate of formation of massive deposits of these crystals on both metal and crystal surfaces.

As indicated in section 1.3, the mechanism of scale formation on a surface would be expected to be comprised of at least two and possibly three steps:

- (1) The initial formation of crystal nuclei either on the surface or in the bulk of the solution followed by attachment to the surface.
- (2) Growth of these crystal nuclei, and possibly -
- (3) Further nucleation either on the existing deposit or in the bulk of the solution followed by attachment to the deposit.

In this chapter, exploratory studies on the form of dihydrate and hemihydrate deposits on both heated and unheated metal surfaces are reported along with measurements of the rate of deposition of these two hydrates on

unheated metal surfaces. Various conclusions are drawn regarding the mechanism of deposition, and an attempt is made to relate the results of the deposition rate measurements to the single crystal growth rates reported in previous chapters.

5.2 Exploratory Investigations of Deposition on Unheated Metal Surfaces

The studies reported in this section are chiefly qualitative in nature. The experiments were carried out, using small volumes (1 to 2 ml) of solution, to provide general information on the conditions favouring crystal deposition on an unheated metal surface.

EXPERIMENTAL

A number of glass tubes of two types, B and D (see figure 4), were prepared for use in these experiments. Equal volumes (about 1 ml) of equimolar solutions (44 millimoles per litre) of sodium sulphate and calcium chloride were introduced into separate legs of these tubes with a long-tipped pipette. In some runs, a few drops of concentrated hydrochloric acid were also added, in order to give the normally neutral solution a lower pH. For the runs in B tubes, a 1.5 inch length of metal wire was dropped into the solution in one leg, and the top of the tube was sealed. For the runs in D tubes, the

wire was inserted in the stirring rod which was then placed in the tube. The tubes were then placed in the constant temperature bath at 100° , and after sufficient time had been allowed for the solutions to reach bath temperature, the tubes were tipped to mix the solutions. In D tubes, stirring was commenced at the time of mixing. Deposition on the wire and elsewhere in solution was observed with a travelling microscope at intervals up to an hour or more.

Eight kinds of metal wires (18 gauge S.W.G.) were used: galvanized iron, steel, copper, aluminium, platinum, nickel-chromium, tungsten and stainless steel. The surface of the wire was prepared in one of the following three ways: (1) no treatment whatsoever, (2) a section of the wire was filed to remove surface impurities and (3) a section of the wire was coated with cellulose acetate paint.

RESULTS

In all of these experiments, the hemihydrate crystals were first observed in the bulk of the solution, as noted previously in section 2.5. Later, crystals were detected on the various surfaces exposed to the solution, and when the wire was unstirred, crystals were sometimes observed in the process of attaching to the metal surface. Although the rate of stirring in the D tubes (about 200

HEMIHYDRATE DEPOSITS ON METAL WIRES

Figure 39

Run 204



Painted galvanized iron wire
with a scraped section
(unstirred 4 hours)

Magnification : 9x

Run 225



Galvanized iron wire with a
filed section (stirred 15
minutes - unstirred 25 minutes)

Magnification : 10x

rpm) was rather low, it was sufficient to give considerable agitation in the solution, and the density of the deposit on the metal surface was generally lower for stirred wires than for unstirred.

In figure 39, photographs of the deposits in two of these experiments are shown. The needle-like hemihydrate crystals were usually attached at one end to the metal surface, as indicated in the first photograph (run 204), and often a cluster of crystals appeared to be attached at a point. No preferred orientation on the surface was apparent.

In table 23, the effect of the type of metal, the surface treatment and the solution acidity on the density of the deposit on stirred wires is summarized. These results indicate that the corrosion resistance of the metal influences the density of the deposit, the deposit being heavier on metals with a low corrosion resistance. Presumably, this is because metals that are easily corroded have a rougher surface, making it easier for crystals to become attached. The photographs in figure 39 illustrate this point. In the first photograph, the visible crystals are all attached to the bare, untreated section of the wire, the outline of which is just discernible, and there are virtually none on the surrounding painted section. In the second photograph,

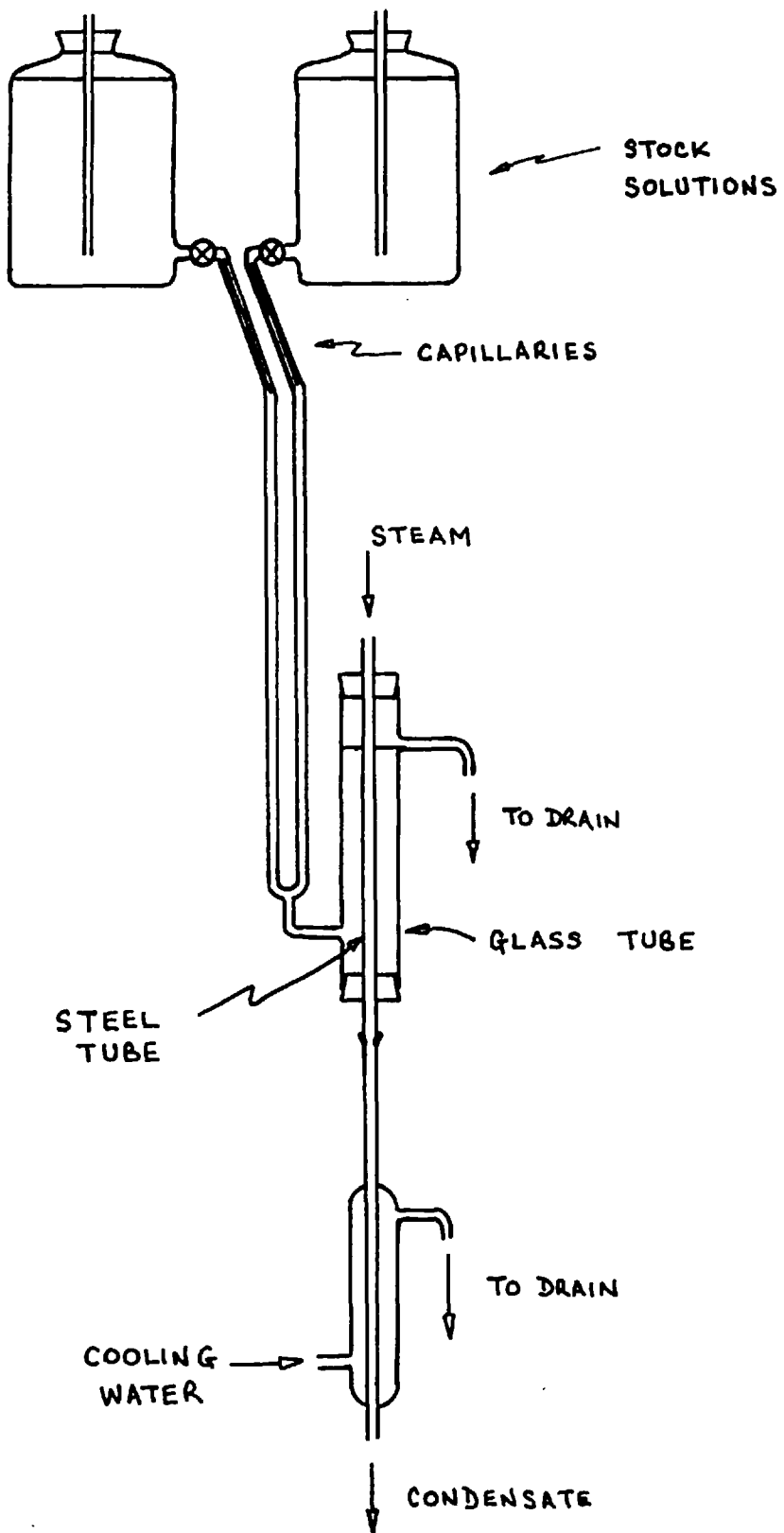
there is a heavy deposit of crystals on the untreated sections of the wire on either side of the filed section (dark vertical strip between) to which no crystals appeared to be attached. It seems that painting or filing a section made the surface smoother and less amenable to crystal attachment.

The deposit density recorded in table 23 is an arbitrary measure of the relative numbers of crystals, but in one unstirred experiment, the numbers of crystals on various surfaces in contact with the solution were counted and the area of the surfaces estimated. In table 24, the resulting deposit densities are listed. It is apparent from these values that the density is much higher on the bare section of the wire than on the painted section. This can also be seen in figure 39 where the first photograph shows this same wire after 4 hours in the solution.

Thus, these results suggest that the crystals nucleate in the bulk of the solution and later become attached to the surface, the number attached depending on the roughness of the surface. Also, attachment is apparently more difficult in agitated solutions.

APPARATUS FOR DEPOSITION ON A HEATED SURFACE

FIGURE 40



5.3 Exploratory Investigations of Deposition on a Heated Metal Surface

In this section, qualitative studies on deposition on a heated metal surface over a limited range of experimental conditions are reported. These experiments were carried out to determine whether the form of the initial deposit on a heated surface was similar to that reported for an unheated surface in the previous section.

EXPERIMENTAL

The apparatus used in these experiments is illustrated in figure 40. The flowrate of each of the feed solutions was controlled by similar capillaries so that equal volumes (135 cc.hr^{-1}) of the equimolar calcium and sulphate feed solutions were mixed just before entering the scaling section. The mixed solution then passed through the scaling section, depositing calcium sulphate on the outside of the 0.5 inch diameter heated steel tube. Heat was provided by passing superheated steam through the steel tube, the flowrate of the steam being controlled to give near boiling to vigorous boiling conditions in the solution. The form of the deposit was observed for periods of up to 90 hours.

In four experiments, the concentration of each of the calcium chloride and sodium sulphate feed solutions was 44 millimoles per litre. In the other experiment, a

DEPOSITS ON A HEATED SURFACE

Figure 41

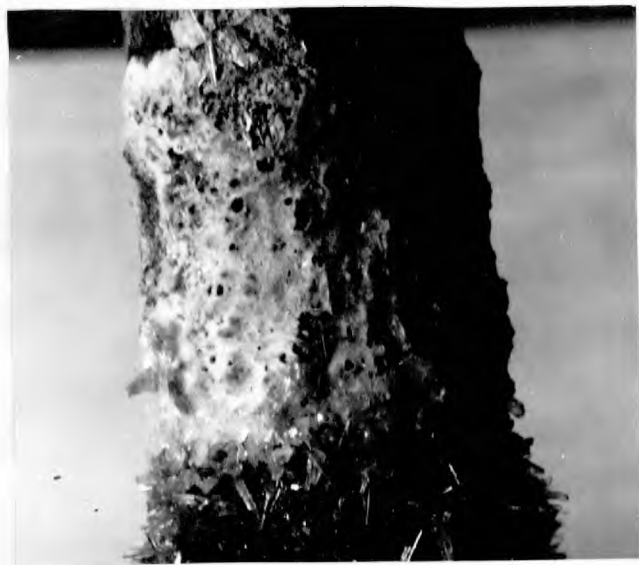


Run 375

Dihydrate crystals

after 64 hours

Magnification : 5x



Run 372

Dihydrate deposit at

solution surface

after 16.5 hours

Magnification : 5x

synthetic sea water brine was prepared by dissolving the major salts in water, as indicated in table 25. The concentration of the brine was about 4.25 times that of normal sea water.

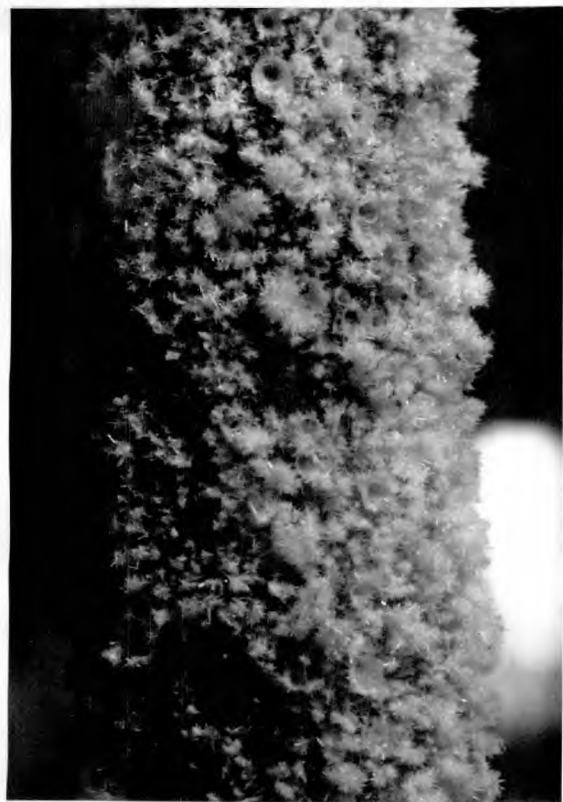
RESULTS

In these experiments, the crystals were observed in the solution and on the glass walls of the scaling section as well as on the heated steel tube, but generally most of them were attached to the heated surface. The deposit, which was thicker at the lower end of the tube where the solution entered the scaling section, developed considerable adhesion to the metal surface over the period of the experiment.

In table 26, the results of these experiments are summarized. The crystals formed in mixed calcium chloride and sodium sulphate solutions were entirely the dihydrate, and the first photograph (run 373) of figure 41 illustrates the nature of the deposit. It had a rather porous structure, being composed of large separate crystals (up to a few mm. long) radiating outwards from the tube surface. The deposit thus resembles that reported in the previous section. (Golightly and McCartney¹³ reported the same sort of structure for dihydrate deposits on a heated surface in experiments carried out under similar conditions.) Although the solution was boiling

DEPOSITS ON A HEATED SURFACE

Figure 42



Run 377
Hemihydrate crystals
after 70 hours
Magnification : 3x



Run 377
Hemihydrate "rings"
after 70 hours
Magnification : 3x

at the surface at the beginning of this run, the boiling ceased as the deposit grew and hence the deposit illustrated in this photograph corresponds to non-boiling conditions.

The deposit on the steel tube at the solution surface was very much different in appearance, as indicated by the second photograph (run 372) of figure 41. This portion was much more compact and was found to consist of tiny dihydrate crystals. This was presumably due to evaporation of the solution at the triple interface (solution - steel tube - air) causing increased nucleation in the thin film of highly supersaturated solution.

In the experiment using synthetic sea water brine, the crystals were entirely hemihydrate and the first photograph of figure 42 illustrates the appearance of the deposit on the lower and middle sections of the steel tube. It is apparent that the hemihydrate crystals were very much smaller than the dihydrate crystals produced in the previous runs, and the structure of the deposit was somewhat less porous. The deposit on the upper end of this tube, where boiling occurred during most of the run, is illustrated in the second photograph of figure 42. Here, an extended form of the rings of crystals, as reported by Partridge⁷ and others, is evident.

As with the dihydrate deposits at the solution surface in the previous runs, the deposit which formed in the boiling region was more compact.

Thus, under these experimental conditions, the initial calcium sulphate deposits formed on a heated surface in non-boiling solutions are similar to those obtained on an unheated surface in the previous section. That is, the deposit is a porous structure of separate crystals radiating outwards from the surface. It appears also that at temperatures approaching 100°C , dihydrate deposits in calcium sulphate solutions whereas hemihydrate deposits in the synthetic sea water brine.

5.4 The Rate of Deposition on a Metal Surface: Isothermal Conditions

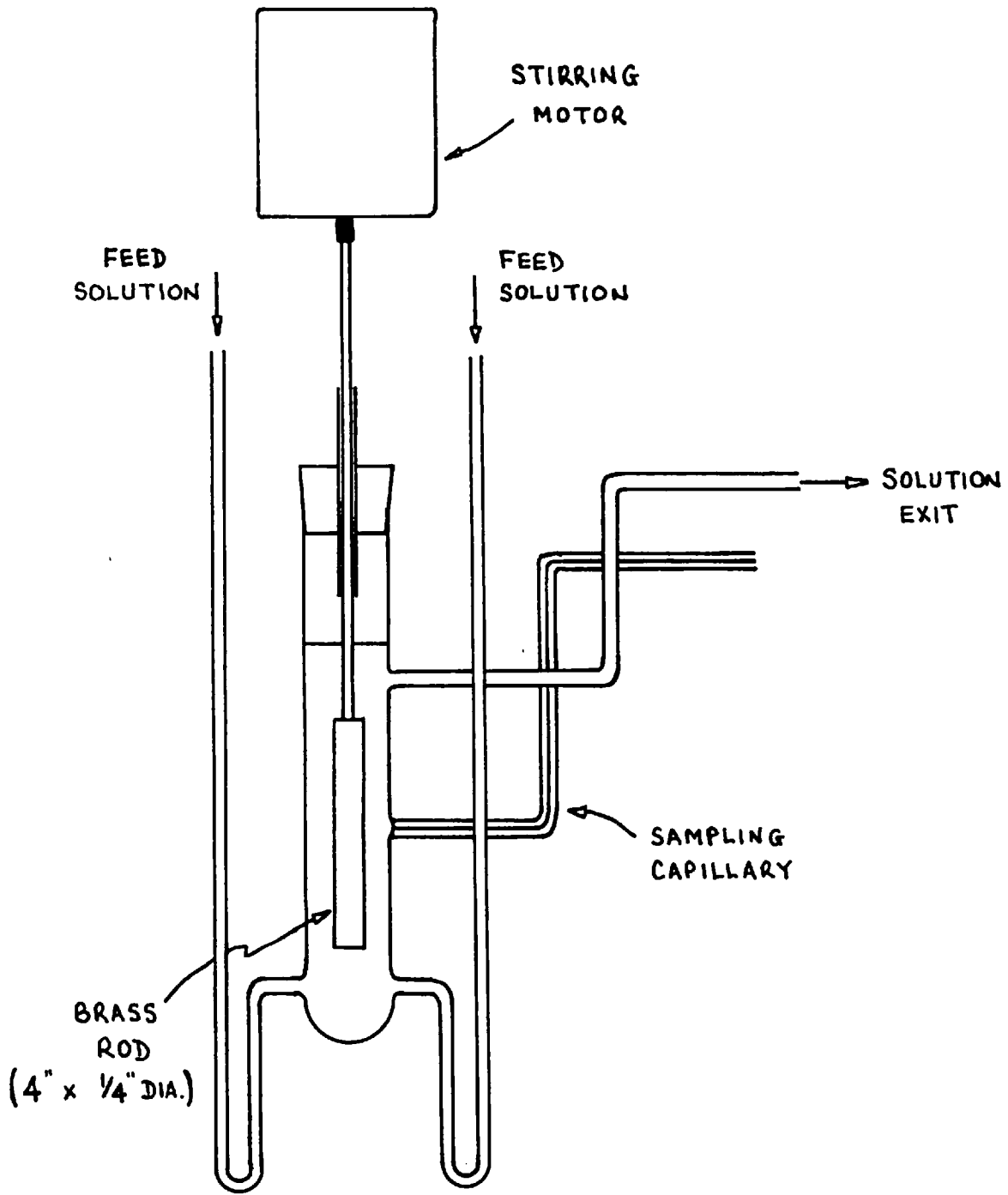
In this section, measurements of the rate of build-up of dihydrate and hemihydrate deposits on a stirred, unheated metal surface under isothermal conditions are reported, and the results are compared to the growth rates of single crystals reported in Chapters 3 and 4.

EXPERIMENTAL

The apparatus used for these measurements was a flow system similar to that illustrated in figure 16: but in place of the glass rod and guide shaft, a brass rod and guide shaft were inserted as illustrated in figure

APPARATUS FOR DEPOSITION RATE MEASUREMENTS

FIGURE 43



43, with the rod positioned midway between the solution inlets and outlet.

The surface of the rod was prepared for the runs in the following way. When a new rod was used, the surface was lightly rubbed with a fine grade of emery paper and then a few crystals of the hydrate desired for growth were deposited on its surface. For dihydrate crystals, the rod was dipped into a calcium sulphate solution at room temperature, removed and allowed to dry in air leaving tiny dihydrate crystals deposited on the rod. For hemihydrate, the rod was immersed in a highly supersaturated calcium sulphate solution at 100° until some crystals attached to the rod. In other runs, a rod with a deposit grown in a previous run was used. One run was started with a rod completely free of any deposit.

For most of these runs, the feed solutions were simple equimolar calcium chloride and sodium sulphate solutions. In a few runs, sodium chloride was added to each of these solutions, making them 1.0 molar in sodium chloride. The flowrate of each solution was controlled by similar capillaries in the feed lines as before, so that equal volumes of the solutions mixed continuously at the bottom of the deposition section. At various times during the run, 5 ml. samples of solution were withdrawn from the deposition section through the capillary (see

figure 43), cooled to room temperature and analysed for calcium ion concentration.

At the start of each run the deposition section, which had been thoroughly cleaned to remove any deposit from the previous run, was filled by starting the flow of the feed solutions. When the section was filled, it was immersed in the constant temperature bath and after sufficient time had been allowed for the solution to reach bath temperature, the brass rod was placed in the solution. After initial measurements of the rod with the travelling microscope (see following paragraph), the rod was started stirring. The relative velocity between the rod and the solution was measured as described in section 3.3.

The following procedure was adopted for measuring the rate of deposition. Stirring was stopped and the rod was set in a fixed position. With a 100 watt lamp illuminating the rod from the rear, the profile of the deposit was observed using a travelling microscope. The cross-hair in the eyepiece of the microscope was lined up along the deposit on each side of the rod and the displacement measured. This was repeated at fixed points 5 mm. apart (approximately the field of view of the microscope) along the length of the rod. Since the deposit was somewhat porous, two displacement measurements were made at each point. The first corresponded to the "base

DEPOSITS ON A STIRRED UNHEATED METAL SURFACE

Figure 44



Run 595
Dihydrate (larger crystals)
and hemihydrate deposit
after 54 hours
Magnification : 3x



Run 595
Hemihydrate deposit at
bottom of rod after 54 hours
Magnification : 3x



Run 594
Hemihydrate deposit after
21 hours
Magnification : 50x

deposit" which extended to the point where the deposit just began to transmit light. The second corresponded to the "tip deposit" which referred to the tips of the crystals extending furthest from the surface. These measurements were made at intervals of three hours or more with the rod in the same position each time, and half the change in the displacement was taken as the increase in the thickness of the deposit over the time interval. Each set of measurements required about 15 minutes to complete, after which stirring was resumed.

These experiments were carried out at 85° and 98° and were up to 80 hours in duration.

RESULTS

In these experiments, the deposit produced at 85° was exclusively the dihydrate, while that at 98° was usually a mixture of hemihydrate and dihydrate. The dihydrate deposits were similar in appearance to those obtained on a heated surface in non-boiling solutions in section 5.3 (see first photograph, figure 41). On the other hand, the hemihydrate deposits were harder and more compact with very good adhesion to the brass rod.

The photographs in figure 44 illustrate the deposits produced at 98° . The first photograph shows a mixed dihydrate and hemihydrate deposit, with the larger dihydrate crystals extending beyond the underlying

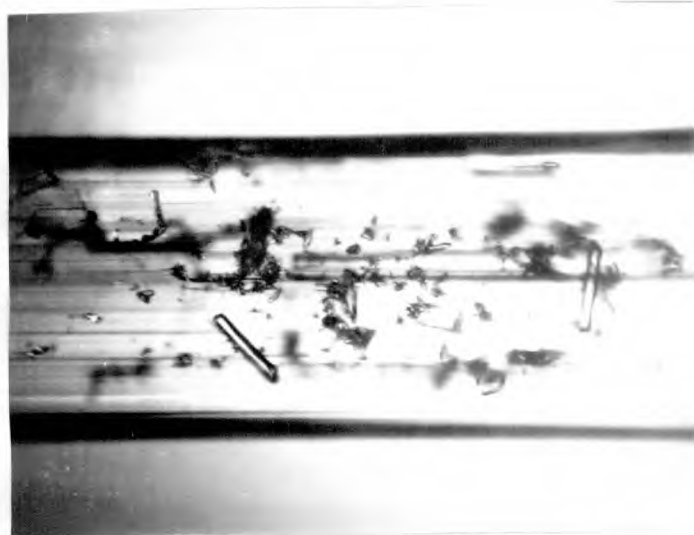
hemihydrate deposit. On the right hand side of this deposit, there are a few hemihydrate needles which grew to somewhat greater lengths than the rest of the hemihydrate crystals in the deposit. Another part of the same deposit is shown in the second photograph. This smooth-looking deposit consists almost entirely of tiny hemihydrate crystals radiating outwards from the rod surface much as the larger dihydrate crystals do. This is illustrated in the third photograph which shows a section of a hemihydrate deposit of this type at a higher magnification.

In the initial stages of the runs at 98° , the deposit appeared to be entirely hemihydrate. However, as the run progressed, a retardation in the hemihydrate growth rate appeared to occur and dihydrate crystals gradually became apparent in the deposit. Over the period of the run, these dihydrate crystals eventually grew to several times the length of the underlying hemihydrate crystals.

Sections of the dihydrate deposit obtained at 85° were also examined at a higher magnification. This examination showed that the relatively large dihydrate crystals visible at the surface of the deposit grew from a continuous base of tiny dihydrate crystals. There were also tiny dihydrate crystals attached to the surface of

DIHYDRATE CRYSTALS ATTACHED TO A LARGER DIHYDRATE CRYSTAL
FROM A DEPOSIT ON A STIRRED UNHEATED METAL SURFACE

Figure 45



Top and side views of a large dihydrate crystal with smaller dihydrate
crystals attached to its surface - from Run 427 after 79 hours

Magnification : 50x

the larger crystals, particularly in the area of the crystal nearest the base, and in some cases these smaller crystals completely covered the surface of the larger ones. In figure 45, the top and side views of one of the large crystals are shown. The presence of these tiny crystals appears to indicate that there is a third step in the mechanism of deposition (see section 5.1) i.e. further nucleation either on the existing deposit, or in the bulk of the solution followed by attachment to the deposit. The question of the source of this nucleation is taken up in the following chapter.

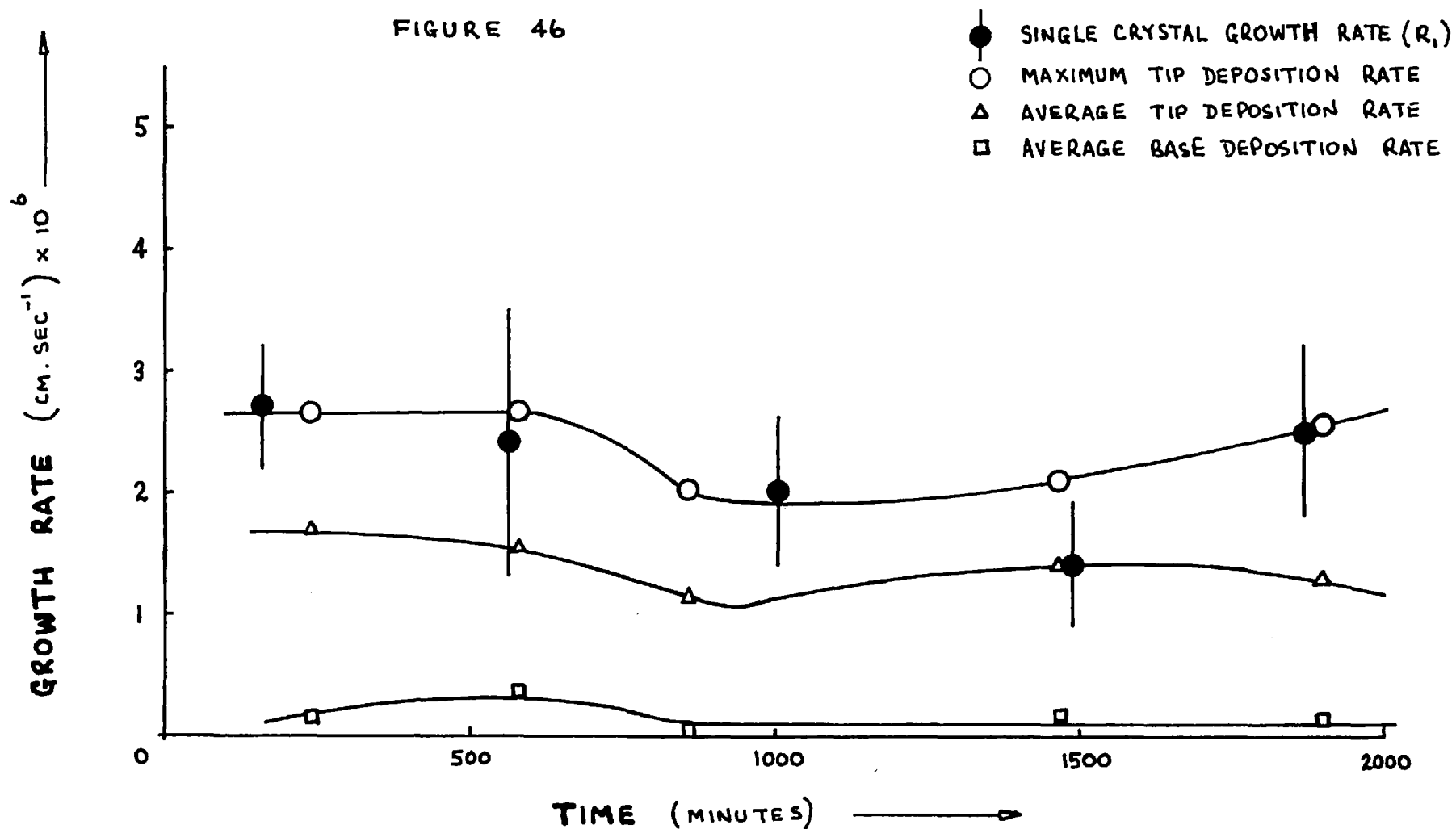
The results of the rate of deposition measurements are listed in tables 27 and 28. The average rate of deposition was taken as the arithmetic mean of the rates at the points of the traverse along the deposit. Also listed in these tables are the maximum rates observed at any point on the traverse.

In table 27, it is evident that the measured solution concentration in the first three runs with the low solution flowrate (about 100 cc.hr^{-1}) decreased as the deposit built up and the surface area of the growing crystals increased. This tendency was not as apparent in later runs with higher solution flowrates.

The average base deposition rates are seen to be generally less than the average tip deposition rates.

COMPARISON OF DIHYDRATE DEPOSITION RATES IN RUNS 422 - 426
 (EACH RUN CONTINUING WITH THE DEPOSIT OF THE PREVIOUS RUN)
 WITH SINGLE CRYSTAL GROWTH RATES AT 85°C

FIGURE 46



Since the former, in the case of the dihydrate deposits at least, is a measure of the rate at which the porous deposit fills in, this difference in rates indicates that the deposit would tend to remain porous as it builds up.

In table 29, the maximum observed tip deposition rates at 85° in these experiments are compared to the growth rates of stirred single dihydrate crystals at the same temperature and supersaturation as reported in Chapter 3. Since these latter growth rates were measured at two solution concentrations only, interpolation of the results of Chapter 3 was necessary in order to estimate the single crystal growth rates corresponding to the measured solution concentrations in the deposition experiments. An equation of the form:

$$R_1 = K(\Delta c)^2$$

was used for this interpolation since this was found to adequately describe the effect of supersaturation on the single crystal growth rate at any one value of stirring velocity.

It is evident from table 29 that the maximum rate of tip deposition is generally equal to or less than (figure 46) the corresponding single crystal growth rate. Since these two growth rates were essentially equal in a number of the runs, this indicates that dihydrate crystals

grow at a similar rate whether in a deposit or in the bulk of the solution. However, the true growth rate of these crystals would be measured only if they were growing horizontally and perpendicular to the direction of observation, and since only a few crystals appeared to do so, it might be expected that in some runs the maximum observed growth rate of the crystals would be less than the growth rates reported in Chapter 3.

In table 30, the maximum observed tip deposition rates at 98° are compared to the growth rates of stirred single dihydrate crystals and unstirred single hemihydrate crystals at the same temperature and supersaturation, reported in Chapters 3 and 4. The growth rates of stirred hemihydrate crystals were found in Chapter 4 to be initially up to three times the rates listed here for unstirred crystals.

These results show that the maximum tip deposition rates were equal to or less than the hemihydrate single crystal growth rates in the early stages of the run and equal to or less than the dihydrate single crystal growth rates in the latter stages of the run. This is in agreement with the observed form of the deposit which was predominantly hemihydrate in the early stages, with dihydrate crystals later becoming apparent and extending past the hemihydrate crystals. As with the dihydrate at

85°, the hemihydrate and dihydrate crystals appear to grow at a similar rate in the deposit as in the bulk of the solution at 98°, but the observed rate is often a fraction of this rate because of the angle of attachment of the crystals to the surface.

The cause of the retardation in the growth rate of the hemihydrate deposit at 98° is somewhat puzzling since no glass dust could have been present in these experiments. It may be that other impurities having a similar effect on the growth rate were present in these solutions.

5.5 Summary

Exploratory investigations have been undertaken into the conditions favouring hemihydrate deposition on an unheated metal surface. These experiments indicated that the crystals appear to nucleate in the bulk of the solution and later become attached at one end to the metal surface. Deposits were heavier on metals with low corrosion resistance probably because the surface of such metals was rougher. Agitation in the solution was found to reduce the density of the deposit on the surface.

A few experiments were also carried out to investigate, over a limited range of experimental conditions, the form of a calcium sulphate deposit on a heated

metal surface. In non-boiling solutions, the deposit was composed of separate crystals radiating outwards from the metal surface, resembling the deposits on unheated metal surfaces. When evaporation occurred at the surface, the crystals were much smaller and the deposit much denser.

Measurements of the rate of deposition of dihydrate and hemihydrate on a stirred unheated metal surface have been made. Both the dihydrate and hemihydrate deposits were composed of separate crystals radiating from the surface, but the latter were much more compact. The maximum rates measured at various points on the deposits approached the corresponding growth rates of single crystals in the bulk of the solution reported in previous chapters, indicating that the crystals grow at a similar rate in the two cases. The average deposition rate, however, was less since the majority of the crystals did not grow perpendicular to the surface and to the direction of observation. A retardation in the growth rate of stirred hemihydrate crystals was also observed in these experiments.

Examination of the large crystals in the dihydrate deposits formed on an unheated metal surface showed that very small dihydrate crystals were attached to the surface, suggesting that nucleation was taking place during growth of the deposit.

CHAPTER 6

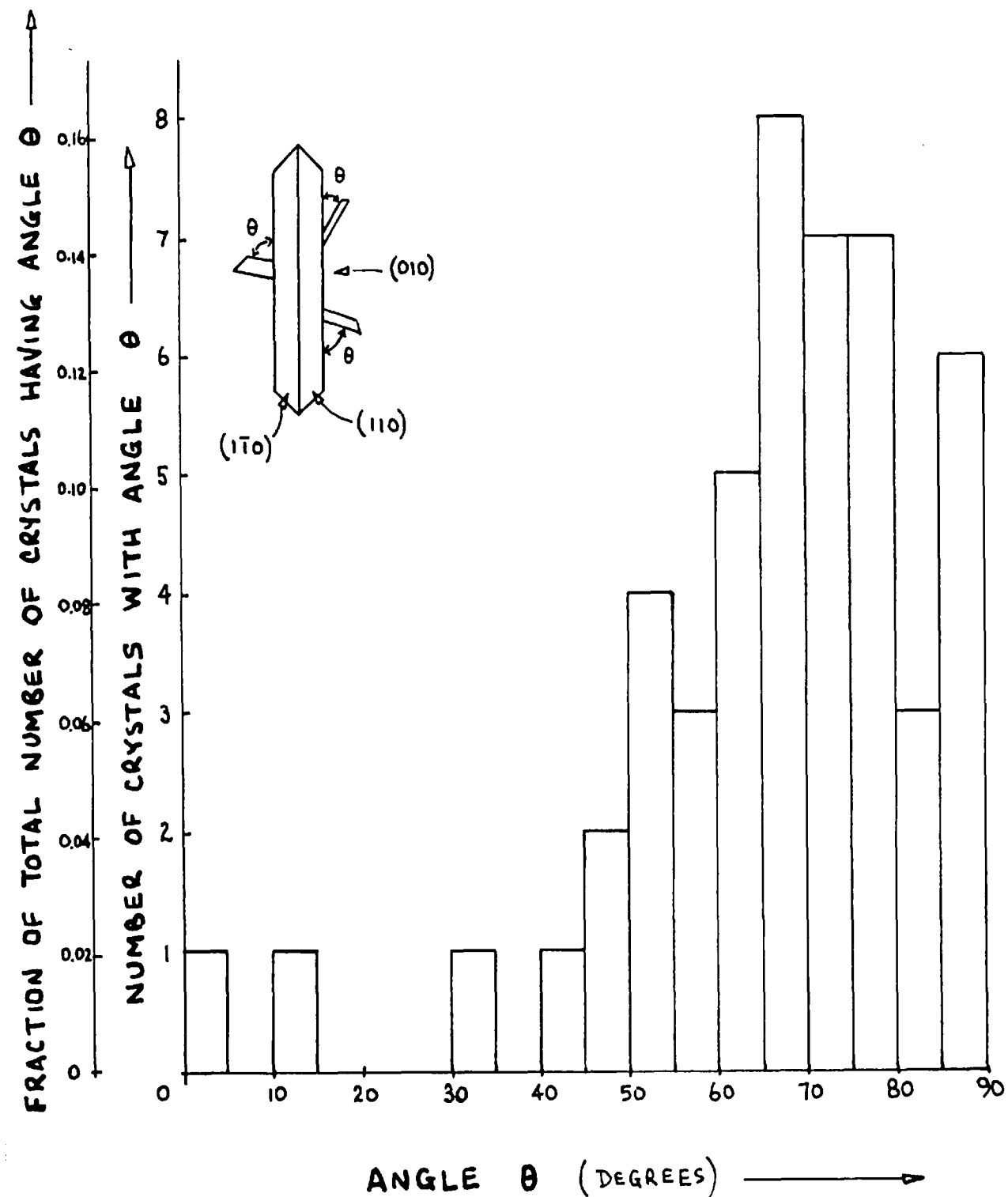
THE FORMATION OF CALCIUM SULPHATEDEPOSITS ON CRYSTAL SURFACES6.1 Introduction

The evidence so far indicates that the mechanism of calcium sulphate deposition on an unheated surface involves all three of the steps outlined in section 5.1 namely, the initial formation of crystal nuclei, the growth of these nuclei, and the formation and growth of further crystal nuclei. The existence of the third step was indicated by the results of section 5.4 where it was found that in deposits of dihydrate on an unheated metal surface, very small dihydrate crystals were attached to the surface of quite large dihydrate crystals.

The first two steps of the mechanism have been investigated in previous chapters. In this chapter, an investigation of the third step is reported. The experiments described below were carried out to determine the effect of various factors on further nucleation and to determine whether this nucleation takes place directly on the deposit or in the bulk of the solution followed by attachment of the crystal nuclei to the deposit.

THE ANGLE θ BETWEEN DIHYDRATE CRYSTALS
AND PARENT DIHYDRATE CRYSTALS

FIGURE 47



6.2 Examination of the Dihydrate Deposits Formed on Stirred Unheated Metal Surfaces

EXPERIMENTAL

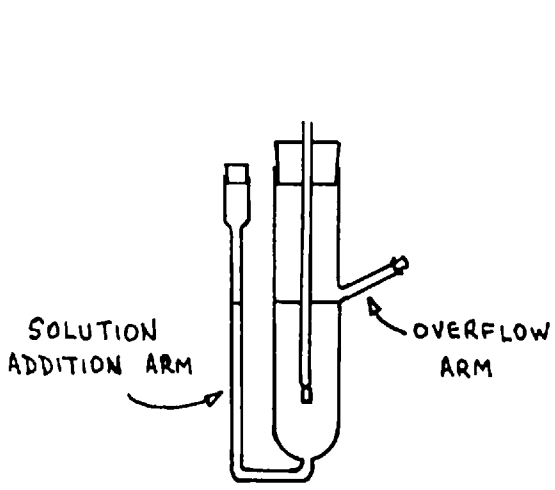
The first part of this investigation was a microscopic examination of some of the dihydrate deposits produced in the runs reported in section 5.4. Several of the large crystals (or parent crystals) radiating outwards from the base of the deposit were mounted on glass rods for easier manipulation, and the dihydrate crystals on their surfaces were observed from all directions at 150x magnification. Measurements were made of the acute angle Θ between the (010) plane of the parent crystal and the c axis of the small crystals projected on the (100) plane of the parent crystal. (The angle Θ is shown in the second photograph of figure 45.)

RESULTS

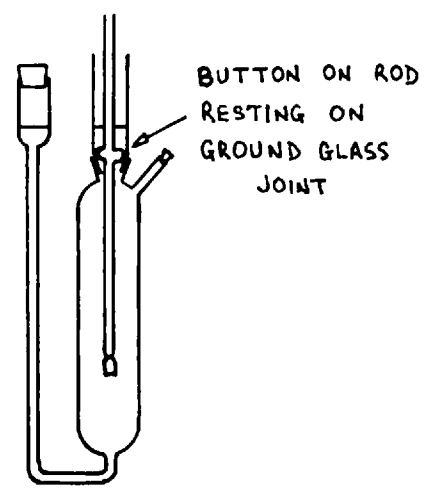
The results of these measurements are listed in table 31 and illustrated in figure 47. It is evident that the crystals tend to point primarily outwards from the parent crystal surface, but no single preferred orientation on the parent crystal is apparent. This tendency was noted when the crystals were observed from any direction.

TUBES USED IN DEPOSITION ON CRYSTAL SURFACE RUNS

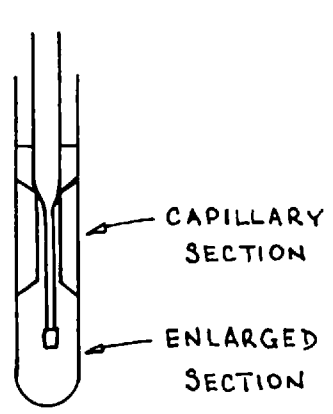
FIGURE 48



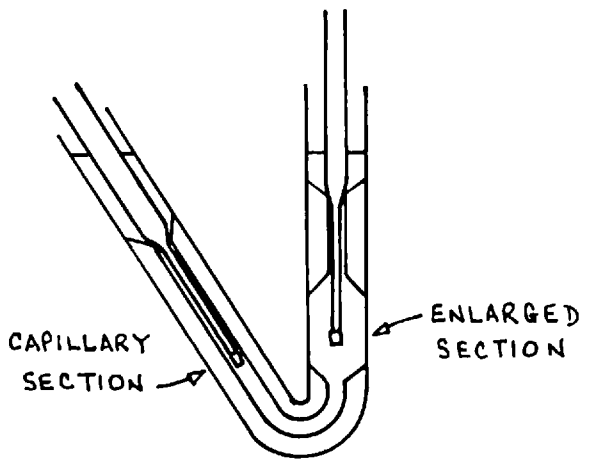
TYPE E TUBE



TYPE F TUBE



TYPE G TUBE



TYPE H TUBE

6.3 Nucleation of Dihydrate Crystals in the Presence of an Unstirred Dihydrate Seed Crystal

In the experiments reported in this section, a dihydrate seed crystal was immersed in a supersaturated calcium sulphate solution in which dihydrate crystals later nucleated. The seed crystal was not stirred during the experiment in order that the surface of the crystal and the surrounding solution could be more readily observed.

EXPERIMENTAL

Dihydrate seed crystals which were free of any visible surface crystals were fixed on glass rods with Araldite adhesive, with the c direction of the crystal parallel to the length of the rod. Relatively large seed crystals, up to several mm. in length, were chosen so that a reasonable surface area could be observed.

A number of glass tubes of two types, E and F (see figure 48), were prepared for use in these experiments. In F tubes, which were a minor modification of E tubes, any crystals which formed on the solution surface were prevented from settling into the solution by a button on the crystal support rod which rested on the ground glass joint. Since the tubes were each used several times, they were thoroughly cleaned before each experiment using the procedure outlined in section 2.6 for D tubes.

At the start of each experiment, the tube was filled with filtered (porosity 4 sintered glass filter) distilled water. The seed crystal was immersed in the water at room temperature for a period of from 10 to 35 minutes and the surface was dissolved to remove any tiny dihydrate crystals present. Measurements made under these conditions indicated that the dissolution rate was about $5 \times 10^{-6} \text{ cm. sec}^{-1}$ so that from 0.003 to 0.010 cm. was dissolved from the seed crystal surface.

A calcium sulphate solution was prepared by mixing equal volumes of equimolar solutions of calcium chloride and sodium sulphate. The solution was added through a sintered glass filter (porosity 4) to the solution addition arm of the tube, displacing the distilled water through the overflow arm.

Analysis of the solution remaining in the tube showed it to have an identical concentration to that of the solution added. The tube was then placed in the constant temperature bath and observation with a travelling microscope was begun. The experiments were all carried out at 85°C with solution concentrations in the range, 19.0 to 24.0 millimoles per litre.

RESULTS

Dihydrate crystals nucleated in all of these experiments and were first observed in the bulk of the

solution in numbers ranging from very few in the solutions at 19.0 millimoles per litre to very many in the 24.0 millimoles per litre solutions. Crystals were generally not observed on the surface of the seed crystal at the lower supersaturations, but as the supersaturation increased, greater numbers of crystals could be seen attached at one end to the seed crystal surface. The time at which the first crystal was observed on the surface decreased with increasing supersaturation and is listed for these experiments in table 32.

Crystals were occasionally observed in the act of settling from the solution onto the seed crystal surface. Some were loosely held and vibration of the support rod was sufficient to dislodge them. Others seemed to be more tightly held, possibly because of subsequent growth of either or both the seed crystal and the attached crystal.

The appearance of the deposit on the seed crystal surface was similar to that illustrated in figure 45. Again, as found in section 6.2, the crystals appeared to take up no particular orientation with respect to the seed crystal. Frequently, greater numbers of crystals were piled up in sheltered areas around the seed crystal and on the Araldite mounting, the surface of which was somewhat rougher than that of the seed crystal.

These results seem to indicate that nucleation takes place in the bulk of the solution and some of the crystals later become attached to the surface of the seed crystal.

6.4 The Effect of the Number of Crystals in the Solution on the Deposit Density on Crystal Surfaces

If nucleation occurs in the bulk of the solution and some of the crystals later become attached to the seed crystal surface, then it should be possible to control the number of crystals on the seed crystal surface simply by controlling the number of crystals present in the solution. To test this hypothesis, three types of experiments were carried out, and these are described in the following sections.

6.4.1 The Effect of the Addition of Barium Ion on Nucleation in the Solution

In these experiments, a small amount of barium ion was added to some of the calcium sulphate solutions, to remove in the barium sulphate precipitate any foreign materials present which could act as nucleation centres for calcium sulphate.

EXPERIMENTAL

Supersaturated calcium sulphate solutions were prepared by mixing equal volumes of equimolar calcium

chloride and sodium sulphate solutions. Equal volumes of the solution were filtered into two test tubes, and to one of these solutions a small volume of barium chloride solution was added giving a barium ion concentration of about 0.6 millimoles per litre (the sulphate ion removed by this precipitation was very small compared to the total concentration). Both solutions were then centrifuged for 10 to 30 minutes at about 2000 rpm. to remove the barium sulphate from the solution. Glass rods with or without dihydrate seed crystals were inserted and the tubes were placed in the constant temperature bath at 85° . Observation was then begun with a travelling microscope.

RESULTS

There was no apparent effect when barium ion was added to these solutions. The dihydrate crystals were first observed in the bulk of the solution as before, and the number of crystals deposited on glass or seed crystal surfaces was at least as great in the solution with added barium ion as in the solution without. In table 33, the time at which the first crystal was observed on the surface is listed for these experiments. Here again, there was no significant effect due to the presence of barium ion.

These results appear to suggest that either the

method used was ineffective in removing all of the foreign particles from the solution or the nucleation of calcium sulphate is not dependent on their presence.

6.4.2 The Effect of the Volume of Solution in Contact with the Seed Crystal

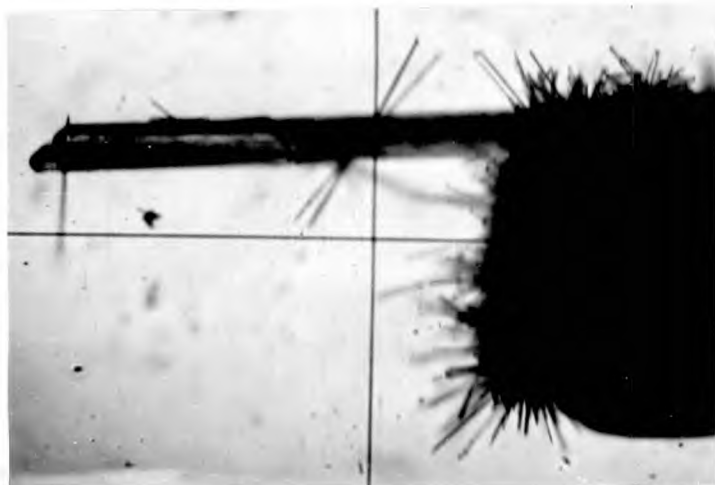
In many of the previous experiments, it was observed that the smaller dihydrate crystals in the solution were carried about by convection currents for quite some time before settling to the bottom of the vessel. In this section, experiments are described in which the effect of restricting convection, and hence the access of these crystals to the seed crystal, was investigated.

EXPERIMENTAL

For these experiments, glass tubes of three types were used: G, H (illustrated in figure 48) and J (simple 3.2 cm. diameter test tube). In the J tubes and the enlarged sections (1.2 cm. dia.) of the G and H tubes, convection was not restricted but in the capillary sections (0.2 cm. dia.) of the latter two types of tubes, movement of crystals in the solution was observed to be very slight. Type H tubes, which were used for the majority of these experiments, had the principal advantage that seed crystals could be immersed simultaneously in the enlarged and capillary sections, as shown in figure 48.

DIHYDRATE CRYSTALS ON DIHYDRATE SEED CRYSTALS FROM
ENLARGED AND CAPILLARY TUBES (RUN 451)

Figure 49



Dihydrate seed crystal
from enlarged tube
after 60 minutes
Magnification : 50x



Dihydrate seed crystal
from capillary tube
after 76 minutes
Magnification : 50x

Solution concentration : 24.0 millimoles per litre

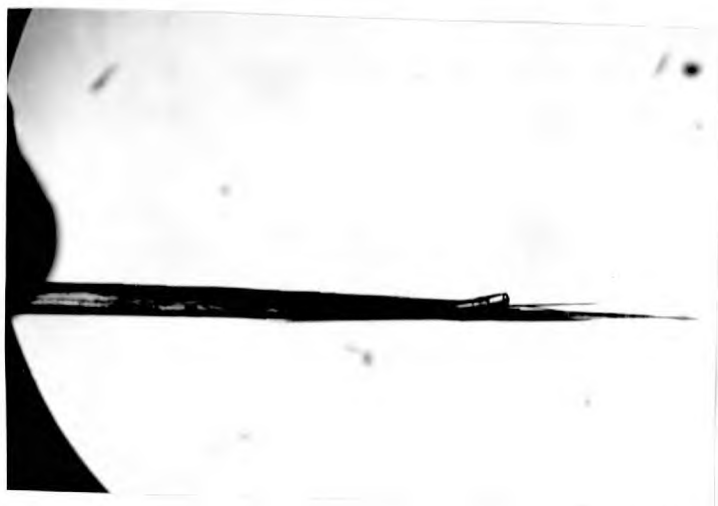
Solution temperature : 85°C

DIHYDRATE CRYSTALS ON HEMIHYDRATE SEED CRYSTALS
FROM ENLARGED AND CAPILLARY TUBES (RUN 615)

Figure 50



Hemihydrate seed crystal
from enlarged tube
after 138 minutes
Magnification : 50x



Hemihydrate seed crystal
from capillary tube
after 126 minutes
Magnification : 50x

Solution concentration : 25.0 millimoles per litre

Solution temperature : 100°C

The calcium sulphate solutions were prepared as before by mixing equal volumes of equimolar solutions of calcium chloride and sodium sulphate at room temperature. The solution, having a concentration in the range 18.5 - 25.0 millimoles per litre, was then added to the tube through a porosity 4 filter.

Seed crystals of dihydrate, hemihydrate and calcite, fixed on glass rods with Araldite adhesive, were used in these experiments. The dihydrate crystals were surface-dissolved before the run. Calcite crystals were prepared by cleaving clear pieces of Iceland Spar along the (100) plane. Seed crystals of hemihydrate and calcite were used as well as dihydrate in these experiments to determine if dihydrate deposits could form equally well on other crystal surfaces.

After inserting the seed crystals into solution, the tube was placed in the constant temperature bath at a temperature between 85° and 100° , and the seed crystal was observed with a travelling microscope. In a few runs, the growth rates of the dihydrate and hemihydrate seed crystals in both the enlarged and capillary tubes were also measured.

RESULTS

The photographs of figures 49 and 50 illustrate the effect of tube size on the number of dihydrate crystals attached to dihydrate and hemihydrate seed crystals

in these experiments (the same effect was observed with the calcite seed crystals). The first photograph in each figure shows the deposit on a seed crystal taken from an enlarged tube, and the second photograph shows the deposit on a seed crystal from a capillary. (In all cases the seed crystal is the horizontal spike protruding from the Araldite and glass rod mounting.) It is apparent that the density of the deposit on the seed crystal is very much reduced in the capillaries over that in the enlarged tubes. While many dihydrate crystals continued to circulate for some time in the solutions in the latter tubes, most of the crystals in the former tubes quickly settled onto the nearest surface and thus few crystals had the opportunity of contacting the seed crystal. It is also apparent that the dihydrate crystals can attach to hemihydrate (and calcite) seed crystals as well as to dihydrate seed crystals. Dihydrate crystals were also observed in large numbers on the Araldite mounting (photograph 1, figure 49) in the enlarged tubes.

In table 34, the times of observation of the first crystal on seed crystals in enlarged and capillary tubes are compared, and it is evident that the times are generally much shorter in the enlarged tubes. It was found also that the growth rates of dihydrate and hemihydrate seed crystals were similar in both types of tubes,

as indicated by the results listed in table 35, and hence the solution supersaturation must have been similar in the two tubes.

Since restricting the approach of crystals to the seed crystal surface has been shown to reduce the number of crystals attached, nucleation must be occurring, to some extent at least, in the bulk of the solution with some of the crystals subsequently attaching to the seed crystal surface. Also, since it was possible in some runs to entirely prevent deposition in this way, this appears to be the sole mechanism of formation of crystals on seed crystal surfaces under these conditions. If the crystals were nucleating directly on the seed crystal surface, such a large and consistent difference between the number of crystals attached to seed crystals in capillary and enlarged tubes would not be expected for solutions of the same supersaturation.

Since dihydrate crystals attached not only to dihydrate seed crystals but also to hemihydrate and calcite seed crystals, to the Araldite mounting and even to the glass rod, it appears that attachment to any suitable surface can occur irrespective of whether that surface is growing or not. Whatever the surface, attachment would be facilitated by the growth of the attached crystal into the irregularities of the surface, and it has been

observed that the fast-growing end of the crystal is often the point of attachment of the crystal to the surface.

6.4.3 The Effect of the Addition of Dihydrate Crystals on the Number of Crystals on the Seed Crystal

In the previous section, the effect of reducing the number of crystals in the solution around the seed crystal was investigated. In this section, experiments are described in which dihydrate crystals were added to the solution in order to increase the number of crystals in the solution around the seed crystal.

EXPERIMENTAL

The seed crystals used in these experiments were dihydrate and calcite, mounted as before on glass rods. In the runs with dihydrate seed crystals, type F tubes were used and the seed crystal was surface-dissolved before the run as outlined in section 6.3. Type J tubes (simple test tubes) were used for the runs with calcite seed crystals.

The calcium sulphate solutions were prepared as described in section 6.4.2 with a concentration ranging from nearly saturated to 22.0 millimoles per litre. The tubes, with the solution added and the seed crystal inserted, were placed in the constant temperature bath at

85° or 95° and observed with a travelling microscope. Several of the seed crystals were stirred in these experiments.

When no crystals were observed on the surface of the seed crystal after some time, a number of dihydrate crystals were added as a slurry in a small volume of the solution retained for this purpose. The size of the added crystals varied from large (up to 1 mm. long) to small (prepared by crushing the large crystals) and in two runs, a mixed sample of these two sizes was added. The effect of this addition on the number of crystals attached to the seed crystal was observed.

RESULTS

In these experiments, while no crystals were observed on the seed crystal surface before addition of the slurry, crystals were generally observed on the surface after the addition. The larger crystals were found to be not as effective as the smaller crystals in attaching to the seed crystal surface since many settled to the bottom of the tube shortly after addition, but some of these larger crystals did become attached, even to stirred seed crystals.

In table 36, the time elapsed between the addition of crystals and the observation of crystals on the seed crystal surface is listed, and it is apparent that

this time is generally much shorter than the corresponding time when no crystals are added, as indicated in table 32. For instance, at a supersaturation of 2.2 millimoles per litre, the first crystal was observed on the seed crystal surface between 5 and 50 minutes after the addition of small crystals to the solution, whereas when no crystals were added generally no crystals were observed on the seed crystal at times ranging from 2 hours to 64 hours. These results therefore confirm those reported in section 6.4.2, since in both cases the density of the crystal deposit on the seed crystal surface is higher when greater numbers of crystals can come into contact with the surface, whether the seed crystal is dihydrate, hemihydrate or calcite. It appears then that the assumed mechanism of nucleation in the bulk of the solution followed by attachment to the surface is valid.

6.5 The Effect of Stirring on the Number of Dihydrate Crystals on a Seed Crystal Surface

In previous experiments in which unstirred seed crystals were immersed in supersaturated calcium sulphate solutions, it has been shown that dihydrate crystals first nucleate in the bulk of the solution and subsequently attach to the surface of the seed crystal. Presumably, the first crystals become attached at some irregularity

on the surface and once attached, they grow to conform to this irregularity forming a mechanical interlock with the surface. Further crystals could find attachment much easier since the crystals already attached would present a very irregular surface for attachment. Stirring the seed crystal should make the initial attachment of the first crystals much more difficult, and the crystals would have to remain attached under these unfavourable conditions until growth made the attachment to the surface more secure.

Over the short range of stirring speeds used in section 6.4.3, it was found that dihydrate crystals often attached to stirred dihydrate or calcite seed crystal surfaces. In this section, experiments are reported in which the effect on the density of the dihydrate deposit of stirring the seed crystal was more fully investigated.

EXPERIMENTAL

These experiments were generally carried out in type J tubes (simple test tubes), but in a few runs type F tubes (figure 48) were used. The supersaturated calcium sulphate solutions were prepared as described in previous sections.

In most of these runs, a seed crystal of dihydrate or calcite fixed to a glass rod was immersed in the

DIHYDRATE DEPOSITS ON STIRRED CALCITE SEED CRYSTALS

Figure 51



Run 664

Dihydrate crystals on calcite
seed crystal and Araldite
mounting after 105 minutes.
Stirring velocity : 1.3 cm./sec.

Magnification : 3x



Run 651

Dihydrate crystals on leading
edge of calcite seed crystal
after 90 minutes.
Stirring velocity : 76.4 cm./sec.

Magnification : 3x



Part of the dihydrate deposit
illustrated in the second
photograph.

Magnification : 18x

Solution concentration : 22.0 millimoles per litre

Solution temperature : 95°C

solution and stirred at a constant speed. Occasionally, one or more glass paddles were also attached to the rod above the seed crystal, to increase further the turbulence in the solution. In a few runs, a glass rod without an attached seed crystal was used. The velocity of the seed crystal or glass rod was measured as described in section 3.3 and ranged up to 120 cm. sec^{-1} in these experiments.

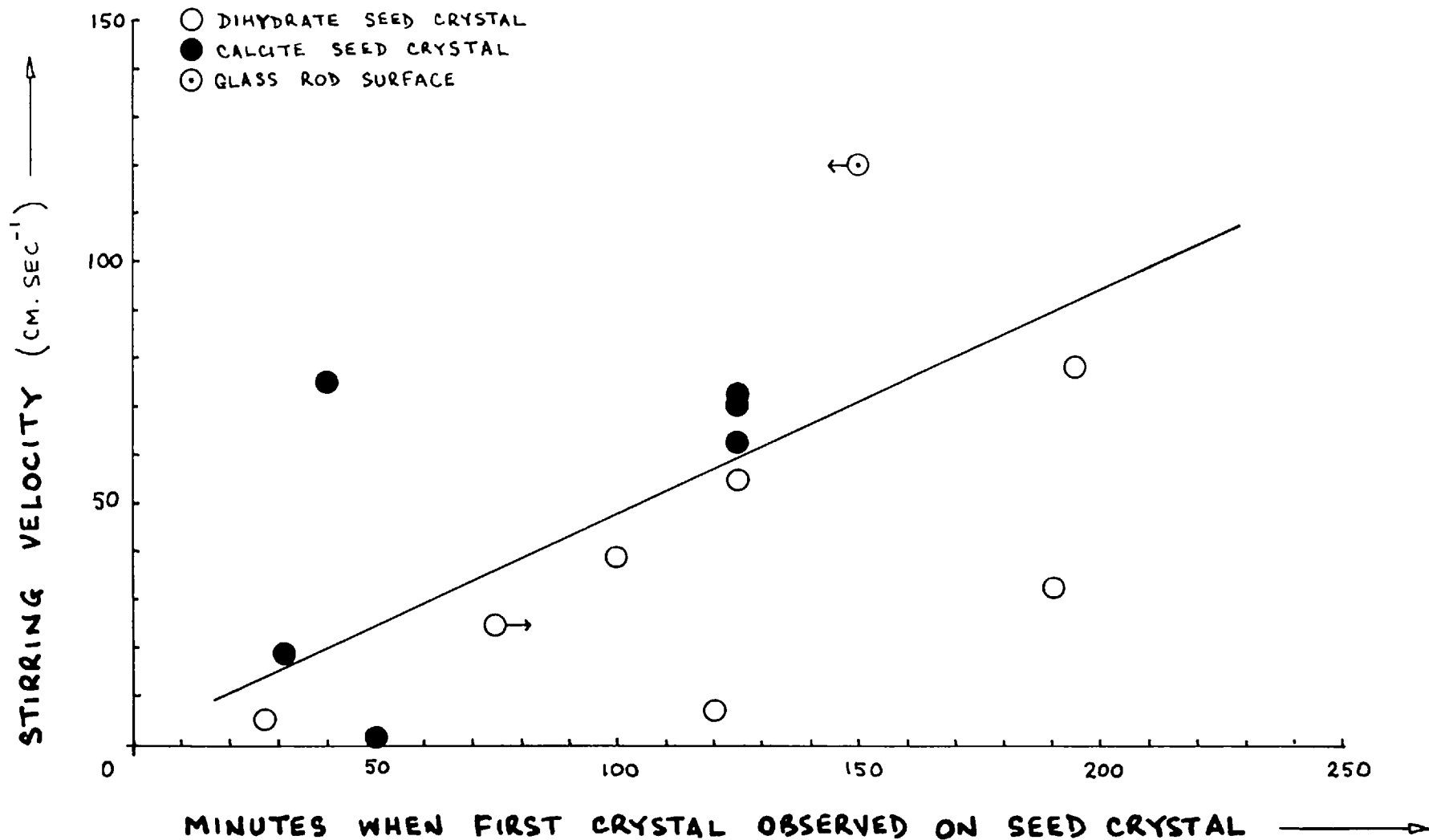
RESULTS

In these experiments, dihydrate crystals were observed to be attached to stirred dihydrate and calcite seed crystals, although usually in smaller numbers than previously found on unstirred seed crystals under similar conditions. Deposits were also observed on the glass rod and the Araldite mounting. At higher stirring rates, the deposits were generally lighter and the crystals tended to lie closer to the surface of the seed crystal. As before, the crystals did not appear to have any preferred orientation on the surface.

The photographs of figure 51 illustrate the nature of the dihydrate deposits on stirred calcite seed crystals. (In all three photographs, the small calcite crystal is shown protruding vertically above the larger glass-Araldite mounting.) In the first photograph, the deposit formed at a low stirring rate is shown. A rather

TIME OF OBSERVATION OF FIRST CRYSTAL ON STIRRED SEED CRYSTALS (95°)
SUPERSATURATION : 5.9 MILLIMOLES / LITRE

FIGURE 52



heavy deposit is observed on the leading and receding edges of the crystal and on the Araldite mounting. There are also a few crystals attached to the glass rod. In the second and third photographs, the deposit formed at a higher stirring rate is illustrated. Here, the deposit has piled up mainly on the leading edge of the seed crystal and on one area of the Araldite mounting. This piling up of crystals was observed over a range of stirring velocities up to 120 cm. per second, and on both types of seed crystal. The presence of glass paddles on the rod, however, considerably increased the turbulence in the solution and the dihydrate deposit was somewhat more evenly distributed over the surface of the seed crystal.

The time of observation of the first crystal on the surface of the stirred seed crystal is listed for these experiments in table 37, and in figure 52 the time is plotted against stirring velocity for some of these experiments. It is apparent that the time tends to increase as the rate of stirring increases, although there is a great deal of scatter in the results illustrated in figure 52 as might be expected considering the probable variation in the nature of the surface of different seed crystals. The tendency to longer times with increasing stirring speeds agrees however with the observation that fewer crystals were attached at the higher stirring rates.

In a few runs, a nearly saturated solution containing many dihydrate crystals was used. This was prepared by stirring a moderately supersaturated calcium sulphate solution for several hours with a glass paddle until a very large number of crystals were present. The rod with attached seed crystal was then inserted and stirred, and it was found that very few crystals were attached to the surface of the seed crystal. This suggests that crystals will more readily attach to the seed crystal if a certain degree of supersaturation exists so that some sort of mechanical interlock with the surface can be formed by growth of the attached crystals or the seed crystal. The fact that any crystals attached at all in these nearly saturated solutions indicates that the mechanism of crystals attaching to the seed crystal is valid since it would be virtually impossible for nucleation to have occurred directly on the surface of the seed crystal.

6.6 Summary

The formation of calcium sulphate dihydrate deposits on various crystal surfaces has been investigated and the mechanism of formation indicated is one of nucleation in the bulk of the solution followed by attachment to the surface of the seed crystal.

In the first part of this investigation, dihydrate deposits from deposition experiments in Chapter 5 were examined. Apart from being directed primarily outwards from the surface, the dihydrate crystals showed no preferred orientation with respect to the parent crystal surface.

Experiments were then carried out in which the formation of dihydrate deposits on unstirred dihydrate seed crystals immersed in supersaturated calcium sulphate solutions was observed. The crystals which were first seen in the bulk of the solution were occasionally observed settling onto the surface of the seed crystal and the deposits appeared to be heaviest in sheltered areas and on rough surfaces. The time at which the first crystals were observed on the seed crystal surface decreased with increasing supersaturation.

In a few experiments, barium ion was added to the solution in an attempt to remove foreign materials which might induce nucleation in the bulk of the solution. However, this was not successful in preventing nucleation and the deposits on seed crystals in these solutions were as heavy as those on seed crystals in solutions without added barium ion.

Experiments were carried out in which the access of dihydrate crystals from the bulk of the solution to

the surface of unstirred dihydrate, hemihydrate and calcite seed crystals was restricted. This caused a reduction in the number of crystals attached to the seed crystal and in some cases entirely prevented deposition, while in unrestricted conditions the deposit on the seed crystal was quite considerable. In another set of experiments, crystals were added to solutions when no crystals were observed on the seed crystal and within a short period after the addition, crystals were observed on the seed crystal surface. The results of these two sets of experiments indicate that nucleation must be occurring in the bulk of the solution followed by attachment of some of the crystals to the seed crystal surface.

The effect of stirring the seed crystal has been shown to be a reduction in the number of crystals attached to the seed crystal. The number of crystals attached was also reduced considerably, but not entirely, when the seed crystal was stirred in a nearly saturated solution. The fact that a few crystals were attached to a stirred seed crystal in such a solution, however, clearly indicates that the proposed mechanism of formation applies under these conditions.

CHAPTER 7

SUMMARY AND DISCUSSION OF RESULTS7.1 The Mechanism of Calcium Sulphate Deposition on an Unheated Surface

The present work has shown that the mechanism of calcium sulphate deposition on an unheated metal surface is comprised of the following three steps:

- (1) The initial formation of crystal nuclei either directly on the surface or in the bulk of the solution followed by attachment to the surface, but probably the latter.
- (2) Growth of these crystal nuclei.
- (3) Further nucleation in the bulk of the solution followed by attachment to the deposit.

In the exploratory studies of deposition on metal wires, the crystals were first detected in the bulk of the solution suggesting that this may be the site of nucleation in the first step. After some time, deposits composed of separate, needle-like crystals were observed on the metal surface. In these deposits, the fast-growing tips of the crystals were directed outwards from the surface, but otherwise the crystals showed no preferred orientation with respect to the surface. The amount of the deposit was found to increase as the corrosion

resistance of the metal decreased, an effect similar to that observed by Freeborn⁵⁰ for calcium carbonate scales formed on heated surfaces in boiling tap water. Presumably, metals that are easily corroded have a rougher surface making it easier for crystals to become attached since treatment of these metals to reduce corrosion caused a reduction in the density of the deposit. It was also observed that the density of the deposit was reduced in agitated solutions.

The rate of formation of these initial crystals, first observed in the bulk of the solution, has been measured for the dihydrate and hemihydrate and these results are discussed in section 7.2. The subsequent rates of growth of single crystals in the bulk of the solution and massive deposits of crystals on a metal surface have also been measured, and these results are discussed in section 7.3.

While the deposit is growing, further crystals nucleate and it has been shown that the site of this nucleation is the bulk of the solution, with some of the crystals subsequently becoming attached to the deposit. The form of dihydrate deposits on a seed crystal immersed in solution is similar to that described earlier for hemihydrate on metal wires, i.e. the crystals are attached at one end and directed outwards from the surface of the seed

crystal, but no preferred orientation is apparent. As before, deposits are heavier in rough and sheltered areas on and around the seed crystal, and lighter in agitated solutions. That the nucleation takes place in the bulk of the solution and not directly on the surface has been clearly shown by three sets of experiments. In the first set, the density of dihydrate deposits on dihydrate, hemihydrate or calcite seed crystals was reduced when access of crystals from the bulk of the solution was restricted. In the second set, crystals were added to the solution and shortly afterwards some crystals were observed on the seed crystal surface on which there were none before the addition. In the third set, crystals were observed on a stirred seed crystal immersed in a nearly saturated solution containing many dihydrate crystals.

The process of attachment of crystals to various surfaces presumably involves two steps. In the first, some of the crystals which come into contact with the surface are trapped at some surface irregularity. In the second step, these trapped crystals grow to conform to the irregularity, forming a mechanical interlock which gives a more secure attachment. It is apparent that for attachment to occur, the crystals must remain in contact with the surface until they are secured by growth. The ease of attachment depends on such factors as the smooth-

ness of the surface, the agitation of the solution and the supersaturation. Smooth surfaces such as glass would offer fewer and less prominent surface irregularities than would rougher surfaces (such as Araldite), and thus fewer crystals would be expected to attach in the former case. Stirring would also tend to reduce the number of crystals attached by making it more difficult for crystals to remain trapped until secured by growth. Attachment would also be more difficult in solutions of lower supersaturation since a longer time would be required for the trapped crystal to grow into the irregularity. All of these effects have been observed in the present work.

It appears therefore that these deposits build up by the growth of the crystals already attached and the trapping in the deposit of crystals nucleated in the solution, with these crystals subsequently growing to partially fill the voids in the deposit. The orientation of the crystals in the deposit is random and as growth progresses, mechanical interlocks and intergrowths are formed between crystals thus developing cohesion in the deposit. (A similar process developing adhesion of a scale to a metal surface has been suggested by Freeborn⁵⁰.) It is evident that deposits composed of smaller crystals would be likely to be more compact, and this was found with the hemihydrate deposits in section 5.4. When a large

number of crystals are present in the solution and the agitation is good, however, the supersaturation is reduced. The deposit does not then build up as quickly since the trapped crystals are less able to grow and become a part of the deposit.

Since the presence of crystals in the solution plays an important part in the deposition of calcium sulphate on an unheated surface, any factor which influences their number could affect the rate of build-up of the deposit. In the case of sea water brines for instance, the soluble and insoluble impurities present could induce or suppress nucleation and hence increase or decrease the number of crystals in the brine. However, when sea water is distilled the brine is generally well agitated, and excess local supersaturation may consequently be rather low. The probability of nucleation would then be much reduced, but any crystals present in the solution could attach to surfaces even in slightly supersaturated brines, as indicated by the results of section 6.5. In this connection, it is interesting to note that one method used to reduce scale formation in sea water distillation is to seed the brine with crystals of the scaling salt. It is apparent from the present results, however, that some of these crystals could deposit on the surfaces of the equipment even though nucleation may be prevented by the reduction in supersaturation brought about by seeding.

The present work has been largely confined to deposition on unheated surfaces, but the results would be expected to apply to heated surfaces as well providing no boiling occurred and the temperature gradient at the surface was not too large. Since the decrease in solubility with increasing temperature for calcium sulphate is relatively small especially for the dihydrate, the corresponding increase in supersaturation in the solution at a heated surface could be less than the decrease in supersaturation due to mass transfer effects. If the temperature gradient is large, however, the supersaturation at the surface could be higher than in the bulk of the solution and in this case, nucleation might take place directly on the surface rather than in the bulk of the solution. The rate of deposition might then be higher and the deposits more compact.

The present work has important implications for the general question of polycrystal formation. There appear to be two possible ways in which polycrystalline masses could form: (1) by the nucleation of crystals either directly on or adjacent to already existing crystals or (2) by the joining together of separate crystals which have nucleated independently in the solution. The first mechanism requires that the existing crystal be able to induce on or in close proximity to its surface

the formation of a new crystal lattice which is in no way orientated to its own lattice. Such an occurrence is very difficult to imagine in view of the commonly accepted theories of crystal growth. In these, the crystal grows by means of adsorption of molecules at fixed points on the lattice, the molecules subsequently migrating from point to point across the surface until the position with the greatest attractive forces is found. In this way, the molecules can be incorporated into the existing crystal lattice. For a new crystal lattice to form, however, the molecules would have to be adsorbed in a non-orientated fashion with respect to the existing crystal lattice. Alternatively, the crystal would need to be capable, through its attractive forces, of arranging unadsorbed molecules in the adjacent solution into a separate lattice, this lattice subsequently becoming disorientated with respect to the crystal and attaching to its surface.

On the other hand, the second mechanism of formation of polycrystals in which separate crystals join together requires only that the crystals come into contact with each other and remain in contact until attachment is made secure by intergrowth or mechanical interlock of the crystals. Clearly, this is the case with calcium sulphate dihydrate crystals which were found to attach

not only to other dihydrate crystals, but also to hemihydrate and calcite crystals, and to non-growing surfaces such as Araldite and glass even in stirred solutions where attachment would be difficult.

7.2 Nucleation of Calcium Sulphate Dihydrate and Hemihydrate

When supersaturated calcium sulphate solutions were prepared and allowed to stand at a temperature in the range, 70° - 110°C , the crystals of dihydrate or hemihydrate which nucleated were usually seen first in the bulk of the solution. An estimate of the rate of formation of these crystals has been made by measuring the induction time, the time elapsed when the first crystal was observed. In unstirred simple calcium sulphate solutions, the induction time for the hemihydrate was found to be shorter than that for the dihydrate in solutions of similar supersaturations. In unstirred mixed calcium chloride and sodium sulphate solutions, the induction time for the hemihydrate was shorter still. One of the possible reasons for this reduction is the presence of sodium chloride in the mixed solutions. (If this is the cause, the induction times in sea water brines in which the concentration of sodium chloride is relatively high could be considerably shorter than those measured in

the present work.) Stirring the solution was also observed to reduce the induction time. These results appear to be one of the few sets of data available at the temperatures of interest in sea water distillation.

The induction time is composed of two parts: the time for crystals to nucleate and the time for these crystals to grow to a visible size. Although the growth rates of dihydrate and hemihydrate crystals have been measured, it is not possible to calculate the nucleation time by subtracting the growth time from the induction time, for two reasons. Firstly, the size of the crystals when they were first detected can be only very roughly estimated. Secondly, the growth rate of these very tiny crystals can again be only very roughly estimated since because of mass transfer effects the growth rate is affected by the size of the crystal. Even though the actual rate of nucleation is not available, the results are likely to be of practical use as they indicate the rate of formation of crystals of a detectable size, albeit an arbitrary one.

As mentioned previously, this rate would very likely be different in sea water brines because of the many other constituents present, but the present results would probably provide a conservative estimate of that rate.

7.3 Growth of Calcium Sulphate Dihydrate and Hemihydrate

The rate of growth of single dihydrate and hemihydrate crystals in the bulk of the solution and massive deposits of these crystals on an unheated surface has been measured. Single dihydrate crystals in mixed calcium chloride and sodium sulphate solutions between 70° and 98° have growth rates approximately proportional to the second power of the supersaturation. A significant increase in growth rate was obtained for stirred dihydrate crystals, particularly at the higher temperatures, indicating that the growth rate is at least partly controlled by the rate of mass transfer. This is supported by the fact that the growth rate of unstirred crystals is dependent on the size of the crystal, and the value of this rate agrees reasonably well with that predicted for conditions of complete mass transfer control. The dihydrate crystals were needle-like and became more so with increasing supersaturation. However, the formation of needle-like crystals cannot be attributed to mass transfer limitations since stirred crystals were even longer and thinner.

There are a few references in the literature to measurements of the rate of decrease in concentration of supersaturated calcium sulphate solutions as dihydrate crystals nucleated and grew (these are discussed later).

In what appears to be the only reference to the direct measurement of the growth rates of specific faces of the dihydrate crystal, Dunn⁵¹ has quoted values obtained by Askey and Bunn in dilute slurries of anhydrite, presumably at room temperature. These are shown in the following table along with selected values from the present work. For purposes of comparison, three runs were carried out by the author at 25° in which the unstirred growth rate R_1 was measured in mixed calcium chloride and sodium sulphate solutions at a supersaturation of 5.1 millimoles per litre, and the average of the three growth rates obtained is included in the table.

Source	Δc millimoles per litre	Stirring velocity cm/sec	$R_1 \times 10^6$ cm/sec	$R_2 \times 10^6$ cm/sec	R_2/R_1
Askey and Bunn	~5*	?	0.6	0.06	0.1
Present Work	25°	5.1	0	--	--
	70°	5.0	0	--	--
	70°	5.0	>15	15.6	--
	85°	5.0	0	3.9	0.4
	98°	5.0	0	6.7	0.4

* Assuming solution is at 25° and saturated with respect to anhydrite

It is apparent that the values of R_1 , R_2 and R_2/R_1 are of the same order of magnitude as those found in the present work.

Other studies have been made¹⁶⁻¹⁸ in which the rate of decrease of concentration in a supersaturated calcium sulphate solution was measured as many dihydrate crystals nucleated and grew. Schierholtz¹⁶ concluded that the growth rate at 25° was dependent on supersaturation to the first power, whereas Moriyama and Utsunomiya¹⁷ and Sugimoto et al.¹⁸ found it to be dependent on the second power of supersaturation in the temperature range, 20° - 60°C. The growth rate constant from one of these studies¹⁷ is compared below to those found for the dihydrate at 70° in the present work. The value obtained by Moriyama and Utsunomiya can be considered as only an estimate of k_1 since these authors did not vary the rate of stirring of the slurry in their investigation. Also included in the table are the growth rate constants at 25° of some sparingly soluble salts, obtained by Reich⁵². These constants were also obtained by measuring the rate of decrease of solution concentration when a slurry of crystals was stirred at a single rate. The value of k_r was calculated from the growth rate at low supersaturations where the rate was assumed to be surface reaction controlled, and the value of k_m from the growth rate at

high supersaturations where the rate was assumed to be mass transfer controlled. In all cases, the constants in the following table were calculated from an equation of the type:

$$\text{Rate} = k_m(c - c_i) = k_r(c_i - c^*)^2 \text{ moles.cm}^{-2}.\text{sec}^{-1}$$

with $(c - c_i)$ and $(c_i - c^*)$ in moles.cm^{-3}

AUTHOR	CRYSTAL	SOLUBILITY	k_m	k_r
		$\frac{\text{mol}}{\text{cm}^3} \times 10^7$	$\frac{\text{cm}}{\text{sec}} \times 10^2$	$\frac{\text{cm}^4}{\text{mol}.\text{sec}} \times 10^{-1}$
Moriyama and Utsunomiya	$\text{CaSO}_4 \cdot 2\text{H}_2\text{O}$	~ 180	--	21.0*
Present Work	$\text{CaSO}_4 \cdot 2\text{H}_2\text{O}$	~ 180	1.7 - 8.0	1400 **
Reich	$\text{MgC}_2\text{O}_4 \cdot 2\text{H}_2\text{O}$	34.0	0.01	0.03
"	$\text{CaC}_2\text{O}_4 \cdot \text{H}_2\text{O}$	0.6	--	1900
"	$\text{SrC}_2\text{O}_4 \cdot \text{H}_2\text{O}$	3.8	1.3	1800
"	$\text{BaC}_2\text{O}_4 \cdot 2\text{H}_2\text{O}$	4.9	3.0	1400
"	TlBr	20.3	3.0	60,000

* This value, which corresponds to growth of the crystal in 3 dimensions, was extrapolated to 70°C for comparison to the present work.

** When averaged for growth in 3 dimensions,

$$k_r \times 10^{-1} \sim 38$$

The values of k_m , except for that of $\text{MgC}_2\text{O}_4 \cdot 2\text{H}_2\text{O}$, are seen to be in quite good agreement. This is not at all an unexpected result since the diffusion coefficient for similar salts is generally of the same order of magnitude, and hence the rate of mass transfer would be rather similar for these salts.

The values of k_r for these salts show somewhat greater variation. However, the value for the dihydrate obtained by Moriyama and Utsunomiya is similar to the value for the dihydrate from the present work, when the latter is averaged for growth in 3 dimensions. The values of k_r obtained by Reich for the sparingly soluble salts also correspond to growth in 3 dimensions, but these are evidently considerably higher than the corresponding values for the dihydrate. The abnormally low value for $\text{MgC}_2\text{O}_4 \cdot 2\text{H}_2\text{O}$ may be due to the method used to evaluate k_r . Reich assumed that at low supersaturations, the growth rate was largely surface reaction controlled but since the value of k_m is also rather low for this salt, mass transfer effects may not have been entirely eliminated in this case.

It is apparent that the value of k_m is generally very much less than that of k_r for these salts. This indicates that except at extremely low supersaturations, the rate of mass transfer will largely control the growth

rate (see equation 23). Indeed, this was found to be the case for the dihydrate in the present work. The value of k_m for the dihydrate shown in the above table corresponds to unstirred growth, and this was found to be very much controlled by the rate of mass transfer.

The present work appears to be the first to provide data on the growth rate of the dihydrate as a function of supersaturation and solution velocity. Also, the temperature range $70^{\circ} - 98^{\circ}\text{C}$ is higher than that of previous investigations and in the range of interest for sea water distillation.

The growth rate of single hemihydrate crystals in the bulk of the solution has been measured in mixed calcium chloride and sodium sulphate solutions at 98° . The growth rate of unstirred crystals was found to be dependent on the supersaturation to the power 1.3 and was higher than the unstirred dihydrate growth rate R_1 at 98° . Differences in seed crystal sizes in the two cases however does not allow a direct comparison of the rates. The growth rate of stirred hemihydrate crystals was found to decrease with time and in many cases was reduced to zero. The cause of this decrease in growth rate appears to be connected with the presence of glass dust in the solution since it was shown that visible deposits of dust on the tip of the crystal could inhibit growth. Dihydrate crystals

immersed simultaneously in the same solution continued to grow when stirred indicating that the dihydrate was not similarly affected by glass dust and also that the decrease in hemihydrate growth rate was not the result of any change in solution supersaturation. Power and Fabuss³⁰ have reported that the hemihydrate is stable in solution at 100°C after 48 hours and therefore transformation to another form of calcium sulphate cannot be occurring. When the formation of glass dust was prevented in these experiments, stirred hemihydrate crystals appeared to grow at a constant rate. Apart from the growth stoppage, the growth rate of stirred hemihydrate crystals appeared to increase somewhat with stirring suggesting that the growth rate may be to some extent controlled by the rate of mass transfer.

The only reference in the literature to the measurement of the growth rate of hemihydrate crystals appears to be that of reference 41. In this, the growth rate of an unstirred hemihydrate crystal transforming from a dihydrate crystal in distilled water at 134°C is reported to be $8 \times 10^{-5} \text{ cm. sec}^{-1}$. This is the same order of magnitude as the present results at 98° in which rates of up to $13.3 \times 10^{-5} \text{ cm. sec}^{-1}$ were measured for solution supersaturations up to 7.8 millimoles per litre. Thus the present work appears to be the first to provide data on

the growth rate of hemihydrate crystals as a function of supersaturation and solution velocity.

The growth rate of single dihydrate and hemihydrate crystals in the bulk of 1 M NaCl solutions has also been measured in a few runs. These rates were of the same order of magnitude as the corresponding growth rates in mixed solutions at the same supersaturation.

It will be observed that in the present work much attention has been devoted to a study of the effect of controlled levels of stirring on the growth rate of single crystals. Such a study has a distinct advantage over the more commonly used method of measuring the change in solution concentration in a stirred slurry of crystals, in that the solution velocity at the growing crystal face can be measured and controlled, and hence its effect on the growth rate can be obtained directly. In the present work for instance, it was possible to show that the fast-growing edge of the dihydrate crystal reached a constant maximum growth rate only at very low supersaturations and high rates of stirring. Under these conditions, the concentration at the crystal-solution interface of the observed crystal approached that in the bulk of the solution and the effects of mass transfer were virtually eliminated. A measure of the true surface reaction rate was then obtained and for the dihydrate, this rate was shown to be

approximately proportional to the second power of the supersaturation. At higher supersaturations and/or lower rates of stirring, the rate of mass transfer had a significant influence on the growth rate.

The rate of growth of massive deposits of dihydrate and hemihydrate on stirred unheated metal surfaces has been measured and the deposition rate has been shown to be related to the corresponding single crystal growth rate in the bulk of the solution. Individual crystals in the deposit appear to grow at the same rate as in the bulk of the solution for solutions of the same supersaturation, but the observed rate of increase in thickness of the deposit is often a fraction of this rate because of the angle of attachment of the crystal to the surface.

The present work appears to be the first in which the rate of build-up of calcium sulphate deposits on unheated metal surfaces has been measured as a function of supersaturation. There are a few references in the literature^{7,13,53} to measurements of the deposition rate of calcium sulphate scale on a heated surface, and a summary of the results is compared below to the present results.

REFERENCE	TEMP. °C	HYDRATE	DURATION OF RUN (hours)	DEPOSITION RATE cm.sec ⁻¹ x 10 ⁶
7	100-130	hemihydrate	48	0.7 - 2.5
13	100	dihydrate	40	0.5
53	45	dihydrate	up to 20	0.2 - 1.4
Present Work	85	dihydrate	up to 80	0.1 - 3.0
	98	hemihydrate	--	0 - 25.2

The deposition rates in the first two references (7, 13) were calculated by weighing or measuring the thickness of the deposit at the end of the run, while that in the third reference (53) was calculated from measurements of the decrease in heat transfer coefficient as the scale deposited. In the case of the first two references, no mention of the solution concentration was made. The form of the dihydrate and hemihydrate deposits on these heated surfaces in the absence of boiling was similar to that described for unheated surfaces in the present work.

It is apparent that these deposition rates are of the same order of magnitude as those in the present work. However, all of these studies were carried out on deposits on heated surfaces where both the temperature and the concentration of the solution at the growing surface varied during the run, and the supersaturation

could at best be known only very approximately. The present work was carried out under isothermal and controlled stirring conditions so that the supersaturation at the growing surface could be more readily determined, and the measured deposition rates could be related to the growth rates of single crystals.

APPENDIX 1EXPERIMENTAL RESULTSTABLE 1

EFFECT OF TEMPERATURE AND SUPERSATURATION ON THE RELATIVE AMOUNTS OF DIHYDRATE AND HEMIHYDRATE

Run	Solution concentration millimoles/l.	Solution temperature °C	Sampling time minutes	Percent hemihydrate
(a) Type A tubes				
500	24.0	85.0	50	0
502	24.0	85.0	50	0
505	24.0	91.3	30	0
501	24.0	98.0	25	33
503	24.0	98.0	25	6
504	24.0	100.1	20	33
534	25.0	98.9	12	100
535	25.0	98.9	25	100
536	25.0	98.9	11	10
537	25.0	98.9	17	100
543	50.0	75.0	10	50
544	50.0	98.9	15	50
(b) Type B tubes				
545	20.0	80.5	40	0
546	20.0	80.5	45	-*
553	20.0	85.2	16	0
547	20.0	98.9	7	100
548	20.0	98.9	18	100
518	25.0	52.0	65	-*
533	25.0	52.0	195	0

* No crystals found.

TABLE 1 (continued)

Run	Solution concentration millimoles/l.	Solution temperature °C	Sampling time minutes	Percent hemihydrate
551	25.0	75.0	35	0
532	25.0	75.0	75	0
529	25.0	80.4	30	50
530	25.0	80.4	35	50
521	25.0	85.8	25	99
522	25.0	85.8	20	100
523	25.0	85.8	20	100
524	25.0	85.8	30	50
519	25.0	89.6	45	100
520	25.0	89.6	25	100
512	25.0	91.3	25	99
514	25.0	91.3	25	99
516	25.0	95.3	15	100
517	25.0	95.3	25	100
513	25.0	100.1	35	100
515	25.0	100.1	8	100
526	50.0	52.0	30	0
542	50.0	52.0	70	0
551	50.0	60.5	11	0
552	50.0	60.5	16	0
549	50.0	70.0	7	90
550	50.0	70.0	10	50
540	50.0	75.0	20	50
541	50.0	75.0	30	90
538	50.0	80.4	12	10
539	50.0	80.4	20	90
527	50.0	85.8	7	100
528	50.0	85.8	10	100
525	50.0	89.6	20	100

TABLE 2

INDUCTION TIMES IN C TUBES

Run	Solution concentration millimoles/l.	Bath temperature °C	Super- saturation S	Induction time ϕ_I seconds	$\frac{10^7}{T^5(\log S)^2}$	$\log \phi_I$
86	12.5	107.8	(1.23)	600	22.9	2.78
85	12.5	109.0	(1.26)	600	18.5	2.78
80	16.0	98.5	(1.35)	240	11.7	2.38
79	16.0	99.0	(1.36)	420	10.7	2.62
78	16.0	100.0	(1.38)	120	9.5	2.08
77	16.0	101.8	(1.43)	90	8.0	1.95
76	16.0	105.5	(1.54)	60	5.3	1.78
75	16.0	106.8	(1.57)	60	4.7	1.78
84	16.0	107.2	(1.58)	65	4.5	1.81
83	16.0	108.0	(1.60)	75	4.4	1.88
82	16.0	109.0	(1.63)	75	4.0	1.88
81	16.0	109.5	(1.65)	50	3.7	1.70
94	16.9	92.3	1.36	270	11.2	2.43
93	16.9	95.7	1.39	190	9.9	2.28
92	16.9	98.3	(1.41)	120	8.7	2.08
91	16.9	100.9	(1.49)	100	6.4	2.00
90	16.9	102.8	(1.54)	80	5.2	1.90
89	16.9	104.0	(1.58)	120	4.7	2.08
88	16.9	106.3	(1.64)	60	4.0	1.78
87	16.9	107.3	(1.67)	50	3.6	1.70
49	18.6	83.6	1.45	330	9.2	2.52
48	18.6	86.0	1.46	330	8.3	2.52
47	18.6	87.2	1.46	330	8.1	2.52
51	18.6	88.0	1.47	210	7.8	2.32
50	18.6	88.8	1.48	165	7.5	2.22

*Bracket denotes hemihydrate.

TABLE 2 (continued)

Run	Solution concentration millimoles/l.	Bath temperature °C	Super- saturation S	Induction time ϕ_I seconds	$\frac{10^7}{T^3(\log S)^2}$	$\log \phi_I$
46	18.6	89.0	1.48	240	7.4	2.58
45	18.6	90.1	1.48	240	7.4	2.58
53	18.6	90.7	1.49	75	7.0	1.88
54	18.6	90.7	1.49	75	7.0	1.88
52	18.6	94.2	1.51	90	6.3	1.96
44	18.6	98.5	(1.56)	75	5.4	1.88
74	19.2	85.1	1.49	195	7.3	2.29
73	19.2	88.1	1.51	165	6.7	2.22
72	19.2	90.4	1.54	100	6.0	2.00
71	19.2	93.5	1.56	75	5.5	1.88
70	19.2	95.5	1.57	70	5.2	1.85
69	19.2	98.5	(1.61)	65	4.5	1.81
68	19.2	100.0	(1.66)	55	4.0	1.74
67	19.2	102.0	(1.72)	50	3.4	1.70
66	19.2	103.8	(1.78)	45	3.0	1.65
65	19.8	78.1	1.48	530	8.1	2.52
64	19.8	80.0	1.50	225	7.3	2.35
63	19.8	84.3	1.54	150	6.3	2.18
62	19.8	88.6	1.56	120	5.7	2.08
61	19.8	90.9	1.59	95	5.2	1.98
60	19.8	92.6	1.60	105	5.0	2.02
59	19.8	94.9	1.62	60	4.5	1.78
58	19.8	96.7	1.64	45	4.4	1.65
57	19.8	98.7	(1.68)	40	3.8	1.60
56	19.8	101.1	(1.75)	35	3.3	1.54
55	19.8	103.1	(1.78)	30	2.9	1.48

TABLE 5

INDUCTION TIMES IN A TUBES

Run	Solution concentration millimoles/l.	Bath tempera- ture °C	Super- saturation S	Induction time ϕ_I seconds	$\frac{10^7}{T^3(\log S)^2}$	$\log \phi_I$
156	12.5	109.7	(1.29)	1140	15.1	3.06
160	14.3	102.0	(1.29)	1800	15.2	3.26
159	14.3	103.5	(1.32)	1140	11.8	3.06
158	14.3	104.5	(1.35)	1000	11.3	3.00
157	14.3	105.5	(1.38)	495	10.0	2.70
129	15.8	100.2	(1.37)	660	10.5	2.82
128	15.8	100.2	(1.37)	650	10.5	2.80
127	15.8	101.5	(1.41)	480	8.3	2.68
126	15.8	102.1	(1.42)	420	8.2	2.62
125	15.8	103.9	(1.48)	240	6.3	2.38
110	16.8	99.8	(1.45)	550	7.3	2.52
108	16.8	105.6	(1.62)	135	4.2	2.13
109	16.8	105.7	(1.62)	120	4.2	2.08
144	17.5	92.7	1.41	900	9.1	2.95
145	17.5	92.7	1.41	1080	9.1	3.05
142	17.5	94.2	1.42	900	8.6	2.95
143	17.5	94.2	1.42	780	8.6	2.89
117	17.8	99.3	(1.52)	285	5.9	2.46
116	17.8	101.0	(1.57)	225	5.0	2.35
115	17.8	103.0	(1.65)	140	4.2	2.15
114	17.8	104.6	(1.68)	90	3.6	1.95
113	17.8	107.2	(1.76)	90	3.0	1.95
111	17.3	107.9	(1.78)	60	2.9	1.78
112	17.8	108.5	(1.80)	65	2.7	1.81

* Bracket denotes hemihydrate.

TABLE 3 (continued)

Run	Solution concentration millimoles/l.	Bath temperature °C	Super- saturation S	Induction time ϕ_I seconds	$\frac{10^7}{T^3(\log S)^2}$	$\log \phi_I$
101	18.3	100.0	(1.58)	180	4.8	2.26
102	18.3	100.0	(1.58)	210	4.8	2.32
103	18.3	105.1	(1.74)	75	5.2	1.88
104	18.3	105.1	(1.74)	90	5.2	1.95
105	18.3	105.1	(1.74)	90	5.2	1.95
107	18.5	92.0	1.49	1000	6.8	3.00
106	18.5	94.8	1.52	390	6.1	2.59
100	19.0	90.0	1.51	210	6.5	2.52
99	19.0	94.9	1.56	150	5.4	2.18
98	19.0	99.9	(1.64)	110	4.1	2.04
97	19.0	99.9	(1.64)	110	4.1	2.04
96	19.0	104.8	(1.80)	80	2.9	1.90
95	19.0	104.9	(1.80)	70	2.9	1.85
141	21.5	77.3	1.60	1000	5.5	3.00
140	21.5	78.3	1.60	840	5.5	2.93
139	21.5	79.6	1.62	600	5.2	2.78
138	23.3	77.1	1.74	420	4.0	2.62
137	23.3	79.7	1.75	300	3.8	2.48
136	23.3	81.5	1.78	270	3.6	2.43
135	23.3	86.0	1.82	150	3.2	2.18
134	23.3	86.0	1.82	180	3.2	2.26
133	23.8	87.9	1.87	120	2.9	2.08
132	23.8	97.2	1.97	60	2.3	1.78
131	23.8	98.4	(2.00)	65	2.2	1.81
130	23.8	99.7	(2.05)	62.5	2.0	1.80
124	24.0	88.1	1.89	115	2.8	2.06

TABLE 3 (continued)

Run	Solution concentration millimoles/l.	Bath temperature °C	Super- saturation S	Induction time ϕ_I seconds	$\frac{10^7}{T^3(\log S)^2}$	$\log \phi_I$
123	24.0	91.2	1.92	100	2.6	2.00
122	24.0	94.8	1.97	65	2.5	1.81
121	24.0	96.4	1.98	65	2.2	1.81
120	24.0	99.5	(2.03)	55	2.0	1.74
119	24.0	101.9	(2.15)	50	1.7	1.70
118	24.0	103.8	(2.23)	45	1.6	1.65
155	25.3	70.0	1.82	450	3.7	2.65
154	25.3	70.7	1.82	420	3.7	2.62
153	25.3	71.8	1.83	300	3.5	2.48
152	25.4	74.3	1.87	225	3.2	2.35
151	25.4	76.2	1.88	200	3.1	2.50
150	25.4	79.2	1.91	180	2.9	2.26
147	50.0	82.5	2.29	90	1.7	1.95
146	50.0	85.4	2.32	80	1.6	1.90
148	50.0	90.5	2.40	40	1.5	1.60
149	50.0	94.0	2.44	45	1.3	1.65

TABLE 4

INDUCTION TIMES IN A TUBES WITH HEAT-UP CORRECTION

Run	Solution concentration millimoles/l.	Average * solution temperature °C	$\frac{10^7}{T^5(\log 3)^2}$ Ave.	$\log \phi_I$
129	15.8	(98.9)	27.5	2.82
128	15.8	(98.8)	28.0	2.80
127	15.8	(99.7)	31.7	2.68
126	15.8	(100.0)	33.2	2.62
125	15.8	(100.1)	45.3	2.38
110	16.8	97.2	13.0	2.52
108	16.8	(98.7)	15.6	2.13
109	16.8	(98.0)	16.9	2.08
144	17.5	91.8	9.9	2.95
145	17.5	92.0	9.8	3.03
142	17.5	93.3	9.5	2.95
143	17.5	93.2	9.6	2.89
117	17.8	96.3	8.8	2.46
116	17.8	97.1	8.8	2.35
115	17.8	96.6	9.5	2.15
114	17.8	94.4	11.3	1.95
113	17.8	96.7	10.5	1.35
111	17.8	92.1	13.5	1.78
112	17.8	95.8	12.6	1.81
101	18.3	95.2	8.1	2.26
102	18.3	95.9	7.8	2.32
103	18.3	92.8	10.1	1.88

* Bracket denotes hemihydrate.

TABLE 4 (continued)

Run	Solution concentration millimoles/l.	Average solution temperature °C	$\frac{10^7}{T^3(\log S)^2}$ Ave.	$\log \phi_I$
104	18.3	94.9	9.1	1.95
105	18.3	94.9	9.1	1.95
107	18.5	91.2	7.3	3.00
106	18.5	92.7	7.3	2.59
100	19.0	86.4	8.1	2.32
99	19.0	89.5	7.7	2.18
98	19.0	92.0	7.9	2.04
97	19.0	92.0	7.9	2.04
96	19.0	93.3	7.6	1.90
95	19.0	91.8	8.3	1.85
141	21.5	76.7	5.8	3.00
140	21.5	77.5	5.5	2.93
139	21.5	78.5	5.4	2.78
138	23.3	75.6	4.2	2.62
137	23.3	77.5	4.0	2.48
136	23.3	79.0	3.9	2.43
135	23.3	81.2	3.8	2.18
134	23.3	82.0	3.7	2.26
133	23.8	81.8	3.5	2.08
132	23.8	83.3	3.6	1.78
131	23.8	85.4	3.4	1.81
130	23.8	85.9	3.4	1.80
124	24.0	81.7	3.5	2.06
123	24.0	83.5	3.4	2.00
122	24.0	82.4	3.5	1.81
121	24.0	83.7	3.5	1.81

TABLE 4 (continued)

Run	Solution concentration millimoles/l.	Average solution temperature °C	$\frac{10^7}{T^3(\log S)^2}$ Ave.	$\log \phi_I$
120	24.0	85.9	5.5	1.74
119	24.0	84.4	5.5	1.70
118	24.0	84.0	5.3	1.65
155	25.3	68.8	5.8	2.65
154	25.5	69.4	5.7	2.62
153	25.3	69.9	5.7	2.48
152	25.4	71.7	5.5	2.35
151	25.4	75.2	5.4	2.30
150	25.4	75.6	5.2	2.26
147	30.0	75.0	2.1	1.95
146	30.0	76.6	2.0	1.90
148	30.0	72.0	2.4	1.60
149	30.0	76.4	2.1	1.65

TABLE 5

INDUCTION TIMES IN B TUBES

Run	Solution concentration millimoles/l.	Super- saturation S	Induction time ϕ_I seconds	$\frac{10^7}{T^3(\log S)^2}$	$\log \phi_I$
186	17.5	1.13	75	66.0	1.87
187	17.5	1.13	60	66.0	1.78
188	17.5	1.13	105	66.0	2.02
189	17.5	1.13	100	66.0	2.00
190	17.5	1.15	100	66.0	2.00
173	20.0	1.23	120	25.0	2.08
174	20.0	1.23	100	25.0	2.00
175	20.0	1.23	60	25.0	1.78
176	20.0	1.23	30	25.0	1.48
177	20.0	1.23	60	25.0	1.78
178	20.0	1.23	43	25.0	1.63
179	20.0	1.23	35	25.0	1.54
180	20.0	1.23	30	25.0	1.48
181	20.0	1.23	25	25.0	1.40
182	20.0	1.23	35	25.0	1.54
183	20.0	1.23	40	25.0	1.60
166	25.0	1.50	25	6.2	1.40
167	25.0	1.50	25	6.2	1.40
168	25.0	1.50	30	6.2	1.48
169	25.0	1.50	30	6.2	1.48
170	25.0	1.50	33	6.2	1.51
171	25.0	1.50	20	6.2	1.30
172	25.0	1.50	20	6.2	1.30

TABLE 6

INDUCTION TIMES IN D TUBES

Solution concentration : 22.0 millimoles/litre

Supersaturation S : 1.35

 $T^{-3} (\log S)^{-2} \times 10^7$: 11.4

Run	Induction time ϕ_I seconds	$\log \phi_I$ *
258	10	1.00
259	10	1.00
263	30	1.48
264	30	1.48
265	30	1.48
266	20	1.30
267	15	1.18

* The line drawn in Figure 13 gives the corresponding induction time in unstirred mixed solutions as 28 seconds ($\log \phi_I = 1.45$).

TABLE 7

UNSTIRRED DIHYDRATE GROWTH RATES AT 70°C

Run	Solution concentration c millimoles/l.	c - c* millimoles/l.	R ₁ x 10 ⁶ cm./sec.
309	19.55	1.92	1.05
301	20.80	3.00	1.46
300	21.50	3.59	0.91
307	21.55	3.65	1.93
313	21.55	3.65	1.29
319	21.55	3.63	1.96
299	22.75	4.66	1.44
298	24.00	5.73	1.67
310	24.55	6.21	5.27
323	24.55	6.21	3.99
302	25.50	7.02	4.15
304	26.55	7.91	11.1
312	27.55	8.76	9.45
313	28.05	9.19	10.1
311	28.55	9.62	18.3
315	29.55	10.48	16.7

TABLE 8

UNSTIRRED DIHYDRATE GROWTH RATES AT 85°C

Run	c millimoles/l.	c - c* millimoles/l.	R ₁ x 10 ⁶ cm./sec.	R ₂ x 10 ⁶ cm./sec.	R ₂ / R ₁
384	19.0	2.18	1.36	--	--
385	19.0	2.18	1.00	0.25	0.25
387	20.0	3.05	2.78	0.28	0.10
388	20.0	3.05	2.77	--	--
391	20.0	3.05	1.89	0.29	0.16
392	20.0	3.05	2.08	--	--
467	20.0	3.05	3.22	--	--
381	21.0	3.95	2.14	0.07	0.03
382	22.5	5.28	3.80	0.29	0.08
389	23.0	5.72	5.08	0.53	0.10
399	23.0	5.72	4.04	--	--
380	24.0	6.60	8.30	--	--

TABLE 9

UNSTIRRED DIHYDRATE GROWTH RATES AT 98°C

Run	c millimoles/l.	c - c* millimoles/l.	R ₁ × 10 ⁶ cm./sec.	R ₂ × 10 ⁶ cm./sec.	R ₂ / R ₁
558	17.0	1.75	1.03	--	--
559	17.0	1.75	1.39	--	--
560	17.0	1.75	1.19	--	--
561	17.0	1.75	1.21	--	--
561	17.0	1.75	1.63	--	--
562	17.0	1.75	1.31	--	--
562	17.0	1.75	1.67	--	--
562	17.0	1.75	0.89	--	--
562	17.0	1.75	1.15	--	--
562	17.0	1.75	0.61	--	--
563	17.0	1.75	1.17	--	--
564	17.0	1.75	1.24	--	--
471	18.5	3.05	2.41	0.49	0.20
565	18.5	3.05	2.90	--	--
566	18.5	3.05	2.78	--	--
567	18.5	3.05	2.10	--	--
568	18.5	3.05	2.50	--	--
571	18.5	3.05	2.42	--	--
574	18.5	3.05	2.84	--	--
578	18.5	3.05	2.11	--	--
581	18.5	3.05	1.54	--	--
582	18.5	3.05	2.38	--	--
465	20.0	4.35	5.13	--	--
476	21.0	5.20	7.85	--	--
495	24.0	7.80	16.7	0.46	0.03

TABLE 10

STIRRED DIHYDRATE GROWTH RATES AT 70°C

Run	c millimoles per litre	c - c* millimoles per litre	v cm./sec.	$R_1 \times 10^6$ cm./sec.	$K \times 10^7$ (cm./sec.) x (l./millimole) ^{1.8}
309	19.55	1.92	0.68	1.33	--
322	19.55	1.92	10.5	2.20	--
350	19.55	1.92	60.7	4.02	--
356	19.55	1.92	74.4	2.60	--
344	20.00	2.30	13.4	3.68	--
342	20.80	3.00	19.3	6.75	--
306	21.55	3.63	0.21	3.93	3.85
308	21.55	3.63	0.37	5.20	5.10
319	21.55	3.63	0.51	6.17	6.05
306	21.55	3.63	0.52	6.45	6.32
307	21.55	3.63	0.68	8.70	8.53
321	21.55	3.63	6.00	9.48	--
320	21.55	3.63	12.0	7.95	--
355	21.55	3.63	56.1	11.0	--
349	21.55	3.63	62.3	11.0	--
352	22.75	4.66	26.9	15.7	--
323	24.55	6.21	0.63	12.8	--
324	24.55	6.21	15.1	17.4	--
325	24.55	6.21	24.5	18.0	--
348	24.55	6.21	57.0	21.8	--
357	24.55	6.21	64.2	21.6	--

TABLE 11

STIRRED DIHYDRATE GROWTH RATES AT 85°C

Run	c milli- moles per litre	c - c* milli- moles per litre	v <u>cm.</u> sec.	$R_1 \times 10^6$ cm./sec.	$R_2 \times 10^6$ cm./sec.	$\frac{R_2}{R_1}$	$K \times 10^7$ (cm./sec.) x (l./millimole) ^{1.8}
387	20.0	3.05	7.6	4.39	--	--	5.90
393	20.0	3.05	13.7	5.21	0.40	0.12	4.50
386	20.0	3.05	25.9	4.17	--	--	5.60
394	20.0	3.05	35.8	4.06	0.29	0.07	5.45
396	20.0	3.05	40.2	6.67	--	--	8.95
398	20.0	3.05	70.0	9.00	--	--	12.1
395	20.0	3.05	71.3	8.33	--	--	11.2
400	23.0	5.72	11.3	8.48	1.80	0.21	3.68
402	23.0	5.72	25.0	12.0	0.85	0.07	5.22
405	23.0	5.72	31.4	18.7	1.40	0.07	8.12
404	23.0	5.72	64.1	30.1	2.15	0.07	13.1

TABLE 12

STIRRED DIHYDRATE GROWTH RATES AT 98°C

Run	c millimoles per litre	c - c* millimoles per litre	v cm./sec.	$R_1 \times 10^6$ cm./sec.	$K \times 10^7$ (cm./sec.) x (l./millimole) ^{1.8}
558	17.0	1.75	16.7	2.64	--
556	17.0	1.75	19.2	2.62	--
559	17.0	1.75	31.4	2.22	--
561	17.0	1.75	35.6	2.19	--
562	17.0	1.75	37.7	2.70	--
574	18.5	3.05	10.7	4.04	5.42
571	18.5	3.05	20.7	3.65	11.6
578	18.5	3.05	39.1	5.22	7.00
570	18.5	3.05	42.7	3.33	11.2
566	18.5	3.05	50.3	14.1	18.9

TABLE 15

CALCULATED MASS TRANSFER COEFFICIENTS FOR UNSTIRRED DIHYDRATE
GROWTH RATES AT 70°C

(All concentrations in millimoles/litre)

Interfacial super- saturation $c_i - c^*$	Bulk solution concentration c	Interfacial concentration c_i	Super- saturation for mass transfer $c - c_i$	Mass transfer coefficient k_m cm./sec.
2.0	23.4	20.8	2.6	0.017
3.0	25.3	22.4	2.9	0.032
4.0	27.2	23.8	3.4	0.045
5.0	28.8	25.2	3.6	0.062
6.0	30.3	26.4	3.9	0.080

TABLE 14

THE EFFECT OF CRYSTAL SIZE ON THE UNSTIRRED GROWTH RATE
OF DIHYDRATE AT 85°C

Run	c millimoles/l.	c - c* millimoles/l.	Crystal tip radius r_t cm.	$R_1 \times 10^6$ cm./sec.
407	20.0	3.05	0.0005	2.94
407	20.0	3.05	0.0005	3.53
407	20.0	3.05	0.0005	2.94
407	20.0	3.05	0.0005	6.67
392	20.0	3.05	0.003	2.08
391	20.0	3.05	0.009	1.89
387	20.0	3.05	0.012	2.78
388	20.0	3.05	0.014	2.77
408	23.0	5.72	0.00075	4.75
408	23.0	5.72	0.00075	9.90
408	23.0	5.72	0.00075	10.6
408	23.0	5.72	0.00125	7.70
399	23.0	5.72	0.008	4.04
389	23.0	5.72	0.016	5.08
390	27.0	9.25	0.0002	27.8 **
405	27.0	9.25	0.0002	16.7 **
406	27.0	9.25	0.0005	20.0
406	27.0	9.25	0.0005	15.3
406	27.0	9.25	0.0005	20.0
405	27.0	9.25	0.008	8.53
390	27.0	9.25	0.009	5.00
406	27.0	9.25	0.010	11.1

** Maximum rate measured.

TABLE 15

UNSTIRRED HEMIHYDRATE GROWTH RATES AT 98°C

Run	Solution concentration c millimoles/l.	c - c* millimoles/l.	R x 10 ⁵ cm./sec.
598	16.5	1.30	1.53
600	16.5	1.30	1.09
473	17.0	1.75	1.00
474	17.0	1.75	1.20
475	17.0	1.75	1.16
487	17.0	1.75	1.01
488	17.0	1.75	1.27
490	17.0	1.75	0.99
492	17.0	1.75	0.89
493	17.0	1.75	0.95
555	17.0	1.75	1.28
555	17.0	1.75	1.53
556	17.0	1.75	0.93
558	17.0	1.75	0.86
561	17.0	1.75	1.05
562	17.0	1.75	1.00
562	17.0	1.75	0.67
469	18.5	3.05	2.36
470	18.5	3.05	2.20
472	18.5	3.05	2.53
481	18.5	3.05	2.65
566	18.5	3.05	2.22
566	18.5	3.05	1.95
567	18.5	3.05	1.40
567	18.5	3.05	2.75

TABLE 15 (continued)

Run	Solution concentration c millimoles/l.	c - c* millimoles/l.	R x 10 ⁵ cm./sec.
571	18.5	3.05	2.13
572	18.5	3.05	2.50
573	18.5	3.05	2.79
573	18.5	3.05	2.20
574	18.5	3.05	2.72
574	18.5	3.05	2.27
578	18.5	3.05	1.40
579	18.5	3.05	1.97
579	18.5	3.05	2.00
579	18.5	3.05	1.67
580	18.5	3.05	2.08
580	18.5	3.05	2.29
580	18.5	3.05	1.09
580	18.5	3.05	1.19
580	18.5	3.05	0.85
580	18.5	3.05	2.35
581	18.5	3.05	2.14
581	18.5	3.05	1.86
581	18.5	3.05	2.67
582	18.5	3.05	2.50
582	18.5	3.05	2.28
582	18.5	3.05	2.69
582	18.5	3.05	3.08
583	18.5	3.05	2.16
583	18.5	3.05	1.86
583	18.5	3.05	1.18
584	18.5	3.05	1.87
584	18.5	3.05	1.56

TABLE 15 (continued)

Run	Solution concentration c millimoles/l.	c - c* millimoles/l.	R x 10 ⁵ cm./sec.
584	18.5	3.05	2.22
585	18.5	3.05	1.57
586	18.5	3.05	1.99
587	18.5	3.05	1.87
588	18.5	3.05	2.34
588	18.5	3.05	2.12
591	18.5	3.05	3.05
591	18.5	3.05	1.92
593	18.5	3.05	1.15
597	18.5	3.05	2.55
597	18.5	3.05	2.86
597	18.5	3.05	1.82
607	18.5	3.05	1.08
610	18.5	3.05	1.81
610	18.5	3.05	2.01
464	20.0	4.35	3.04
466	20.0	4.35	3.70
468	20.0	4.35	3.46
602	20.0	4.35	2.39
609	20.0	4.35	3.09
609	20.0	4.35	3.41
611	20.5	4.80	3.33
462	21.0	5.20	4.67
463	21.0	5.20	5.05
477	21.0	5.20	4.44
494	24.0	7.80	13.3
496	24.0	7.80	13.3

TABLE 16

STIRRED HEMIHYDRATE GROWTH RATES AT 98°C

Run	c - c* millimoles per litre	Crystal velocity v cm./sec.	R x 10 ⁵ cm./sec.		Time for growth to stop minutes
			Initial	Final	
BATCH SYSTEM					
492	1.75	5.9	0	0	0
495	1.75	5.9	1.33	0	5
491	1.75	10.0	0.48	0	7
489	1.75	15.7	2.67	0	5
484	3.05	3.2	4.00	0	23
486	3.05	6.3	2.67	0	24
483	3.05	9.3	5.81	0	25
480	3.05	10.4	0	0	0
482	3.05	16.2	4.44	1.03	>40
605	3.05	65.0	0	0	0
FLOW SYSTEM					
555	1.75	4.2	1.33	1.00	>57
556	1.75	9.5	0	0	0
555	1.75	9.9	0	0	0
555	1.75	15.4	0	0	0
555	1.75	42.0	0	0	0
573	3.05	5.9	2.71	0	64
584	3.05	8.4	0.93	0	18
572	3.05	8.8	1.67	0	19
573	3.05	30.9	0.56	0	6
570	3.05	42.7	1.78	1.78	>124
567	3.05	55.0	0.91	0	172

TABLE 17

SIMULTANEOUS GROWTH OF DIHYDRATE AND HEMIHYDRATE AT 98°C

Run	c - c* millimoles per litre	Crystal velocity v cm./sec.	Run time minutes	Growth rate (cm./sec.) x 10 ⁶		
				Dihydrate (constant)	Hemihydrate	
					Initial	Final
561	1.75	10.1	137	2.20	1.20	0
562	1.75	12.6	74	2.70	3.20	0
558	1.75	16.7	101	2.60	3.60	1.50
559	1.75	31.4	30	2.20	0	0
571	3.05	20.7	104	8.70	40.0	0
566	3.05	50.3	30	14.1	10.5	10.3

TABLE 18

THE EFFECT OF A GLASS DUST DEPOSIT ON THE UNSTIRRED
GROWTH RATE OF HEMIHYDRATE

Run	c - c* millimoles per litre	Growth rate (cm./sec.) x 10 ⁵		
		Before visible deposit	Deposit present	After deposit removed
577	1.90	1.09	0	0.74
577	1.90	0.74	0	0.91
577	1.90	0.91	0	--
580	3.05	1.85	0.56	1.67
580	3.05	1.67	0	0.83
580	3.05	0.83	0	2.00
580	3.05	2.00	0	--
582	3.05	2.69	1.20	3.08

TABLE 19

EFFECT OF SURFACE DISSOLUTION ON THE SUBSEQUENT UNSTIRRED
GROWTH RATE OF HEMIHYDRATE

Run	c - c* millimoles per litre	Time of dissolution minutes	Growth rate after dissolution (cm./sec.) x 10 ⁵
564	1.75	0.3	0
565	1.75	3.0	0
562	1.75	6.0	1.00
562	1.75	8.0	0.67
606	1.75	9.0	0
596	3.05	2.0	0
593	3.05	4.0	1.80
597	3.05	4.5	0
597	3.05	6.0	0
587	3.05	9.0	0

TABLE 20

HEMIHYDRATE GROWTH RATE IN THE ABSENCE OF GLASS DUST

Run	c - c* millimoles per litre	Crystal velocity v cm./sec.	R x 10 ⁵ cm./sec.	Duration of run minutes
BRASS ROD IN BRASS SLEEVE				
578	3.05	0	1.41	
578	3.05	29.3	1.91	115
582	3.05	0	2.50	
582	3.05	20.2	2.13	47
RIGID COUPLING				
583	3.05	0	2.16	
583	3.05	29.0	2.01	98
584	3.05	0	2.22	
584	3.05	8.8	1.68	111
584	3.05	8.8	1.61	60**

** Growth suddenly stopped at 60 minutes.

TABLE 21

MAXIMUM STIRRED HEMIHYDRATE GROWTH RATES

Run	c - c* millimoles per litre	Crystal velocity v cm./sec.	Maximum growth rate (cm./sec.) x 10 ⁵
355	1.75	4.2	1.17
493	1.75	5.9	1.33
491	1.75	10.0	0.48
561	1.75	10.1	1.19
562	1.75	12.6	0.32
489	1.75	15.7	2.67
558	1.75	16.7	0.36
484	3.05	3.2	4.00
573	3.05	5.9	2.22
486	3.05	6.3	3.30
584	3.05	8.4	1.48
572	3.05	8.8	1.67
584	3.05	8.8	1.68
584	3.05	8.8	0.95
584	3.05	8.8	1.61
483	3.05	9.3	3.81
574	3.05	10.7	2.67
482	3.05	16.2	4.44

TABLE 21 (continued)

Run	c - c* millimoles per litre	Crystal velocity v cm./sec.	Maximum growth rate (cm./sec.) x 10 ⁵
582	3.05	20.2	1.98
571	3.05	20.7	4.00
583	3.05	29.0	2.04
578	3.05	29.3	1.94
578	3.05	29.3	1.78
578	3.05	29.3	1.33
573	3.05	30.9	0.56
570	3.05	42.7	2.58
570	3.05	42.7	2.22
566	3.05	50.3	1.90
567	3.05	55.0	0.91
567	3.05	55.0	1.00
567	3.05	56.5	1.21

TABLE 22

HEMIHYDRATE AND DIHYDRATE GROWTH RATES IN 1.0 MOLAR
SODIUM CHLORIDE SOLUTIONS AT 98°C

Run	c millimoles per litre	c - c* millimoles per litre	Crystal velocity v cm./sec.	Growth rate (cm./sec.) x 10 ⁶	
				Dihydrate	Hemihydrate
576	46.0	2.90	0	3.78	19.1
577	45.0	1.90	0	3.51	9.50
577	45.0	1.90	10.0	6.67	9.10**

** This rate was maintained for 22 minutes after which growth stopped.

TABLE 25

HEMIHYDRATE DEPOSITS ON STIRRED METAL WIRES AFTER 30 MINUTES

SUMMARY OF RESULTS

Type of metal	Surface treatment			pH of solution		Density* of deposit
	Unprepared	Painted	Filed	Neutral	Acidic	
Galvanized	x			x		5
iron		x		x		4
			x	x		3
	x				x	5
			x		x	2
Steel	x			x		4
			x	x		2
	x				x	4
			x		x	2
Copper	x			x		3
			x	x		1
	x				x	4
			x		x	2
Aluminum	x			x		3
	x				x	5
Platinum	x			x		2
	x				x	2
Nickel-chromium	x				x	2
Tungsten	x			x		1
Stainless steel	x			x		1
	x				x	1

* These values represent relative deposit densities from 1 (no crystals) to 5 (heavy deposit).

TABLE 24

DENSITY OF HEMIHYDRATE CRYSTALS ON AN UNSTIRRED GALVANIZED
IRON WIRE AND OTHER SURFACES AT VARIOUS TIMES (RUN 204)

Surface	Approximate number of crystals per cm. ²		
	<u>20 minutes</u>	<u>40 minutes</u>	<u>60 minutes</u>
Untreated section of wire	150	270	540
Painted section of wire	5	14	14
Glass tube walls	2	5	2
Glass tube bottom	16	23	39
Solution surface	13	32	52

TABLE 25

FORMULA OF THE SYNTHETIC SEA WATER USED IN RUN 377
(APPROXIMATELY 4.25 x NORMAL SEA WATER CONCENTRATION)

Feed solution	Salt	Concentration gm. per litre
Ca ⁺⁺ solution	CaCl ₂	8.7
	NaCl	115.0
SO ₄ ⁻ solution	Na ₂ SO ₄	12.5
	NaCl	112.0
	KCl	7.1
	MgSO ₄	20.0
	MgCl ₂	26.5

Mixed solution	Concentration gm. per litre	4.25 x normal sea water (reference 1) gm. per litre
Cl ⁻	80.5	80.6
Na ⁺	45.6	44.9
SO ₄ ⁻	13.2	11.5
Mg ⁺⁺	5.6	5.4
K ⁺	1.7	1.6
Ca ⁺⁺	1.6	1.7

TABLE 26

DEPOSITION ON A HEATED SURFACE

Run	Solution	Duration of run hours.	Hydrate formed
371	Calcium chloride and sodium sulphate	90	Dihydrate
372	"	16.5	Dihydrate
373	"	64	Dihydrate
376	"	65	Dihydrate
377	Synthetic sea water brine	70	Hemihydrate

TABLE 27

DEPOSITION RATES ON A STIRRED METAL SURFACE IN MIXED CALCIUM CHLORIDE AND SODIUM SULPHATE SOLUTIONS

Run	Solution Temp. °C	Hydrate Deposited on Rod		Solution Flow-rate cc/hr	Rod Velocity cm/sec	Time min.	Solution Concentration millimoles/litre	Deposition Rate cm/sec x 10 ⁶		
		At start of run	During run					Average Base	Average Tip	Maximum Tip
415	85	A few dihydrate seeds	Dihydrate	96.9	36.6	0	20.3±0.2	-	-	-
						202	-	-	0.08	0.48
						217	20.5±0.3	-	-	-
						316	-	-	0.27	0.99
						330	19.5±0.2	-	-	-
416	85	Dihydrate deposit from run 415	Dihydrate	114.5	41.9	130	18.2±0.4	-	-	-
						170	18.4±0.4	-	-	-
						252	-	0.84	1.39	1.94
						356	17.4±0.2	-	-	-
						882	-	0.90	1.46	1.71

TABLE 27 (continued)

Run	Solution Temp. °C	Hydrate Deposited on Rod		Solution Flow-rate cc/hr	Rod Velocity cm/sec	Time min.	Solution Concentration millimoles/litre	Deposition Rate cm/sec x 10 ⁶		
		At start of run	During run					Average Base	Average Tip	Maximum Tip
417	85	Dihydrate deposit from run 416	Dihydrate	102.5	39.3	189	-	0.10	0.37	1.42
						300	16.8±0.3	-	-	-
						822	-	0.44	0.33	0.88
						1310	16.2±0.3	-	-	-
418	85	A few dihydrate seeds	Dihydrate	1110	40.6	342	-	0	0.80	2.15
						358	19.0±0.3	-	-	-
419	85	Dihydrate deposit from run 418	Dihydrate	1190	47.0	120	18.4±0.3	-	-	-
						190	-	0	0.64	1.07
						296	18.6±0.2	-	-	-
420	85	Dihydrate deposit from run 419	Dihydrate	1200	31.4	180	18.6±0.3	-	-	-
						230	-	0	0.41	1.20
						300	18.5±0.2	-	-	-
421	85	Dihydrate deposit from run 420	Dihydrate	1200	40.0	256	-	0.08	0.54	1.10
						275	18.8±0.3	-	-	-

TABLE 27 (continued)

Run	Solu- tion Temp. °C	Hydrate Deposited on Rod		Solu- tion Flow- rate cc/hr	Rod Velo- city cm/sec	Time min.	Solution Concen- tration millimoles/ litre	Deposition Rate cm/sec x 10 ⁶		
		At start of run	During run					Average Base	Average Tip	Maximum Tip
422	85	Dihydrate deposit from run 421	Dihyd- rate	1140	42.0	160	18.8±0.2	-	-	-
						241	-	0.16	1.69	2.64
423	85	Dihydrate deposit from run 422	Dihyd- rate	1140	44.0	145	18.6±0.5	-	-	-
						161	-	0.35	1.55	2.64
424	85	Dihydrate depcsit from run 423	Dihyd- rate	1160	47.5	149	-	0.05	1.16	2.00
						295	18.4±0.3	-	-	-
425	85	Dihydrate deposit from run 424	Dihyd- rate	1160	40.8	257	-	0.14	1.39	2.10
						282	18.2±0.3	-	-	-
426	85	Dihydrate deposit from run 425	Dihyd- rate	1148	49.7	185	18.6±0.3	-	-	-
						216	-	0.12	1.29	2.56
427	85	A few dihydrate seeds	Dihyd- rate	740	46.5	120	19.8±0.4	-	-	-
						385	19.7±0.3	-	-	-
						935	-	0.24	2.19	2.88

TABLE 27 (continued)

Run	Solution Temp. °C	Hydrate Deposited on Rcd		Solution Flow-rate cc/hr	Rod Velocity cm/sec	Time min.	Solution Concentration millimoles/litre	Deposition Rate cm/sec x 10 ⁶		
		At start of run	During run					Average Base	Average Tip	Maximum Tip
427 (continued)				700	40.0	1470	19.7±0.3	-	-	-
						1662	-	0.43	2.03	2.87
						2410	-	0.38	1.53	2.39
				730	49.0	2960	19.8±0.3	-	-	-
						3133	-	0.78	1.89	2.99
				700	53.5	3210	20.2±0.5	-	-	-
						3815	-	0.50	1.56	1.97
						4470	19.4±0.3	-	-	-
				705	48.8	4509	-	0	1.19	1.70
557	98	A few hemi-hydrate seeds	Dihydrate	710	44.9	0	17.0	-	-	-
						190	16.9±0.1	-	-	-
						837	-	0.05	1.30	1.58
575	98	A few hemi-hydrate seeds	Dihydrate and Hemi-hydrate	680	35.0	0	18.5	-	-	-
						235	-	-	6.30	8.30
						893	-	-	1.17	1.98

TABLE 28

DEPOSITION RATES ON A STIRRED METAL SURFACE IN 1.0 MOLAR SODIUM CHLORIDE AND 0.045 MOLAR CALCIUM SULPHATE SOLUTIONS

Run	Soln- tion Temp. °C	Hydrate Deposited on Rod		Soln- tion Flow- rate cc/hr	Rod Velo- city cm/sec	Time min.	Solution Concen- tration millimoles/ litre	Deposition Rate cm/sec x 10 ⁶		
		At start of run	During run					Average Base	Average Tip	Maximum Tip
590	98.7	A few hemi- hydrate seeds	Dihyd- rate and hemi- hydrate	665	23.3	0	45.0	-	-	-
						131	-	0.97	4.04	5.16
						302	-	0	1.90	3.85
						894	-	0.06	1.41	2.29
594	98	None	Hemi- hydrate and a little dihyd- rate	670	19.9	0	45.0	-	-	-
						70	-	3.44	15.6	25.2
						171	-	0.06	2.91	5.35
						308	-	0.40	2.52	4.31
595	98	Mixed deposit from run 594	Hemi- hydrate and di- hydrate	670	19.9	0	45.0	-	-	-
						138	-	2.32	5.31	7.12
						331	-	1.72	4.23	10.5
						898	-	0.83	2.54	3.58
						1605	-	-	1.65	2.30
						2325	-	0.23	1.95	2.39
3044	-	0.35	2.06	3.14						

TABLE 29

COMPARISON OF MAXIMUM OBSERVED TIP GROWTH RATES WITH SINGLE CRYSTAL GROWTH RATES OF THE DIHYDRATE AT 85°

Run	Time min.	Rod Velocity cm/sec	c - c* millimoles litre	Growth Rate cm/sec x 10 ⁶	
				Maximum Tip Rate	Single Crystal Rate
415	0	36.6	3.3 ± 0.2		6.4 ± 0.7
	202			0.5	
	217				7.2 ± 1.0
	316			1.0	
	330				4.0 ± 0.5
416	130	41.9	1.5 ± 0.4		1.5 ± 0.7
	170				2.3 ± 1.2
	252			1.9	
	356				0.4 ± 0.2
	882			1.7	
417	189	39.3		1.4	
	300		0.3 ± 0.3		0.1 ± 0.1
	822			0.9	
418	342	40.6		2.2	
	358		2.1 ± 0.3		2.9 ± 0.7
419	120	47.0	1.6 ± 0.3		2.0 ± 0.6
	190			1.1	
	296				2.3 ± 0.4
420	180	31.4	1.8 ± 0.3		1.9 ± 0.5
	230			1.2	
	300				1.7 ± 0.3

TABLE 29 (continued)

Run	Time min.	Rod Velocity cm/sec	c - c* millimoles litre	Growth Rate cm/sec x 10 ⁶											
				Maximum Tip Rate	Single Crystal Rate										
421	256	40.0	2.0 ± 0.3	1.1	2.6 ± 0.7										
	275														
422	160	42.0	2.0 ± 0.2	2.6	2.7 ± 0.5										
	241														
423	145	44.0	1.8 ± 0.4	2.6	2.4 ± 1.1										
	161														
424	149	47.5	1.7 ± 0.3	2.0	2.0 ± 0.6										
	295														
425	257	40.8	1.5 ± 0.3	2.1	1.4 ± 0.5										
	282														
426	185	49.7	1.8 ± 0.3	2.6	2.5 ± 0.7										
	216														
427	120	46.5	2.9 ± 0.4	2.9	5.9 ± 1.4										
	385					2.8 ± 0.3	5.4 ± 1.0								
	935														
	1470							40.0	2.8 ± 0.3	4.9 ± 0.9					
	1662										2.9				
	2410											2.4			
	2960												49.0	2.9 ± 0.3	6.1 ± 1.1
	3133														

TABLE 29 (continued)

Run	Time min.	Rod Velocity cm/sec	c - c* millimoles litre	Growth Rate cm/sec x 10 ⁶	
				Maximum Tip Rate	Single Crystal Rate
427 (con- tin- ued)	3210	53.5	3.3 ± 0.5		8.1 ± 2.2
	3815			2.0	
	4470		2.5 ± 0.3		4.9 ± 1.0
	4509	48.8		1.7	

TABLE 30

COMPARISON OF MAXIMUM OBSERVED TIP GROWTH RATES WITH SINGLE CRYSTAL GROWTH RATES OF THE DIHYDRATE AND HEMIHYDRATE AT 98°

Run	Time min.	Rod Velo- city cm/sec	c - c* millimoles litre	Growth Rate cm/sec x 10 ⁶	
				Maximum Tip Rate	Single Crystal Rate Stirred Dihydrate Unstirred** Hemihydrate
557	0	44.9	1.8		3.9 10.0
	190		1.7 ± 0.1		3.5 ± 0.4 9.5 ± 0.5
	837			1.6	
575	0	35.0	3.1		9.7 21.0
	235			8.3	
	893			2.0	
590	0	23.3	1.0		~6.7 ~9.5
	131			5.2	
	302			3.9	
	894			2.3	
594	0	19.9	1.0		~6.7 ~9.5
	70			25.2	
	171			5.4	
	308			4.3	
595	0	19.9	1.0		~6.7 ~9.5
	138			7.1	
	331			10.5	

TABLE 30 (continued)

Run Time min.	Rod Velo- city cm/sec	c - c* millimoles litre	Growth Rate cm/sec x 10 ⁶	
			Maximum Tip rate	Single Crystal Rate Stirred Dihydrate Unstirred** Hemihydrate
595	898		3.6	
(con- tin- ued)	1605		2.3	
	2325		2.4	
	3044		3.1	

** Initial stirred hemihydrate single crystal growth rates were up to 3 times the unstirred rates shown here.

TABLE 31

ACUTE ANGLE BETWEEN DIHYDRATE CRYSTALS AND PARENT
DIHYDRATE CRYSTAL (ALL ANGLES IN DEGREES)

<u>First parent crystal</u>	<u>Fourth parent crystal</u>
12.0	3.0
49.9	50.0
61.4	59.0
63.7	60.5
63.7	68.0
72.7	68.5
72.7	69.0
79.6	69.5
	71.5
<u>Second parent crystal</u>	71.5
33.1	75.2
53.0	82.0
54.4	82.5
54.5	86.0
59.5	86.0
62.0	86.0
70.4	87.5
70.4	88.0
70.5	
74.1	<u>Fifth parent crystal</u>
75.6	52.0
75.6	57.1
75.6	69.0
77.0	77.0
77.0	85.0
	<u>87.0</u>
<u>Third parent crystal</u>	Overall 66.4
41.6	average
65.9	

TABLE 32

TIMES OF OBSERVATION OF DIHYDRATE CRYSTALS ON UNSTIRRED
DIHYDRATE SEED CRYSTALS AT 85°C

Run	Tube type	Dissolution time minutes	c - c* millimoles per litre	Observation time minutes	
				First crystal	No crystals
442	F	15	2.2	< 3840**	
438	F	30	2.2		125
440	F	35	2.2		220
437***	F	10	2.2		3840
435	F	20	2.6		1113
433	E	20	4.5	51	
436	F	30	4.5	85	
434	F	25	4.5	< 945	
430	E	30	6.6	29	
432	E	24	6.6	30	

** Only one crystal on the seed crystal.

*** Two seed crystals mounted on the same rod.

TABLE 33

THE EFFECT OF THE ADDITION OF BARIUM ION ON NUCLEATION
IN THE BULK OF THE SOLUTION

Run	c - c* millimoles per litre	$[Ba^{++}]$ millimoles per litre	Surface**	Observation time minutes	
				First crystal	No crystals
499	4.0	0.6	DS		325
499	4.0	0	DS		325
497	6.6	0.6	D	< 105	
497	6.6	0	D	< 105	
498	6.6	0.6	G	15	
498	6.6	0	G	15	

** SYMBOLS

DS - dihydrate seed crystal, surface dissolved.

D - dihydrate seed crystal, no preparation.

G - glass rod.

TABLE 34

TIMES OF OBSERVATION OF DIHYDRATE CRYSTALS ON SEED CRYSTALS
IN ENLARGED AND CAPILLARY TUBES

Run	Tube type	Seed* crys- tal	Solu- tion Temp. °C	Solution super- saturation c - c* millimoles litre	Observation time (minutes)				
					Capillary Tube		Enlarged Tube		
					First crys- tal	No crys- tals	First crys- tal	No crys- tals	
451	G	D	85	6.6	76**			21	
452	H	D	85	6.6				<249	
453	H	D	85	6.6			37		
454	H	D	85	6.6			65		
455	H	D	85	6.6					46
456	H	D	85	6.6			65		47
457	H	D	85	6.6					55
458	H	D	85	6.6			55		
459	H	D	85	6.6					24
460	H	D	85	6.6					55
461	H	D	85	6.6	<1380***				33
616	H	D	100	8.7			69		69
617	H	H'	95	2.9			1000		1000
614	H	H'	100	8.7	48				12
615	H	H'	100	8.7	126**				9
625	J	C	95	4.2					33
619	J	C	95	5.9					27
640	H	C	95	8.5	48				31
642	H	C	95	8.5	45				35

* D = dihydrate; H' = hemihydrate; C = calcite.

** Only one crystal on seed crystal.

*** Only two crystals on seed crystal.

TABLE 35

GROWTH RATES OF SEED CRYSTALS IN ENLARGED AND CAPILLARY TUBES

Run	Seed** crystal	Solution tempera- ture °C	c - a* millimoles per litre	Growth rates (cm./sec.) x 10 ⁶		
				Capillary tube	Enlarged tube	Chapters 3 & 4***
453	D	85	6.6	6.06	6.35	7.5
454	D	85	6.6	6.06	5.88	7.5
455	D	85	6.6	--	6.56	7.5
459	D	85	6.6	--	5.45	7.5
461	D	85	6.6	--	5.33	7.5
614	H'	100	8.7	92.0	24.0	~170
615	H'	100	8.7	90.0	82.0	~170

**
SYMBOLS

D - dihydrate

H' - hemihydrate

Approximate growth rates for unstirred crystals from
chapters 3 and 4.

TABLE 56

THE EFFECT OF ADDITION OF DIHYDRATE CRYSTALS ON TIMES OF
OBSERVATION OF CRYSTALS ON SEED CRYSTAL SURFACES

Run	Tube type	Seed** crystal	Solution tempera- ture °C	c - c* millimoles per litre	Crystal velocity cm./sec.	Crystal*** addition		Observation time, minutes	
						Wt. gm.	Size	First crystal	No crystals
438	F	D	85	2.2	0	--	large		46
458	F	D	85	2.2	0	--	small	5	
440	F	D	85	2.2	0	--	mixed	10	
440	F	D	85	2.2	0	--	small	30	
440	F	D	85	2.2	0	--	small	7	
439	F	D	85	2.2	3.7	--	mixed	18	
446	F	D	85	2.2	5.9	--	small	50	
633	J	C	95	~ 0	13.7	--	small	180	
670	J	C	95	4.2	1.3	0.02	small	30	
668	J	C	95	4.2	2.0	0.01	small	80	
649	J	C	95	4.2	31.2	--	large	40	
665	J	C	95	4.2	31.4	0.40	small		60
666	J	C	95	4.2	33.5	0.01	small		60
646	J	C	95	5.9	13.7	--	large	70	

**
SYMBOLS

D - dihydrate

C - calcite

Dash indicates an unmeasured quantity of crystals added.

TABLE 37

THE EFFECT OF STIRRING ON TIMES OF OBSERVATION OF DIHYDRATE CRYSTALS ON SEED CRYSTAL AND GLASS SURFACES

Run	Tube Type	Sur-face**	Solu-tion Temp. °C	Solution Super-saturation (c - c*) millimoles litre	Crystal Velo-city cm/sec	Pad-dles	Observation Time (mins)	
							First	No
							crys-tal	crys-tals
439	F	D	85	2.2	3.7			60
441	F	D	85	2.2	6.3		245	
444	F	D	85	2.2	8.2			137
439	F	D	85	2.2	14.9		87	
635	J	D	95	~0	4.1			66
636	J	D	95	~0	4.1	X		197
637	J	D	95	5.9	5.5		27	
644	J	D	95	5.9	7.1		120	
647	J	D	95	5.9	14.0			1000
654	J	D	95	5.9	23.6	X	190	
645	J	D	95	5.9	24.6			76
653	J	D	95	5.9	39.2		100	
657	J	D	95	5.9	55.0	X	120	
655	J	D	95	5.9	78.6		195	
660	J	C	95	~0	>0		< 1200	
662	J	C	95	~0	>0		< 445	
632	J	C	95	~0	13.3		86	
659	J	C	95	~0	18.4	X		240
639	J	C	95	~0	48.4			90

** D = dihydrate; C = calcite; G = glass.

TABLE 37 (continued)

Run	Tube Type	Sur-face	Solu-tion Temp. °C	Solution Super-saturation (c - c*) millimoles litre	Crystal Velo-city cm/sec	Pad-dles	Observation Time (mins)	
							First crys-tal	No crys-tals
674	J	C	95	1.6	>0	X		1105
673	J	C	95	4.2	>0	X	120	
672	J	C	95	4.2	1.0		90	
671	J	C	95	4.2	1.3		30	
630	J	C	95	4.2	21.0		61	
648	J	C	95	4.2	28.5		50	
664	J	C	95	5.9	1.3		50	
631	J	C	95	5.9	19.1		31	
643	J	C	95	5.9	45.0		<1080	
641	J	C	95	5.9	63.0		120	
650	J	C	95	5.9	70.0		120	
638	J	C	95	5.9	72.5		120	
651	J	C	95	5.9	76.4		40	
663	J	G	95	~0	>0	X	<345	
634	J	G	95	4.2	30.0	X	<970	
661	J	G	95	5.9	>0	X	<1020	
656	J	G	95	5.9	120		<150	
658	J	G	95	9.0	70.7	X	45	

APPENDIX 2PHYSICAL DATA

PROPERTY		DIHYDRATE	HEMIHYDRATE
Molecular weight		172.18	145.15
Specific gravity		2.32	2.75
Refractive index	α	1.521	1.554
	γ	1.530	1.580
	β	1.523	1.555
Crystal system		monoclinic	hexagonal
Extinction angle		oblique	parallel

APPENDIX 3NOMENCLATURE

a	a constant
A	surface area of crystal (cm^2)
A'	proportionality constant in nucleation rate equation
A _H	area for heat transfer (cm^2)
b	a constant
B	proportionality constant in nucleation rate equation
c	concentration of solute in bulk of the solution (millimoles per litre)
c*	solubility of large crystals of the solute in solution (millimoles per litre)
Δc	$c - c^*$
c _i	concentration of solute at the crystal-solution interface (millimoles per litre)
c _r	solubility of a crystal with radius r (millimoles per litre)
c _∞	concentration of solute in the solution at an infinite distance from the crystal tip (millimoles per litre)
c _s	specific heat of the solution ($\text{cal. gm}^{-1} \cdot ^\circ\text{C}^{-1}$)
d	characteristic dimension of a system
D	diffusion coefficient ($\text{cm}^2 \cdot \text{sec}^{-1}$)
E	activation energy (kilocalories per mole)
f	fractional rate of surface renewal
ΔG	change in the total free energy due to homogeneous nucleation (ergs)
$\Delta G'$	change in the total free energy due to heterogeneous nucleation (ergs)

J	molar flux (millimoles per second)
k	Boltzmann constant, 1.38×10^{-16} (ergs.degree ⁻¹)
k_m	coefficient of mass transfer (cm.sec ⁻¹)
k_r	surface reaction coefficient
K	coefficient for overall solute transfer
K'	constant in an Arrhenius type equation
M	gram molecular weight
n	number of moles of solute transferred
N	rate of nucleation, number of nuclei per unit volume per unit time
p	a constant
r	radius of spherical crystal particle (cm)
r_c	critical radius of spherical crystal (cm)
r_t	radius of tip of crystal (cm)
R	gas constant per mole; growth rate of tip of hemihydrate crystal (cm.sec ⁻¹)
R_1	growth rate of edge of (111) and ($\bar{1}\bar{1}\bar{1}$) planes of dihydrate (cm.sec ⁻¹)
R_2	growth rate of edge of (110) and ($\bar{1}\bar{1}0$) planes of dihydrate (cm.sec ⁻¹)
Re	Reynolds number
S	supersaturation c/c^*
Sc	Schmidt number
Sh	Sherwood number
t	time (seconds)
T	temperature (°K)
T_B	temperature of constant temperature bath (°K)

T_0	temperature of solution at time zero ($^{\circ}\text{K}$)
T_{ave}	average solution temperature during nucleation experiment, as defined by equation 14 ($^{\circ}\text{K}$)
U	overall heat transfer coefficient ($\text{cal.cm}^{-2}.\text{sec}^{-1}.\text{C}^{-1}$)
v	relative velocity between solution and crystal ($\text{cm}.\text{sec}^{-1}$)
V	volume of solution (cm^3)
Z	$(c_i - c^*)^{p-1}$
\bar{c}	laminar diffusion layer thickness (cm)
θ	acute angle between parent dihydrate crystals and small dihydrate crystals on their surface (degrees)
μ	solution viscosity
ρ	density of crystal ($\text{grams}.\text{cm}^{-3}$)
ρ_s	density of solution ($\text{grams}.\text{cm}^{-3}$)
σ	specific surface free energy ($\text{ergs}.\text{cm}^{-2}$)
ϕ	time (seconds)
ϕ_I	induction time (seconds)

APPENDIX 4REFERENCES

1. Sverdrup, Johnson and Fleming, The Oceans, Prentice-Hall, New York 1942.
2. Parker, A., Nature 149, 184 (1942).
3. Ridge, M.J. et al., Aust. J. Sci., 9, 163 (1958); 10, 218 (1959); 11, 180, 385 (1960).
4. Ridge, M.J. et al., J. Appl. Chem., 12, 252 (1962).
5. McCartney, E.R. and A.E. Alexander, J. Colloid. Sci. 13, 383 (1958).
6. Cunningham, W.A. et al., Ind. Eng. Chem. 44, 2402 (1952).
7. Partridge, E.P., Dept. of Eng. Res., Univ. of Mich., Eng. Res. Bull. No. 15, 1930.
8. Badger, W.L. and Associates, Inc., Office of Saline Water, U.S. Dept. of Int., R. & D. Progress Report No. 25, 1959.
9. Couste, Ann. mines (5) 5, 69 (1854).
10. Hall, R.E., Ind. Eng. Chem. 17, 283 (1925).
11. Hall, R.E. et al., Carnegie Inst. Tech., Mining and Met. Investigations, Bull. 24 (1927).
12. Freeborn, J. and D. Lewis, J. Mech. Eng. Sci. 4, 46 (1962).
13. Golightly, D.R. and E.R. McCartney, The Chem. Eng. 169, 170 (1963)
14. Gordon, K.F. and G.C. Smith, Sonderdruck ans Dechema - Monographien Band 47 (1962).
15. Lurie, R.M., M.E. Berg and A. Giuffrida, Office of Saline Water, U.S. Dept. Int., R. & D. Progress Report No. 48 (1961).
16. Schierholtz, O.J., Can. J. Chem. 36, 1057 (1958).

17. Moriyama, T. and T. Utsunomiya, J. Chem. Soc. Japan, Ind. Chem. Sect. 60, 238, 1268 (1957).
18. Sugimoto, K., K. Irie and M. Funaoka, Report of Asahi Glass Research Lab, 3, 205 (1953).
19. Kelley, K.K., J.C. Southard and C.T. Anderson, U.S. Dept. Interior, Bureau of Mines, Tech. paper 625 (1941).
20. Volmer, M., Z. Electrochem. 35, 555 (1929).
21. Becker, R. von and W. Döring, Ann. Phys., Lpz. 24, 719 (1935).
22. Jones, W.J. and J.R. Partington, J. Chem. Soc. 107, 1019 (1915).
23. van't Hoff, J.H., F. Weigert, W. Hinrickson and G. Just, J. physik. Chem. 45, 257 (1903).
24. Caspari, W.A., Proc. Roy. Soc. (London), A155, 41 (1936).
25. Gallitelli, P., Periodico mineral, 4, 132 (1933); Neues Jahrb. Mineral. Geol., Referate I, 472 (1933).
26. Partridge, E.P. and A.H. White, J. Am. Chem. Soc. 51, 360 (1929).
27. Weiser, H.B., W.O. Milligan and W.C. Ekholm, J. Am. Chem. Soc. 58, 1261 (1936).
28. Posnjak, E., Am. J. Sci., 35A, 247 (1938).
29. Bunn, C.W., J. Sci. Instru. 18, 70 (1941).
30. Power, W.H. and B.M. Fabuss, Annual Report to O.S.W., U.S. Dept. Int., Contract No. 14-01-0001-294 (1963).
31. Hulett, G.A. and L.E. Allen, J. Am. Chem. Soc., 24, 667 (1902).

32. Bock, E., Can. J. Chem. 39, 1746 (1961).
33. Booth, H.S. and R.M. Bidwell, J. Am. Chem. Soc., 72, 2567 (1950).
34. Riddell, W.C., private communication quoted in reference 19.
35. Sborgi, U. and C. Bianchi, Gazz. Chim. Ital., 70, 823 (1940).
36. Chassevent, L., Ann. Chim. (10) 6, 244 (1926).
37. Hall, R.E., J.A. Robb and C.E. Coleman, J. Am. Chem. Soc., 48, 927 (1926).
38. Dickson, F.W., C.W. Blount and G. Tunell, Am. J. Sci., 261, 61 (1963).
39. Hill, A.E., J. Am. Chem. Soc. 59, 2242 (1937).
40. Fischer, W.M., Z. Anorg. Chem., 145, 311 (1925).
41. Smith, G.C. et al., Final Report on O.S.W. Graduate Research Fellowship Grant No. 14-01-0001-283, Office of Saline Water, U.S. Dept. Interior, 1963.
42. Nernst, W., Z. Phys. Chem. 47, 52 (1904).
43. Higbie, R., Trans. A.I. Ch. E., 31, 365 (1935).
44. Danckwerts, P.V., Ind. Eng. Chem., 43, 1460 (1951).
45. Toor, H.L. and J.M. Marchello, J.A.I. Ch.E., 4, 97 (1958).
46. Volmer, M., Kinetik der Phasenbildung, Dresden and Leipzig, Steinkopff (1939).
47. Frank, F.C., Symposium on Crystal Growth, Disc. Far. Soc., No. 5, 48 (1949).
48. Hixson, A.W. and K.L. Knox, Ind. Eng. Chem., 43, 2144 (1951).

49. Hixson, A.W. and S.J. Baum, Ind. Eng. Chem., 33, 478 (1941); 34, 120 (1942).
50. Freeborn, J.D., Ph.D. Thesis, Battersea College of Science and Technology, London, 1964.
51. Dunn, J.S., Chem. & Ind. (Rev.) 16, 144 (1938).
52. Reich, R., Ph.D. Thesis, University of Göttingen, 1965.
53. Final Report on Contract No. 14-01-001-164, ORA Project No. 02811, Office of Saline Water, U.S. Dept. Interior, 1964.